LUND UNIVERSITY

Iron Carbonyl Clusters as Proton Reduction Catalysts

Rahaman, Ahibur

2016

[Link to publication](#)

Total number of authors:
1

Creative Commons License:
Unspecified

Iron Carbonyl Clusters as Proton Reduction Catalysts

AHIBUR RAHAMAN | CHEMICAL PHYSICS | LUND UNIVERSITY

Ph

H₂

H'

H

P

P'

Fe

Fe'

2H⁺ + 2e⁻
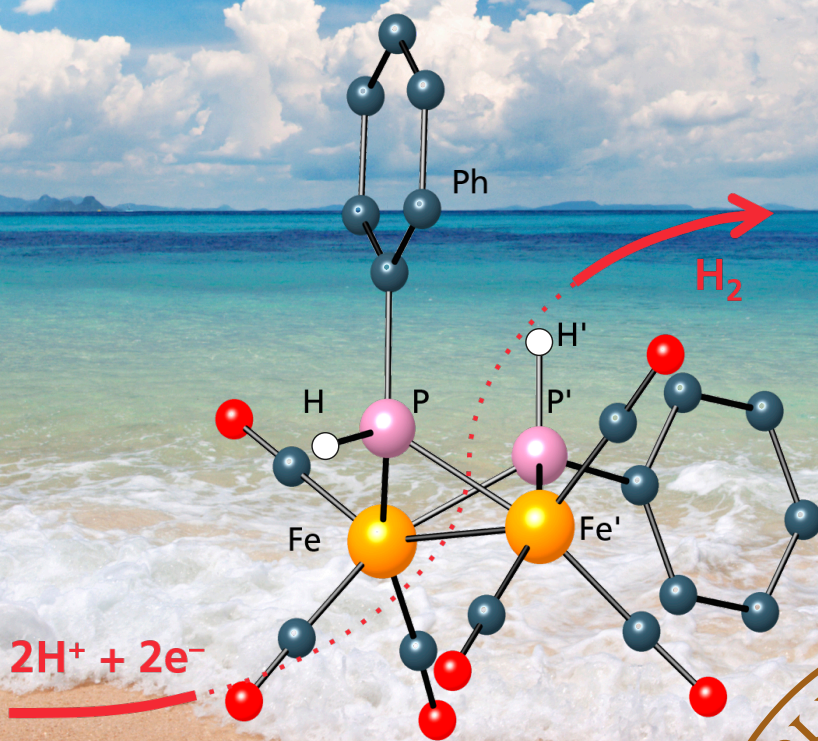
Structure versus Electro-Catalysis

Iron Carbonyl Clusters
as Proton Reduction Catalysts

Ahibur Rahaman

LUND
UNIVERSITY

DOCTORAL DISSERTATION

by due permission of the Faculty of Natural Science, Lund University, Sweden.

To be defended at Lecture Hall B, Kemicentrum, Lund.

Friday 3rd June 2016, at 9.30

Faculty opponent
Professor Philippe Schollhammer
Université de Bretagne Occidentale,
Brest, France

Organization Lund University	Document name DOCTORAL DISSERTATION
	Date of issue: June 3, 2016
Author: Ahibur Rahaman	Sponsoring organization: European Union

Title and subtitle Iron Carbonyl Clusters as Proton Reduction Catalysts

Abstract – The mixed-valence triiron complexes [Fe$_3$(CO)$_{7-x}$(PPh$_3$)$_x$(μ-edt)$_2$] (x = 0, 1, 2; edt = SCH$_2$CH$_2$S) and 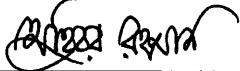[Fe$_3$(CO)$_5$(κ^2-diphosphine)(μ-edt)$_2$] (diphosphine = dppv, dppe, dppb, dppn) have been prepared and structurally characterized. In comparison to the diiron complex [Fe$_2$(CO)$_6$(μ-edt)], [Fe$_3$(CO)$_7$(μ-edt)$_2$] catalyzes proton reduction at 0.36 V less negative potentials, which is a significant energetic gain. In all complexes the HOMO comprises an iron-iron bonding orbital localized between the two iron atoms not ligated by the semi-bridging carbonyl, while the LUMO is highly delocalised in nature and is anti-bonding between both pairs of iron atoms but also contains an anti-bonding dithiolate interaction.

The clusters [Fe$_3$(CO)$_9$(μ$_3$-E)$_2$] (E = S, Se, Te), [Fe$_3$(CO)$_7$(μ$_3$-E)$_2$(μ- κ^2-diphosphine)] (E = S, Se, Te), [Fe$_3$(CO)$_7$(μ$_3$-CO)(μ$_3$-E)(μ-dppm)] (E = S, Se) and [Fe$_3$(CO)$_8$(μ$_3$-Te)$_2$(κ^2-diphosphine)] have been prepared and examined as proton reduction catalysts. The reduction potentials for the tellurium-capped clusters occur at lower potentials than for their sulfur and selenium analogues, and the redox processes also show better reversibility than for the S/Se analogues. The 52-electron clusters [Fe$_3$(CO)$_8$(μ$_3$-Te)$_2$(κ^2-diphosphine)] consist of Fe$_2$(CO)$_6$(μ-Te)$_2$ "butterfly" units that are capped by a Fe(CO)$_2$(κ^2-diphosphine) moiety. Cyclic voltammetry studies reveal that their redox behaviour and properties as proton reduction catalysts largely stem from the Fe$_2$(CO)$_6$(μ-Te)$_2$ entities, although computational modelling indicates that their LUMOs are centered on the briding tellurium ions and the unique "capping" iron ion.

The influence of the substitution, orientation and structure of the phosphido bridges on the electrochemical and electrocatalytic properties of [Fe$_2$(CO)$_6$(μ-phosphido)$_2$] clusters and bis(phosphinidene)-capped triiron carbonyl clusters, including electron-rich derivatives formed by substitution with chelating diphosphines, have been studied. The electrochemistry and electrocatalyses of the [Fe$_2$(CO)$_6$(μ-PR$_2$)$_2$] dimers show subtle variations with the nature of the bridging phosphido group(s), including the orientation of bridgehead hydrogen atoms. The reduction potential of the phosphinidene-capped clusters shift negative way to increase the electron density on the iron centers.

Key words: iron-only hydrogenase, phosphine-substitution, proton reduction, electrocatalysis

Classification system and/or index terms (if any)	
Supplementary bibliographical information	Language: English

ISSN and key title	ISBN 978-91-7422-457-3

Recipient's notes	Number of pages 256	Price
	Security classification	

Signature _____Date May 10. 2016

Iron Carbonyl Clusters
as Proton Reduction Catalysts

Ahibur Rahaman

The cover picture depicts the abundance of resources of unlimited energy, e.g. the sun and water, and the molecular diagram representes a source of ultimate clean fuels.

Supervisor: Professor Ebbe Nordlander
                         Lund University, Sweden.

Co-supervisor: Professor Sofi Elmroth
                         Lund University, Sweden.

Dedicated to

My mother Dudmeher Begum

The soul of my father late Abul Hasem (Hasi)

My beloved wife Rupa &

To my loving son Ta-seen

All praise belongs to Allah, Lord of the worlds,

The Gracious, the Merciful, Master of the Day of Judgement.

The Holy Qur'an

List of papers

This dissertation is based on the following publications, which are referred to in the text by the roman numbers I-VI.

I. "Bio-inspired hydrogenase models: The mixed-valence triiron complex [$Fe_3(CO)_7(\mu$-edt$)_2$] and phosphine derivatives [$Fe_3(CO)_{7-x}(PPh_3)_x(\mu$-edt$)_2$] (x = 1, 2) and [$Fe_3(CO)_5(\kappa^2$-diphsophine)($\mu$-edt$)_2$] as proton reduction catalysts."

   A. Rahaman, S. Ghosh, D. Unwin, S. B. Modi, K. B. Holt, S. E. Kabir, E. Nordlander, M. G. Richmond, G. Hogarth.   Organometallics 2014, 33, 1356-1666.

II. "Bio-inspired proton-reduction catalysts: A comparison of the catalytic proton-reduction properties of chalcogenide-capped triiron clusters [$Fe_3(CO)_9(\mu_3$-E$)_2$],[$Fe_3(CO)_7(\mu_3$-CO)(μ_3-E)(μ-dppm)] and [$Fe_3(CO)_7(\mu_3$-E$)_2(\mu$-dppm)] (E = S, Se)." Submitted.

   A. Rahaman, S. Ghosh, S. B. Modi, A. F. Abdel-Magied, S. E. Kabir, M. Haukka, M. G. Richmond, G. C. Lisensky, E. Nordlander, G. Hogarth.

III. "Electrocatalytic proton-reduction behaviour of telluride-capped triiron clusters: tuning of overpotentials and stabilization of redox states relative to lighter chalcogenide analogues." Manuscript

   A. Rahaman, G. C. Lisensky, M. G. Richmond, E. Nordlander, G. Hogarth.

IV. "Synthesis and molecular structures of the 52-electron triiron telluride clusters [$Fe_3(CO)_8(\mu_3$-Te$)_2(\kappa^2$-diphosphine)]: Electrochemical properties and activity as proton reduction catalysts." Manuscript.

   A. Rahaman, D. A. Tocher, G. C. Lisensky, M. G. Richmond, G. Hogarth, E. Nordlander.

V.   "Bridgehead isomer effects in bis(phosphido)-bridged diiron hexacarbonyl proton reduction electrocatalysts." Submitted.

A. Rahaman, C. G. Suriñach, G. E. Ball, M. Bhadbhade, M. Haukka, L. Higham, E. Nordlander, S. B. Colbran.

VI.   "Proton reduction by phosphinidene-capped triiron clusters". Manuscript.

A. Rahaman, G. C. Lisensky, M. Haukka, D. A. Tocher, S. B. Colbran, E. Nordlander.

My contribution to papers I-VI

I.   I performed all synthesis and reactivity studies, and participated in the electrochemical studies. I wrote major parts of the paper.

II.   I performed all synthesis and reactivity studies, and carried out the electrochemistry and electrocatalysis experiments in CH_2Cl_2. I wrote the initial draft of the paper and participated in all stages of the completion of the manuscript.

III.   I performed all synthesis and reactivity studies, and carried out the electrochemistry and electrocatalysis experiments. I wrote the initial draft of the paper and participated in all stages of the completion of the manuscript.

IV.   I performed all synthesis and reactivity studies, and carried out the electrochemistry and electrocatalysis experiments. I wrote the initial draft of the paper and participated in all stages of the completion of the manuscript.

V.   I performed all synthesis and reactivity studies, and carried out the electrochemistry and electrocatalysis experiments. I wrote the initial draft of the paper and participated in all stages of the completion of the manuscript.

VI.   I performed all synthesis and reactivity studies, and carried out the electrochemistry and electrocatalysis experiments. I wrote the initial draft of the paper and participated in all stages of the completion of the manuscript.

Contents

List of the abbreviations

CO	Carbon monoxide
CN^-	Cyanide
FTIR	Fourier Transform Infrared Spectroscopy
CO_2	Carbon dioxide
DFT	Density Functional Theory
pdt	Propane-1,3-dithiolate
adt	2-aza propane-1,3-dithiolate
edt	1,2-ethanedithiol
bdt	Benzene-1, 2-dithiol
PPh_3	Triphenylphosphine
IR	Infrared
NMR	Nuclear magnetic resonance
MHz	Megahertz
E°	Formal potential
(i_{pa})	Anodic peak current
(i_{pc})	Cathodic peak current
WE	Working electrode
RE	Reference electrode
CE	Counter or auxiliary electrode
i_{cat}	Catalytic current
C_{HA}	Concentration of acid,
C_{cat}	Concentration of catalyst.
CH_2Cl_2	Dichloromethane
MeCN	Acetonitrile
NBu_4PF_6	Tetrabutylammonium hexafluorophosphate

[Cp$_2$Fe][PF$_6$]	Ferrocenium hexafluorophosphate
CV	Cyclic voltammetry
EPR	Electron paramagnetic resonance
TsOH	*p*-toluenesulfonic acid
HBF$_4$.Et$_2$O	Tetrafluoroboric acid diethyl ether complex
XRD	X- ray diffraction
HOMO	Height occupied molecular orbital
LOMO	Lowest occupied molecular orbital
dppm	1,1-Bis(diphenylphosphino)methane
dppe	1,2-Bis(diphenylphosphino)ethane
dppv	1,2-Bis(diphenylphosphino)ethylene
dppb	1,2-bis(diphenylphosphino) benzene
dppp	1,3-bis(diphenylphosphino)propane
dppf	1,1'-Bis(diphenylphosphino)ferrocene
dppbn	2,2′-Bis(diphenylphosphino)-1,1′-binaphthalene
dcpm	Bis(dicyclohexylphosphino)methane
dppa	Bis(diphenylphosphino)iso-propylamine

Chapter 1. General perspectives of my research

1.1 Introduction

The "hydrogen economy" envisages the use of hydrogen as a primary energy carrier, rather than the hydrocarbons that constitute the mainstay of much energy production today. More recently, research in the field of hydrogenases has been given considerable attention because the potential application for the production of clean and renewable hydrogen as a fuel. Hydrogenases are natural enzymes that act as catalysts for the production and oxidation of molecular hydrogen, according to the reaction: $H_2 \leftrightarrow 2H^+ + 2e^-$, using highly abundant metals. Most work in the research area of hydrogenase biomimics has been focused on the use of binuclear complexes. In this thesis, the synthesis of functional models for hydrogenases based on dithiolato-, chalcogenide-capped or diphosphido-bridged di- and triiron clusters, and their phosphine-containing derivatives, is described. The ability of these compounds to act as proton reduction catalysts to produce molecular hydrogen has been investigated.

1.2 Background

Our present society is completely dependent on fossil fuels. It has become increasingly urgent to develop an energy economy that is based on alternatives to petroleum. The demand for energy has never been greater in the history of human civilization. Within the last 150 years, the human energy consumption has increased enormously, from 5×10^{12} kWh/year to 1.2×10^{14} kWh/year.[1] While the population of human beings has increased by a factor of 4 in the last century, the energy demand has increased by a factor of 24. Over 80% of this energy is based on hydrocarbons such as oil and gas. However, the fossil fuels stored in the earth's crust are limited and are not viable for a sustainable energy economy. Day by day, the emission levels of CO_2 and other greenhouse gases increase due to combustion of fossil fuels.[2] The consumption of fossil fuels together with deforestation lead to the net increase in CO_2 in the atmosphere due to human activities being approximately 3×10^{12} kg/year, which corresponds to an annual increase of 0.4% of the CO_2 concentration in the atmosphere.[3] Due to the greenhouse effect, the earth is facing problems such as rising sea levels, floods, droughts etc., the results of which render presently inhabitable land uninhabitable. In addition to potential energy scarcity, modern civilization must

also solve the second urgent problem of the global greenhouse effect. Energy resources that are abundant and do not emit greenhouse gases into the atmosphere are thus urgently needed.

Solar radiation and wind energy are well established alternative energy sources but unreliable. As the sun's energy is still fairly unexplored and almost unused, and will be available for many millions of years, it may offer a solution to the energy challenge faced. However, the one major drawback is that sunlight, wind and virtually all renewable sources of energy have periodic variations in intensity, and it is thus necessary to store collected energy in batteries during low activity periods, e.g. night time or short winter days.

Considerable attention has been paid to the fact that hydrogen is a promising/potential energy vector that may function as an alternative to fossil fuels in the future. Dihydrogen is an ultimate clean burning energetic molecule and its use as an energy source for human activity, e.g. in automotive use, is constantly being developed. It is well known that hydrogen may be produced electrochemically using energy generated from solar or biofuel cells. However, current electrochemical catalysts for H_2 production suffer from inefficiency and the fact that they are based on expensive platinum catalysts. In contrast, nature has solved this problem using a class of enzymes called hydrogenases. Research on hydrogenases is driven not only by scientific curiosity but also by the interest in hydrogen production for future energy challenges.

1.3 Hydrogenase Enzymes

Hydrogenases are enzymes that catalyze the reduction of protons to form dihydrogen and/or the oxidation of hydrogen according to the reaction $H_2 \leftrightarrow 2H^+ + 2e^-$;[4,5] both the forward and backward reactions are of direct relevance to the use of hydrogen as an energy vector. Most of the hydrogenases are found in archaea, bacteria and eucarya. They were first discovered in 1931 by Stephenson and Stickland in colon bacteria.[6] Today, all hydrogenase enzymes found in a variety of bacterial and microbial organisms are estimated to both produce and utilize a total of about 200 million tons of H_2 a year.[7] There are three types of hydrogenases that differ in the metal content in their active sites (Figure 1.1): The [FeNi] hydrogenases are widely distributed in nature and relatively well studied. In their active sites, they contain a dinuclear unit where an Fe-Ni cluster is coordinated by CO and CN$^-$ ligands. The active sites of

[FeFe] hydrogenases, formerly known as iron-only hydrogenases, contain a binuclear Fe cluster that is connected with a {4Fe-4S} cubane. The dinuclear cluster is coordinated by CO and CN⁻ ligands. The [Fe]-hydrogenases, formerly known as metal-free hydrogenases, contain one Fe atom coordinated by two CO and one H_2O ligand in their active sites.[8, 9]
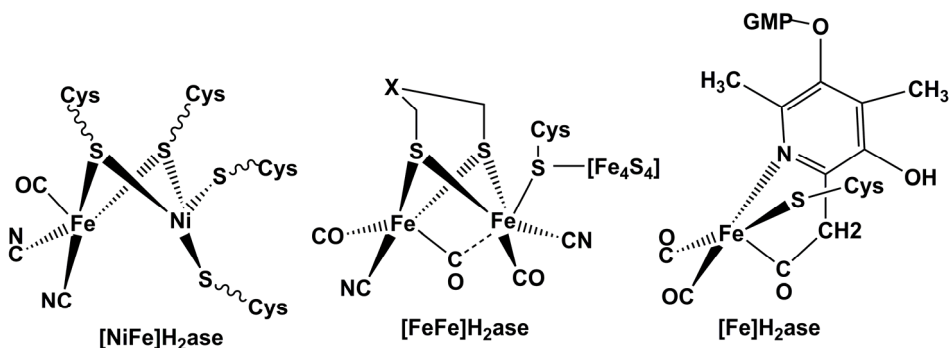
Figure 1.1 Structures of the active sites of the three types of hydrogenase enzymes.

The [FeFe] hydrogenases are more engaged in hydrogen production while [NiFe] hydrogenases catalyze preferentially the oxidation of hydrogen.[10] Furthermore, the catalytic activity of [FeFe] hydrogenases is better than that of [NiFe] hydrogenases;[11] for example, the [FeFe] hydrogenase enzyme has a turnover rate of 9000 moles of hydrogen per mole enzyme and second at 30 °C.[7,8,11,12] Considerable attention has been paid to the use of [FeFe] hydrogenase enzymes for the production of molecular hydrogen as a fuel.[11,13] For these reasons, and due to the fact that biomimetic complexes of the dinuclear active site are relatively easy to synthesize, diiron carbonyl dithiolate complexes of the general formula $[Fe_2(CO)_6(\mu\text{-SRS})]$ have been far more investigated as biomimetic model complexes for [FeFe] hydrogenases than any [NiFe] hydrogenase mimics.

1.4 The structure and catalytic mechanism of the [FeFe] hydrogenase active site

The active site structure of an [FeFe] hydrogenase enzyme was first discovered by Peters *et al.* in 1998 by determination of the crystal structure of the enzyme from the anaerobic soil micro-organism *Clostridium pasteurianum.*[14,15] The active site, known as the 'H-cluster', contains a total of 6 Fe atoms. It consists of two components: a conventional [4Fe4S] ferredoxin cubane cluster that is linked by a 12.5 Å protein backbone to a catalytic two iron [2Fe2S] unit bound by a dithiolate bridge (Figure 1.2). The latter site is called the $[2Fe]_H$ sub-cluster. The ferredoxin [4Fe4S] cluster, that is linked to the $[2Fe]_H$ sub-cluster via a bridging cysteinate side chain, provides a pathway for electron transfer to or from the [2Fe2S] sub-site cluster that is buried deep inside the protein. The electron transfer chain within the protein also contains several other, non-linked, [Fe-S] clusters.[16]
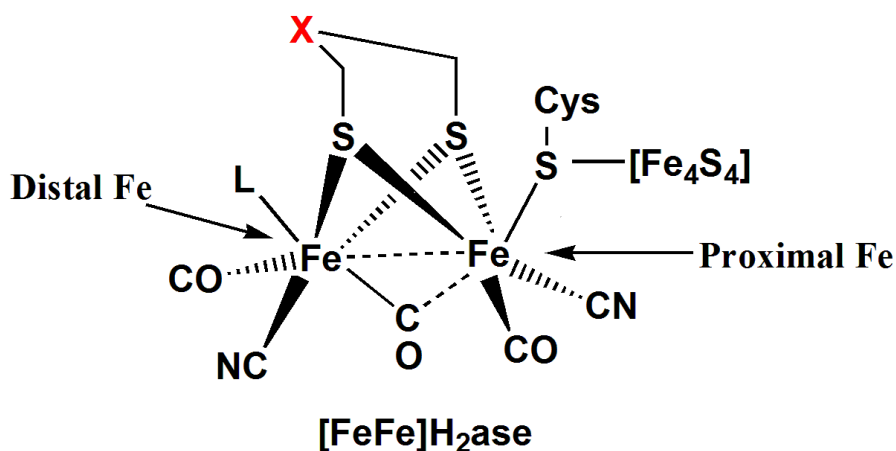
Figure 1.2 The active site of an [FeFe] hydrogenase

The $[2Fe]_H$ sub-cluster contains a bridging dithiolate ligand and is surrounded by five carbon-based diamagnetic π-acceptor ligands that stabilize the low oxidation states of the metals. These ligands have been assigned as either CO or CN^- by FTIR spectroscopy.[8,13] They also play an important role to observe the reactions at the active site because they provide strong and distinctive IR bands that are informative to electron density on the metal centers and electronic structure. The ligand coordination environment consists of two square pyramids

with their respective Fe centers antisymmetric with respect to each other.[17] The Fe atom that is linked to the [4Fe4S] cluster is called the proximal Fe while the other Fe atom is called the distal Fe. One of the carbonyl ligands is semi-bridging between the two iron centers, which leads to a vacant terminal coordination site that may be coordinated by an exchangeable ligand. This vacant site is believed to act as a proton binding site.[18] It is occupied by a water molecule in the reduced state of the enzyme, and can bind a CO molecule, which leads to catalytic inhibition.[19] The center of the [2Fe2S] sub-site cluster is bridged by a three-membered dithiolate bridge, $-SCH_2-X-CH_2S-$, where the atom X remains unidentified; numerous crystallographic measurements have not been able to unambiguously distinguish this moiety. The current proposals are that it is either a carbon (propane-1,3-dithiolate, $-SCH_2CH_2CH_2S-$ (pdt)) or a nitrogen (2-aza propane-1,3-dithiolate, SCH_2NRCH_2S) (adt)) or an oxygen (SCH_2OCH_2S).

The catalytic mechanism of the [FeFe] hydrogenase enzyme is not yet known; several viable mechanisms have been proposed. The initial crystallographic assignment modelled the bridging moiety as μ-adt.[20] On the basis of the key assumption that atom X is a nitrogen (NH), the catalytic cycle depicted in Scheme 1.1 has been proposed.[21] The first step of this proposed mechanism is a reduction followed by loss of the labile H_2O ligand, which creates a vacant coordination site where protons may bind. The second step involves protonation at the N and Fe center. The proton is transferred to the vacant coordination site and reduced to a hydride, which concurrently oxidizes the Fe centers to Fe(II)Fe(II). A second proton binds at the N, and the Fe centers are reduced again to Fe(I)Fe(II). The proton combines with the hydride to form dihydrogen, which is liberated to close the catalytic cycle. In the enzyme, this process is reversible, with the release or uptake of the hydrogen ligand being dependent upon the concentration of hydrogen at the active site.
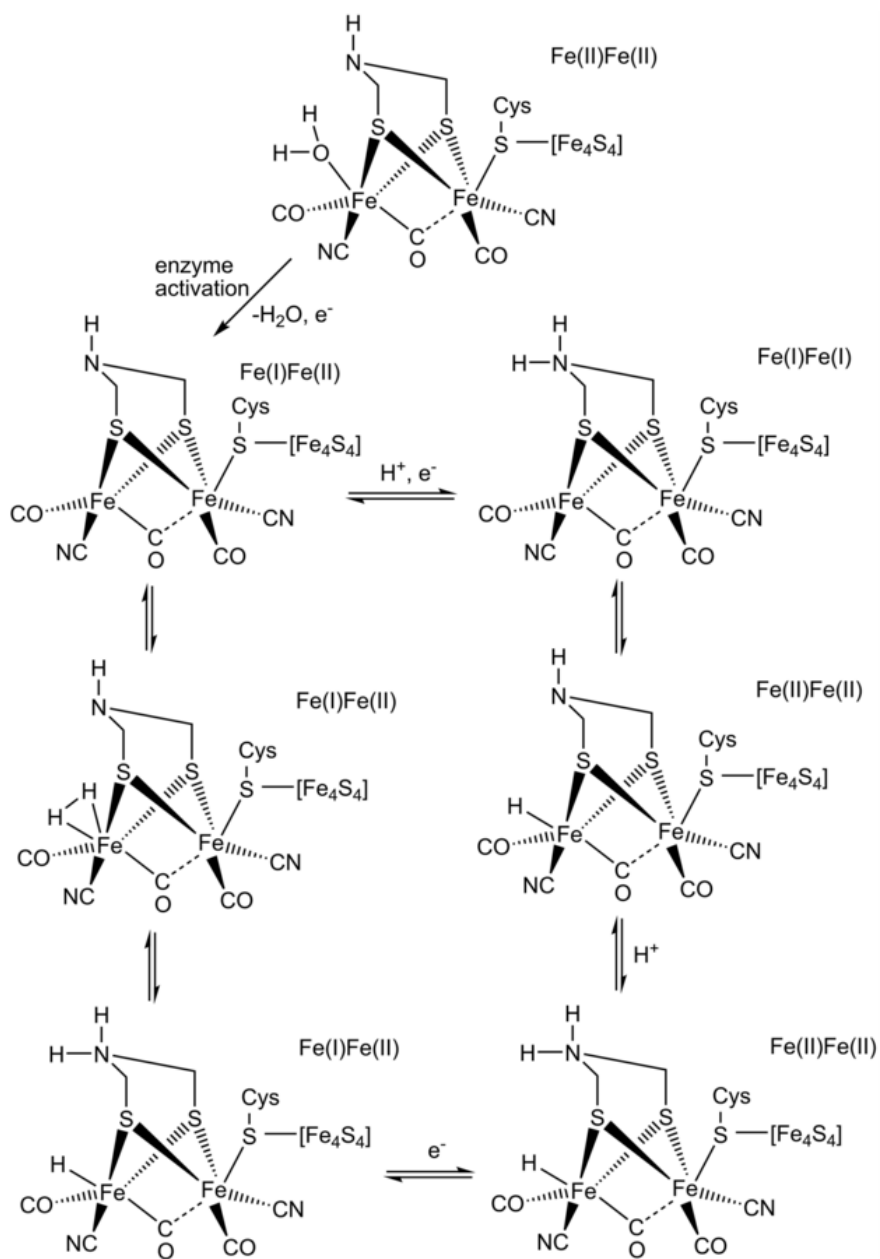
Scheme 1.1 Proposed mechanism for catalytic hydrogen production by the [FeFe] hydrogenase (adapted from ref. 21).

Gioa and coworkers have proposed a mechanism for the reduction of protons by [FeFe] hydrogenase based on DFT calculations,[18] assuming that the $[2Fe]_H$ sub-cluster is bridged by a propanedithiolate (pdt, -SCH$_2$CH$_2$CH$_2$S-) (Scheme 1.2).
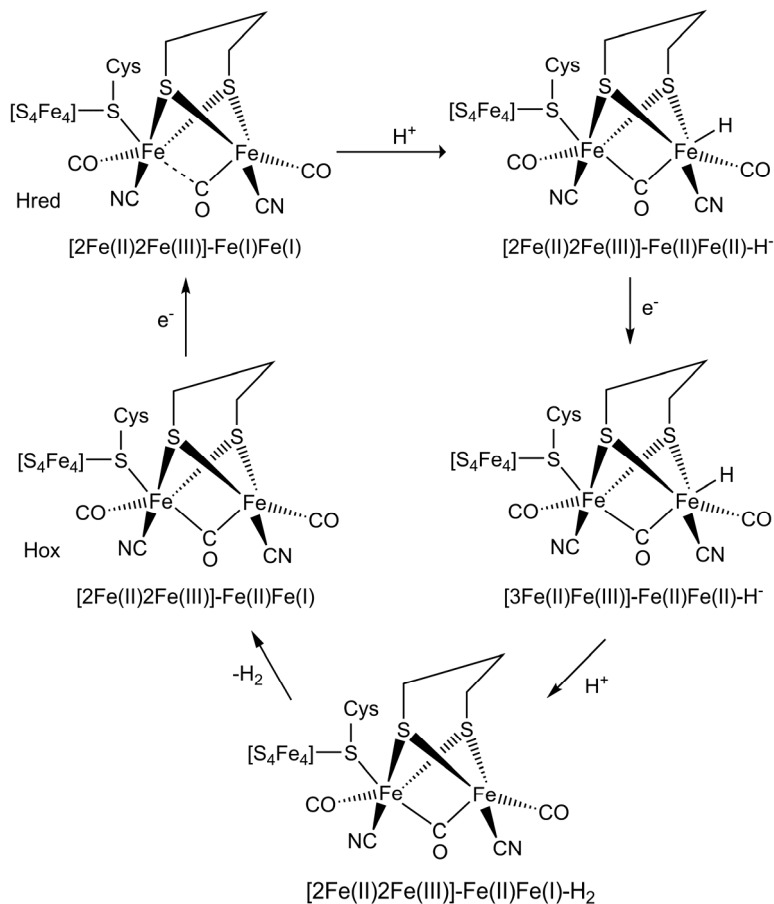
Scheme 1.2 Proposed catalytic mechanism for hydrogen production by a computational model for the [FeFe]-hydrogenase active site containing a propanedithiolate bridge. The iron oxidation states for the [4Fe4S] cluster are given in square brackets (adapted from ref. 18).

Here, the $[2Fe]_H$ sub-cluster oxidation state is [Fe(I)Fe(II)] that is reduced to the catalytically active {H$_{red}$} state that has a formal oxidation state of [Fe(I)Fe(I)]. The {H$_{red}$} complex is protonated to make a [Fe(II)Fe(II)] complex with a terminal hydride bound at the distal iron atom. This then leads to subsequent

protonation and ultimately the evolution of H_2, reforming the original $\{H_{ox}\}$ state and closing the cycle.

1.5 First mimics of the hydrogenase enzyme

After the discovery of the structure of the [FeFe] hydrogenase enzyme, many successful syntheses of mimics of the hydrogenase enzyme ensued. In 1929, Reihlen pioneered the reaction of $[Fe(CO)_5]$ with a thiol RSH to provide a diiron hexacarbonyl complex $[Fe_2(CO)_6(\mu\text{-SR})_2]$ that is a close mimic of the active site.[22] The iron(0) carbonyl precursors $[Fe_3(CO)_{12}]$ and $[Fe_2(CO)_9]$ have also been used to synthesize mimics of the hydrogenase active site. Different synthetic routes to diiron thiolate hexacarbonyl complexes and the chemistry of their precursors are summarized in Scheme 1.3. The $[2Fe]_H$ sub-cluster is similar to that of the diiron dithiolate hexacarbonyl complexes $[Fe_2(CO)_6(\mu\text{-}$ SXS)] [edt, X = $(CH_2)_2$; pdt, X = $(CH_2)_3$; bdt, X = 1,2-C_6H_4] (Figure 1.3) that can be easily prepared.[23,24] Electrochemical properties and catalytic abilities of these diiron dithiolate hexacarbonyl complexes have been extensively studied.[24, 25] Many related compounds and their derivatives have since been prepared and characterized[26,27,28] and common preparative routes to diiron carbonyl dithiolate complexes are summarized the Scheme 1.3. Several groups have reported the synthesis of the dianion $[Fe_2(CO)_4(CN)_2(\mu\text{-pdt})]^{2-}$ [20,29,30] and Rauchfuss and coworkers have reported that $[Fe_2(CO)_4(CN)_2(\mu\text{-adt})]^{2-}$ can also be easily prepared.[31] All of these clusters were found to function as catalysts for proton reduction.

[edt, X = $(CH_2)_2$; pdt, X = $(CH_2)_3$; bdt, X = 1,2-C_6H_4]
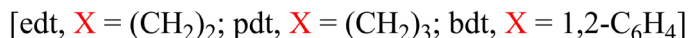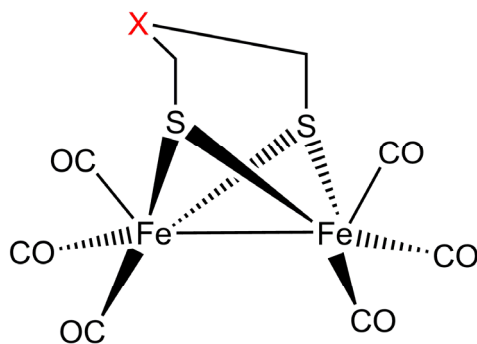
Figure 1.3 Examples of structural/functional mimics of the $[2Fe]_H$ sub-cluster of the active site of [FeFe] hydrogenase.

HS-R-SH → [Fe₂(CO)₆(μ-SRS)]

HS-R-SH $\longrightarrow$ $[Fe_2(CO)_6(\mu\text{-}SRS)]$

$[Fe_3(CO)_{12}]$

HS-R-SH

HS-R-SH $\quad$ $Na_2[Fe(CO)_4]$

Na/Hg

$[Fe_2(CO)_6(SR)_2]$ $\xleftarrow{RSH}$ $Fe(CO)_5$ $\xrightarrow{h\nu}$ $Fe_2(CO)_9$

$[Fe_2(CO)_6(\mu\text{-}SCH_2SCH_2S)]$

S_8, KOH $\Big|$ CH2=RH

$[Fe_2(CO)_6(\mu\text{-}SCH_2\text{=}RHS)_2]$ $\xleftarrow{CH2=RH}$ $[Fe_2(CO)_6(\mu\text{-}S)_2]$

$\xrightarrow[(ClCH_2)_2NR]{LiEt_3BH/}$ $[Fe_2(CO)_6(\mu\text{-}SCH_2NRCH_2S)]$

$Fe_2(CO)_9$

$(CH_2O)_n/$ RNH_2

LiEt₃BH/ (CF_3CO_2H)

$[Fe_3(CO)_9(\mu_3\text{-}S)_2]$ $(CH_2O)_n/$ RNH_2

RNH_2

$[Fe_2(CO)_6(\mu\text{-}SCROH)_2]$ $\xleftarrow{ORC\text{-}CRO}$ $[Fe_2(CO)_6(SH)_2]$

CH_2O

$[Fe_2(CO)_6(SCH_2OH)_2]$ $\xrightarrow{H_2SO_4}$ $[Fe_2(CO)_6(\mu\text{-}SCH_2OCH_2S)]$
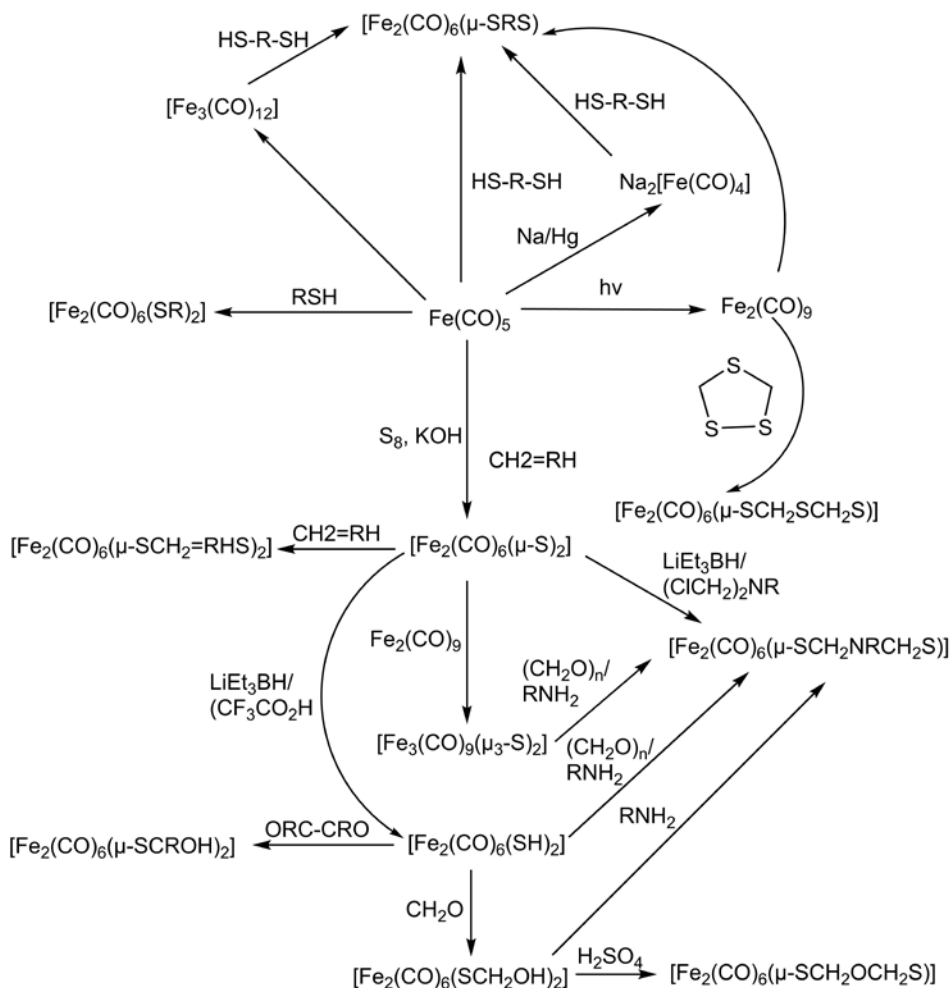
Scheme 1.3 General synthetic routes of diiron hexacarbonyl complexes which are the mimic of the hydrogenase enzyme active site (adopted from 32).

1.6 Variation of the ligand sets in hydrogenase mimics

Two general mechanisms for electrocatalytic proton reduction by dinuclear hydrogenase mimics are considered (Scheme 1.4): (a) The first option is initial protonation of the neutral complex, which could be followed by a reduction and then a protonation, finally a further reduction and liberation of molecular dihydrogen. (b) The second option is an initial reduction of the neutral complex making the Fe centres sufficiently basic to be protonated. The protonated

complex undergoes a second reduction and finally a further protonation and liberation of molecular dihydrogen.
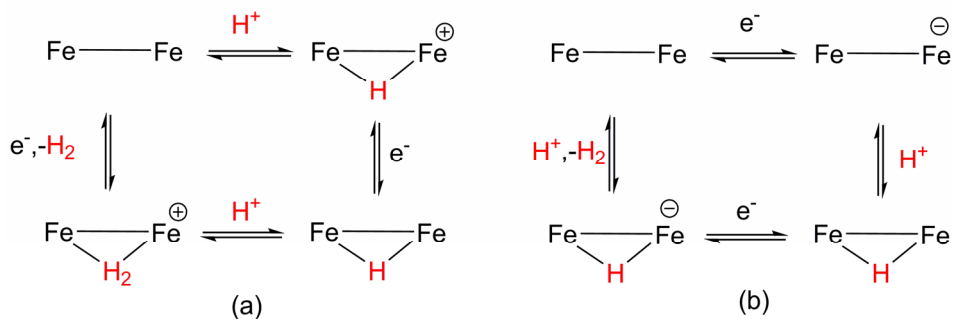
Scheme 1.4 two different general routes of catalytic mechanisms for proton reduction on diiron complexes.

The reduction potentials of the Fe centers initiating catalysis is a key property that may determine the overpotential at which catalysis will occur. These potentials are related to the electron densities on the Fe centers-less electron density means reduction will occur at less negative potentials as the metal center is relatively electrophilic, which is required for catalysis. Diiron dithiolate hexacarbonyl complexes have a more complicated set of ligands and they cannot usually be protonated at the metal centers in the neutral form. In attempts to improve the catalytic performance and increase the basicity on the metal centers, CO ligands have been exchanged with alternative ligands that are more electron-donating in order to direct electron density towards the Fe centers, and thus make them more basic. The hydrogenase enzymes contain CN^- and CO ligands that fulfil this role. Recently, many phosphine-based ligands have been used as they impart the same basicity onto the Fe centres.[33] Substitution of an electron donating ligand by a monodentate phosphine such as PPh_3 is not able to make the Fe centers of diiron dithiolate hexacarbonyl complexes sufficiently basic for protonation.[30]

However, a low potential is desirable for an energetically effective catalytic mechanism. If the substitution creates more electron density on the Fe centers, the reduction potential of the complex will as a result shift to more negative potential. For a diphosphine substituted diiron carbonyl complex the reduction of the neutral complex shifts even further to negative potential. Such negative shifts are counterproductive in the context of proton reduction. However, if the substitutions are made strategically, the complexes can now protonate.[30] When the protonation has occurred electron density is removed from the Fe centers to

form the hydride bond, and therefore the reduction potential of the protonated complex is shifted in a positive direction, which is an improved (i.e smaller) overpotential.

1.7 Synthesis of an accurate H-cluster framework in a model complex

In 2005, Pickett and coworkers reported a metallosulfur cluster involved in small molecule catalysis that is the most accurate structural model of the H-cluster to date.[34] In this model complex, $[Fe_4S_4(L)_3\{Fe_2(CH_3C(CH_2S)_3)(CO)_5\}]^{2-}$ (L=1,3,5-tris(4,6-dimethyl-3-mercaptophenyl-thio)-2,4,6-tris(*p*-tolylthio)benzene), (L = the entire iron-sulfur framework of the active site of [FeFe] hydrogenase had been assembled (Scheme 1.5).

$[Fe_4S_4(SR)_{4-n}\{Fe_2(CH_3C(CH_2S)_3(CO)_5\}_n]^{2-}$, n= 1 to 4
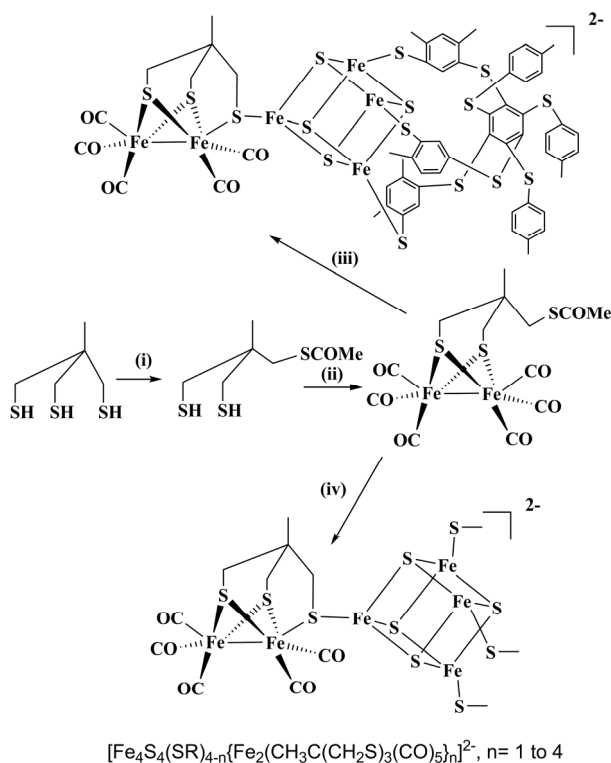
Scheme 1.5 Synthetic path to the assembly of an accurate structural model of the H-cluster of [FeFe]-hydrogenase. (adapted from ref. 34) Consider using a different font in the drawing.

The {4Fe4S} ferredoxin link in this model catalyst was found to be easier to reduce than the {2Fe3S} moiety that mimics the $[2Fe]_H$ sub-cluster, which can transfer the added electron to the latter site[35] (Scheme 1.6).
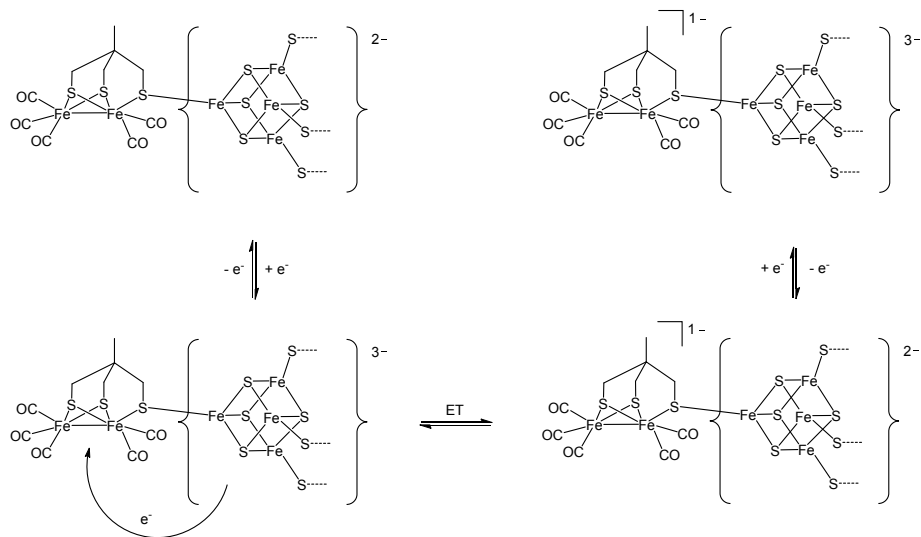
Scheme 1.6 Intramolecular electron transfer between {4Fe4S} and {2Fe3S} sites in the structural model of the H-cluster (adapted from 35).

1.8 Protonation studies

As discussed earlier, there are two options for the first step of a catalytic mechanism – it is either a protonation or a reduction process. It is thus important to know whether or not a model complex is protonated in the presence of a Brönsted acid. Infrared (IR) spectroscopy may be used to probe whether protonation occurs.

The IR frequencies that the CO bonds absorb are of importance for the research presented in this dissertation. There are two synergistic Fe-CO bonding interactions, as illustrated in Figure 1.4: i) Fe-CO σ-bonding is present between the Fe and C atoms, where the CO ligand is donating electron density to the Fe atom. ii) metal to CO π-back bonding where the Fe donates electron density through a d-orbital to the π* orbital of the CO molecule. The electron density at the metal center in coordination complexes affects the strength of the CO-bond

14

and thereby its frequency. A terminally coordinated carbonyl ligand generally absorbs at higher frequencies (1850-2125 cm^{-1}; 2143 cm^{-1} for free CO) than a bridging CO (1700-1860 cm^{-1}).
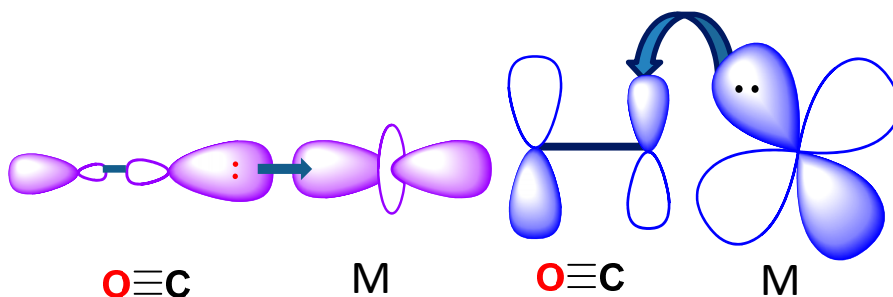
Figure 1.4 Metal-CO bonding interactions

Protonation of a model complex may occur either at a metal or at a ligand. Protonation at a metal center is important to the catalytic activity. A ligand-bound proton is not necessarily involved in the actual formation of molecular hydrogen but it has strong dominance on the reduction potentials that can be shifted up to 0.3-0.6 V.[36a] When protonation occurs at a metal center, the electron density of the complex will be decreased as the proton is reduced to a hydride, resulting in less electron density on the metal (iron) center(s). The back-bonding into the CO ligands will therefore be reduced, thus strengthening the CO bond and shifting the corresponding IR bands to higher wavenumbers. The addition of protons to the metals in iron carbonyl clusters results in IR shifts of about 50-70 cm^{-1} compared to the non-protonated parent complex.[36a,37,38] Ligand protonation at a dithiolate/azadithiolate bridge has been widely considered in the discussion of the catalytic mechanism of hydrogenases and their model complexes. If protonation occurs in a thiolate sulfur (e.g. in ethanedithiolate, edt) or a nitrogen (in azadtihiolate, adt), a shift of the absorption in the CO region of the IR spectrum about 15-20 cm^{-1} is expected.[36a] In the complexes described in this dissertation protonation is expected to occur either at the metal (Fe) centers or a dithiolate sulfur, or a bridging chalcogenide atom (if present).

1.9 Electrochemistry and electrocatalysis

In this thesis, the electrochemical behaviour of the synthesized complexes and their proton reduction abilities have been studied by cyclic voltammetry, which is the most versatile and broadly used electrochemical technique for the determination of redox reaction parameters. In cyclic voltammetry, the potential of an electrode is changed with time; the current passed through this electrode is measured simultaneously. The potential is scanned at a constant rate between two values - the initial potential (V_1) and the final potential (V_2). The rate at which the potential is scanned with time is called scan or sweep rate (Vs^{-1}). During the experiment the potential scanned from a value where the molecule under investigation is redox inactive (i.e no electrochemical reaction take place) to a value where oxidation or reduction occurs; this is followed by a reverse scan back to the initial potential value (Figure 1.5a). The resulting plot of the applied potential *vs* measured current is known as a cyclic voltammogram (Figure 1.5b) and generally contains peaks on both forward and return scans. The magnitude of a peak is called peak current and the potential at which the peak current reaches its maximum value is called the peak potential. Using the values of peak current and peak potential obtained from a cyclic voltammogram for a particular electron transfer reaction, a number of thermodynamic and kinetic parameters associated with that redox reaction can be deduced. The peak potential at maximum anodic current is often denoted E_{pa} and maximum cathodic current is denoted E_{pc}. The formal potential (E°) of a redox couple is determined by averaging the anodic current and cathodic current.
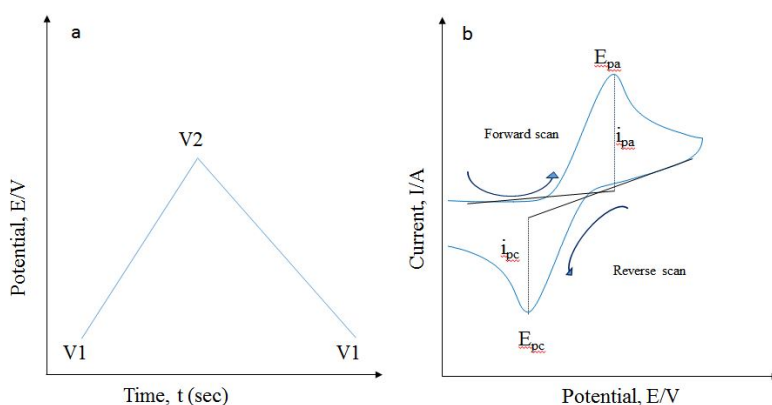
Figure 1.5 Representation of cyclic voltammetry technique

$$E^0 = \frac{E_{pa} + E_{pc}}{2} \tag{1}$$

The figure of the peak on a cyclic voltammogram depends on the chemical and electrochemical reversibility of the redox process. For a chemically reversible system, the peak currents for the forward and reverse scans are equal, which means that the electrogenerated species is stable during the experimental timescale. The electrochemical reversibility depends on the rate of the heterogeneous electron-transfer reaction under the experimental duration, and the difference of peak potential (ΔE_p) is used to determine the electrochemical reversibility. Electrochemical reversibility is observed when the rate of the heterogeneous electron-transfer is very large and for an electrochemicaly reversible one-electron transfer process, ΔE_p does not change with the scan rate and the peaks for the forward and reverse scans are always separated by ~59 mV (298 K) at all scan rates for a one-electron process (Equation 2, n=1).

$$\Delta E_p = E_{pa} - E_{pc} = \frac{59}{n} \, mV[\text{at } 298 \text{ K}] \tag{2}$$

The ratio of the anodic peak current (i_{pa}) and the cathodic peak current (i_{pc}) for an electrochemical reversible one-electron transfer reaction is always equal to 1.

$$\frac{i_{pa}}{i_{pc}} = 1 \tag{3}$$

For a quasi-reversible and an irreversible electron transfer process, ΔE_p changes with increased scan rate. Irreversible couples have a larger peak separation ΔE_p, as a bigger overpotential is required to drive the electron transfer. The size of the backward peak is smaller relative to the forward peak and depends on the voltage scan rate, as does the potential of the peaks E_P. The peak separation and dependence on the scan rate are therefore diagnostic of the nature of the electrode kinetics. "Reversible" and "irreversible" electrode kinetics refer to limiting cases of reaction but often electrode kinetics are intermediate in nature, and these are termed "quasi-reversible". Quasi-reversible reactions have a forward and backward peak current ratio of close to unity, like reversible reactions, but the peak separation is dependent on scan rate. The shape of the current peak of a cyclic voltammogram for an electrochemically and chemically irreversible process does not show a current peak on the backward scan. It means that the electrogenerated species is not stable or decomposes completely, or is consumed rapidly in a subsequent process that is a redox-initiated chemical reaction.

In the case of diffusion-controlled reversible and irreversible processes, the peak current response depends not only on the analyte concentration and diffusion coefficient but also on scan rate as related on the Randles-Sevcik equation (4).

$$ip = 0.4463 \, nFAC \, (nFvD/RT)^{1/2} \tag{4}$$

When the solution is at 25 °C, this equation can be expressed as follows

$$ip = (2.69 \times 10^5) \, n^{3/2} \, AD^{1/2} \, C^{1/2} \, v^{1/2} \tag{5}$$

Where; n = number of electrons transferred
A = area of the the electrode (cm^2)
D = diffusion constant (cm^{2}s^{-1})
v = scan rate (Vs^{-1})
C = bulk concentration of the electroactive species (mol, cm^{-3})

According to the Randles-Sevcik equation, the peak current increases linearly as a function of the square root of the scan rate of a reversible system (eqn 6), a plot of i_p and $v^{1/2}$ should therefore be linear and pass through origin and the diffusion coefficient (D) may then be calculated from the slope.

$$ip \, \alpha \, \sqrt{v} \tag{6}$$

1.10 Electrochemical setup; electrocatalysis measurements

A glass cell has been used for all electrochemical experiments in this thesis (Fig 1.6). A lid of the glass cell with four tightly-fitting holes was used to prevent oxygen entering the cell during the experiment. Typically, a three-electrode set up has been used for the cyclic voltammetry measurements. The electrodes are known as the working electrode (WE), where the reaction of interest occurs, the reference electrode (RE), which provides a stable potential to measure against, and a counter or auxiliary electrode (CE) to complete the circuit. The fourth hole of the lid has been used for a narrow tube for nitrogen gas to de-oxygenate the cell. During the experiment, the RE is placed as close to the WE as possible to minimize the voltage drop in solution and the current is only allowed to flow around the circuit between WE and CE to preserve the chemical composition of the RE throughout the measurement. The mass transport of the substances

during the investigation is allowed to occur only by diffusion which means that the redox reaction at the electrode only affects the molecules within the diffusion layer of the electrode. As a result only irreversible peaks are observed during electrochemical proton reduction, since the H_2 molecules formed during catalysis leave the system.
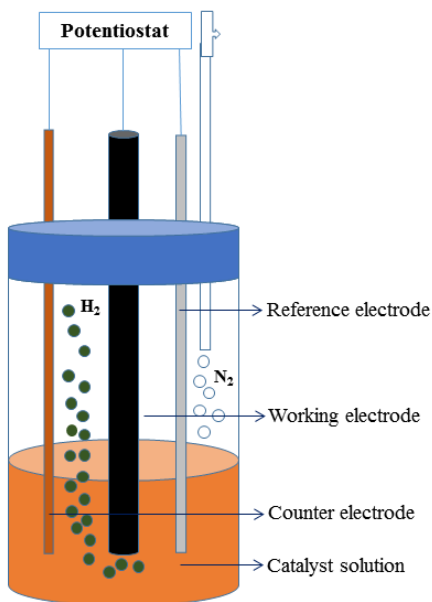
Figure 1.6 Schematic depiction a cyclic voltammetry cell used in the electrochemical experiments described in this thesis.

The height of the catalytic peak increases with the concentration of acid and the voltammograms obtained by varying the concentration of acid also provide qualitative information about catalytic efficiency. The simple ratio of the catalyst current and the current for the reduction of the catalyst in the absence of acid gives a qualitative description of the catalytic efficiency.[32] According to this method, the catalytic efficiency (C.E.) is given by the following equation:

$$C.E. = \frac{\frac{i_{cat}}{i_d}}{\frac{C_{HA}}{C_{cat}}} \tag{7}$$

Where i_{cat} = catalytic current, i_d = current for the reduction of the catalyst in absence of acid, C_{HA} = concentration of acid, C_{cat} = concentration of catalyst.

1.11 Aims and outline of this thesis

My research has focused on the preparation of functional models for hydrogenases that may be good electrocatalysts for proton reduction. The model complexes consist of di and triiron dithiolato, diphosphido-bridged, phosphinidine-capped and chalcogenide-capped clusters. Mono and bidentate phosphines have been coordinated to the different parent cluster frameworks in order to perturb both the steric and electronic nature of the diiron and triiron cores and the investigate the influence of such ligand substitution on protonation mechanisms and catalytic activities of the model complexes. A summary of the work reported in the enclosed papers and manuscripts is as follows.

Paper **I** reports the synthesis and characterization of the mixed-valence dithiolate-bridged triiron complexes $[Fe_3(CO)_7(\mu\text{-edt})_2]$ (edt = SCH_2CH_2S), the monodentate phosphine derivatives $[Fe_3(CO)_{7-x}(PPh_3)_x(\mu\text{-edt})_2]$ (x = 0, 1, 2), and the bidentate phosphine derivatives $[Fe_3(CO)_5(\kappa^2\text{-diphosphine})(\mu\text{-edt})_2]$. The protonation have been studied for all of the complexes. The electrochemical and electrocatalytic properties (for proton reduction) have been investigated for all complexes.

Paper **II-IV** describe the synthesis and characterization of chalcogenide-capped triiron clusters $[Fe_3(CO)_9(\mu_3\text{-E})_2]$ (E = S, Se, Te) and various diphosphine derivatives thereof. The electrochemical and electrocatalytic properties has been investigated in the presence and absence of acid for all the complexes

Papers **V** describes the influence of the substitution, orientation and structure of the diiron phosphido bridges in different isomers of $[Fe_2(CO)_6(\mu\text{-PR}_2)_2]$ electrocatalysts of proton reduction has been studied.

Paper **VI** describe the synthesis and characterization of bis(phosphinidene)-capped triiron carbonyl clusters, including electron rich derivatives formed by substitution with chelating diphosphines, and an investigation of their properties as proton reduction catalysts.

Chapter 2. Transition metal clusters and common ligands

2.1 Introduction

Metal complexes constitute one of the most important groups of chemical compounds in coordination chemistry. Although complex compounds date back to the 18th century, during the 20th and this century thousands of metal complexes have been obtained, characterized and widely applied.

Metal clusters are a class of metal complexes having two or more metal atoms in which there are substantial and direct bonds between the metal atoms.[39,40,41,42] Much of the progress in transition metal cluster chemistry has been made since the mid-1960s. Many of the advances could not have been made without the development of spectroscopic methods and more effective means of structure determination. Transition metal clusters have played an important role in the development of many fields of research with applications in the areas of catalysis, materials science and biological activities.[43,44,45] As discrete molecules, they can react with substrates in homogeneous phases. They can be isolated and characterized like mononuclear complexes using various spectroscopic and crystallographic techniques, and they show phenomena related to polynuclear metal surfaces such as multimetal ligand binding and delocalized metal-metal bonds.
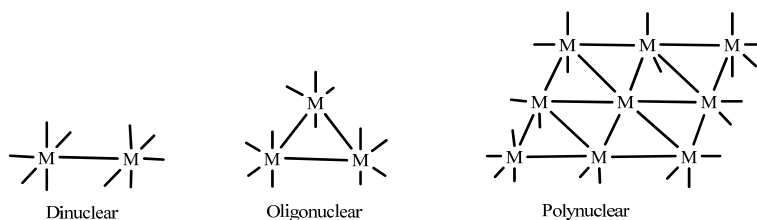
Figure 2.1 Schematic representation of transition metal cluster framework

2.2 Transition metal clusters

Depending on the presence and nature of the ligands that the cluster contains, transition metal cluster may be classified into three different classes as follows.

(a) Naked clusters: These clusters are generated by reduction of metals or semimetals and alkali metals and they do not contain any ligand. These clusters are called Zintl clusters/Zintl anions. Examples of naked clusters are Ag_6, $[Bi_3]^3$, $[Sn_5]^{2-}$.

(b) High-valence clusters: These clusters contain good π-donors such as halides,e.g. $[Mo_6Cl_8]^{4+}$. Metal oxidation states in this type of cluster are commonly +2 and +3 and even higher.

(c) Low-valence clusters: These clusters contain good π-acceptor ligands such as carbon monoxide, phosphines, olefins, cyclopentadienes, etc. Examples include $[Fe_3(CO)_{12}]$, $[Ru_3(CO)_{12}]$ etc. Metal oxidation states in this type of cluster are usually zero or negative.

2.3 Transition metal carbonyl clusters

As mentioned previously (section 1.7), carbon monoxide is a common ligand in transition metal chemistry, in part due to the synergistic nature of its bonding to d-block transition metals. Metal carbonyl clusters are the most widely studied kind of low valent clusters, and have found applications in many areas of research, especially catalysis. As this thesis is concerned with iron carbonyl clusters, the various known ways by which a CO ligand may coordinate to one or more metal atoms of clusters will be describe in detail below. The known coordination modes are as follows:[46]

(i) Terminal attachment to one metal atom by a linear or nearly linear M-C-O unit (Figure 2.2a).

(ii) Bridging (μ) between two metal atoms, coordinating exclusively through the carbon atom (i.e. monohapto, μ-η^1:η^1) the C-O axis being perpendicular to the M-M axis, or nearly so. This three centered two-electron edge bridge can usually be found in association with a metal-metal bond and may be symmetric or asymmetric (Figure 2.2b).

(iii) Doubly bridging in such unsymmetrical ways as to imply dihapto coordination to one of the metal atoms, with M→CO bonding (Figure 2.2c).

(iv) Triply bridging (μ_3-) between three metal atoms, found in association with an M_3 triangular face and may show varying degrees of asymmetry (Figure 2.2d).

(v) The unsymmetrical bonding modes shown in Figure 2.2(e-g) seldom occur in binary metal carbonyls, but they have been identified in metal carbonyl anions or in substituted derivatives.[47] In these coordination modes, there is π-interaction including the C-O bonding orbitals and one or more metals.

(a)   (b)   (c)   (d)

(e)   (f)   (g)
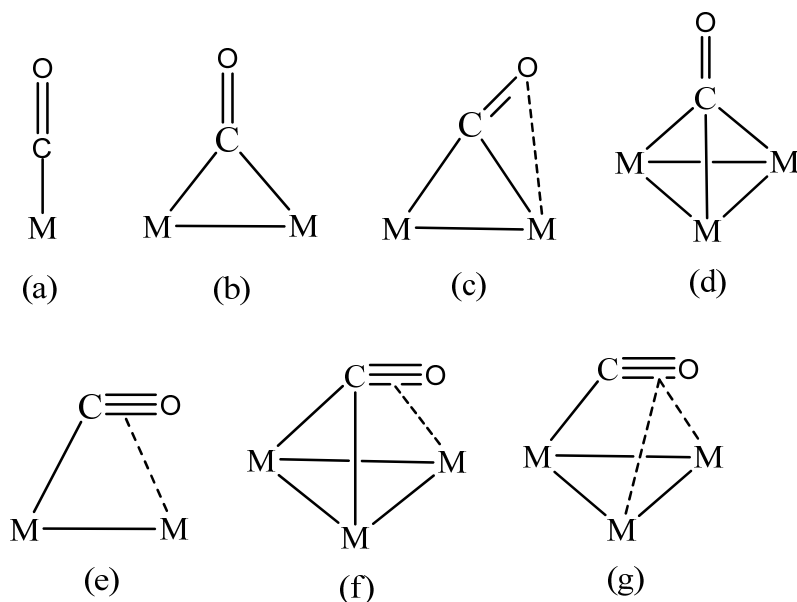
Figure 2.2 Various coordination modes of carbonyl ligand

2.4 Binary iron carbonyl clusters

Much of the interest in the study of carbonyl compounds lies in the importance of iron in homogeneous and heterogeneous catalysis. A wide variety of reduction reactions are promoted by iron carbonyl species.[48] In particular, carbonylation reactions such as the water-gas shift reaction[49] and hydroformylation[50] are promoted by iron carbonyl species. As this thesis is directly concerned with the catalytic application of iron carbonyl clusters in

electrochemical proton reduction, the two most common binary carbonyl clusters, which may be considered parent compounds for di- and trinuclear carbonyl clusters, are briefly described below.

(a) $[Fe_2(CO)_9]$

Di-iron ennacarbonyl, $[Fe_2(CO)_9]$ has been obtained by irradiating iron pentacarbonyl in glacial acetic acid solvent.[51]

$$2Fe(CO)_5 \xrightarrow{\text{UV}} Fe_2(CO)_9 + CO$$

The major use of $[Fe_2(CO)_9]$ (Figure 2.3) is as a source of reactive $Fe(CO)_4$ fragments.
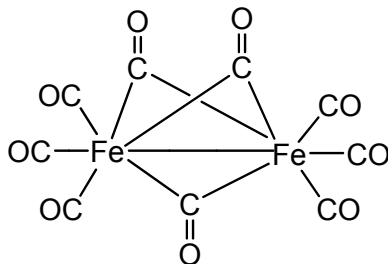
Figure 2.3 Schematic depiction of the molecular structure of $[Fe_2(CO)_9]$

(b) $[Fe_3(CO)_{12}]$

Considerable attention has been focused on the structure and dynamics of $[Fe_3(CO)_{12}]$. This interest arises from

(i)   The crystallographic disorder associated with the solid-state (see fluxionality, below)
(ii)   The presence of more than one isomer in solution, one directly related to the solid state structure (Figure 2.4), and one with all terminal ligands.
(iii)   The observed fluxionality of the compound, where CO ligands are intermittently bridging (μ-η^1:η^1, see above) and terminal, even in the solid state.

24

Solid-state variable-temperature NMR spectra at -93 °C are consistent with the solid-state structure (Figure 2.4).[52]
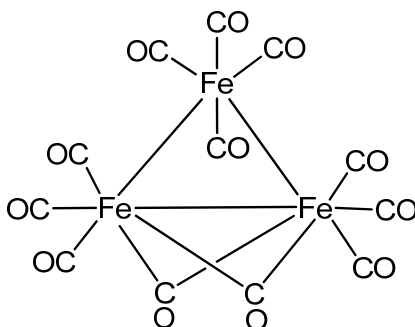
Figure 2.4 Schematic depiction of the molecular structure of [$Fe_3(CO)_{12}$]

2.5 Iron-sulfur clusters

Iron-sulfur clusters are important chemical species, forming a large class in metal cluster chemistry. A very large number of iron-sulfur clusters have been synthesized and structurally characterized and their properties have been investigated. Particularly, the iron-sulfur cubane clusters have attracted the attention of a wide range of scientists because the Fe_4S_4 core is found in biological systems as the active site of several non-heme iron proteins such as high potential iron proteins and ferredoxins. Many iron-sulfur cubane clusters have been synthesized as model compounds and their electron-transfer ability has been investigated under various conditions.[53] Most of these clusters have thiolates as supporting ligands and therefore can be classified as inorganic clusters. There is another large class of iron-sulfur clusters in which the cluster core is surrounded by soft organic ligands *via* iron-carbon bonds and can be classified as organometallic clusters. Early and typical examples are the cyclopentadienyl cluster [$Cp_4Fe_4S_4$][54] and the carbonyl cluster [$Fe_3(CO)_9S_2$],[55] the catalytic properties of which is investigated in this thesis. The oxidation addition of the E-E linkage of [(μ-E_2)$Fe_2(CO)_6$] (E = S, Se, Te) to various low valent, transition metal species have yielded many mixed-metal complexes bridged by chalcogen atoms, and the triiron carbonyl clusters that are discussed in Paper VI are dkrectly related to such clusters.

2.6 Phosphines as ligands in transition metal clusters

Phosphine ligands play a major role in the synthesis of many stable metal clusters. Furthermore, as already discussed in Chapter 1, phosphine ligands can be used to control the electronic and steric properties of transition metal cluster by varying the organic substituents of the phosphines.[56] Many types of phosphines have been used in metal cluster chemistry. In this thesis, mono- and didentate phosphines have been used to modify the basicities of iron carbonyl clusters.

Monodentate phosphines includ such common ligands as triphenylphosphine, tricyclohexylphosphine, tri(tertbutyl)phosphine and trimethyl phosphine. These type of phosphine contains only one phosphorus atom that coordinates to a metal center of the cluster unit. Chiral monodentate phosphines are of considerable interest as they have been found to be very effective ligands for metal complexes used in asymmetric homogenous catalysis.[57] Monodentate phosphines tend to occupy sites remote from one another when more than one substituent is present in cluster.

Didentate phosphines contain two phosphorus atoms that may be coordinated to the metal atoms of the cluster unit, e.g. bis(diphenylphosphino)methane (dppm) and 1,2-bis(diphenylphosphino)ethane (dppe) (Fig. 2.5), which are used in the research described in this thesis. Diphosphine ligands can be used to form intra-molecular bridging or chelating coordination modes, and they can also support the binding of two or more cluster fragments via intermolecular bridging coordination modes. Ligands such as dppe, dppp and dppf (Fig. 2.5) are flexible enough to adopt different modes of attachment to a cluster, e.g. chelating to a single metal center, bridging a metal-metal edge, or linking two metal units together. On the other hand bis(diphenylphosphino) ethene (dppv) is ideally suited to chelation at a single metal center where it can form a planar five-membered chelate ring. The carbon backbone of the dppm ligand is too short for a chelating mode to be favourable, but its geometry is ideal to permit the dppm ligand to bridge between adjacent metal centers.

Bis(diphenylphosphino) methane (dppm)

Bis(dicyclohexylphosphino)methane (dcpm)

Bis(diphenylphosphino) ethane (dppe)

Bis(dimethylphosphino) methane (dmpm)

Bis(diphenylphosphino) ethene (dppe)

Bis(diphenylphosphino) propane (dppp)

1,1'-Bis(diphenylphosphino) ferrocene (dppf)

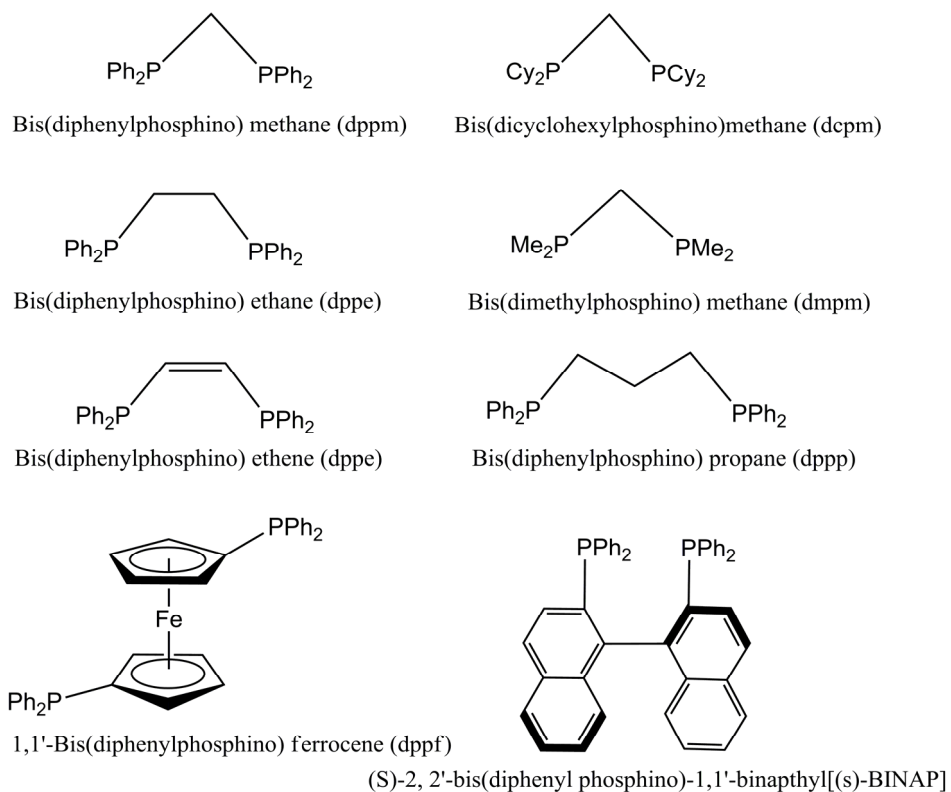(S)-2, 2'-bis(diphenyl phosphino)-1,1'-binapthyl[(s)-BINAP]

Figure 2.5 Samples of different types of didentate phosphine ligands

Chapter 3. Linear triiron bis-dithiolate complexes as proton reduction catalysts (Paper I)

3.1 Background

As described in Chapter 1, most of the research on hydrogenase biomimics has been focused on the chemistry of dithiolate-bridged diiron complexes,[58,59,60] as they closely resemble the $[2Fe]_H$ sub-cluster of [FeFe] hydrogenases.[61,62,63,64] While good structural models have been prepared (*cf.* chapter 1) the discovery of such models that are also good functional models (*i.e.* electrocatalysts with low overpotential, high turnover number and turnover frequency) remains to be achieved.

Much less studies related to proton reduction catalysis have been made on iron carbonyl clusters of higher nuclearities (*i.e.* ≥ 3). However, such clusters do possess the properties that are required for effective proton reduction catalysis, *i.e.* the ability to loosely coordinate labile ligands that can mask a vacant coordination site, the ability to coordinate dihydrogen, and the ability to coordinate protons at their metal centers and, in the course of doing so, reduce the protons to hydrides. Therefore, increased attention has been paid in the recent decade to the potential of higher nuclearity iron carbonyl clusters to act as functional hydrogenase models. Rauchfuss and coworkers have synthesized a number of triiron complex $[Fe_3(pdt)_3(CO)_4(PR_3)]$ (R = Et, Bu, Ph) upon reduction of $FeCl_2$ by zinc or phosphines in the presence of $Na_2(pdt)_3$.[65] In earlier work, Rudolph and Weigand have prepared interesting trinuclear complexes from the reaction of $[Fe_2(CO)_9]$ with 1,2,4-trithiolane (a sulfur heterocycles containing disulfide linkage , SCH_2SCH_2S), 1,2,5-trithiepane (a sulfur heterocycles containing disulfide linkage, $S(CH_2)_2S(CH_2)_2S$) and 1,2,6-trithionane (a sulfur heterocycles containing disulfide linkage, $S(CH_2)_3S(CH_2)_2S$) gave $[Fe_3(CO)_9S_2]$, $[Fe_3(CO)_9(\mu\text{-BTES})]$ and $[Fe_3(CO)_8(S(CH_2)_2S(CH_2)_2S]$, respectively, BTES = bis(thiolato)ethylene sulfide,[66] but electrochemistry has not been done yet on these.

Pickett and coworkers have prepared the stable tetrairon cluster $[Fe_4(CO)_8\{\mu_3\text{-}(SCH_2)_3CMe\}_2]$, which may be viewed as comprising two fused {2Fe3S} sub-units in "butterfly" configuration that are linked via two bridging thiolates (Scheme 3.1).[67]

It has been suggested that this is formally a mixed-valence complex comprising a chain of Fe(I)-Fe(II)-Fe(II)-Fe(I) ions, where the two central iron ions, which are coordinated by four thiolates, are in the Fe(II) oxidation state, while the peripheral irons, which are coordinated by three carbonyl ligands, are in the Fe(I) oxidation state.[68] This cluster undergoes two successive one-electron reduction steps at -0.71 and -1.07 V (*vs* Ag/AgCl), and it is capable of catalysing proton reduction at the all-Fe(I) level, *i.e.* at the second reduction. The difference between the two steps (primary and secondary reduction ca. 310 mV) suggests moderately strong electronic communication. This is attributed to a cleavage of the central iron-iron bond (Scheme 3.1).
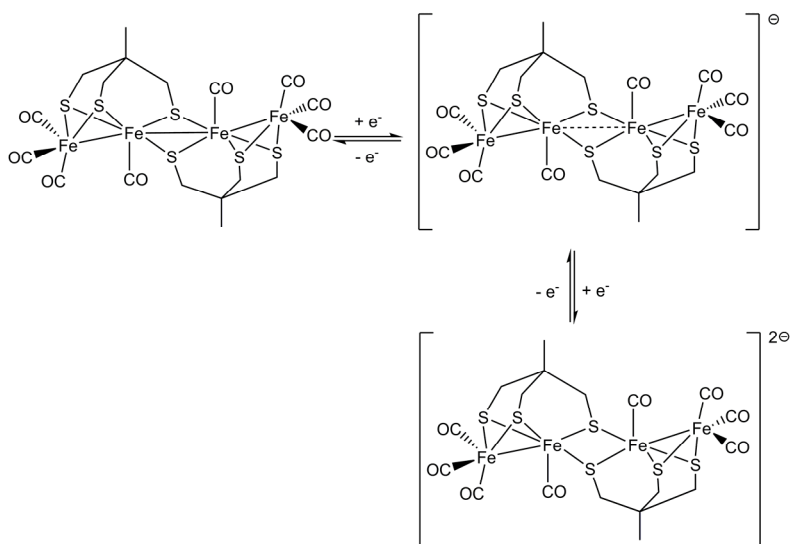
Scheme 3.1 The cluster $[Fe_4(CO)_8\{\mu_3\text{-}(SCH_2)_3CMe\}_2]$ and its corresponding anions, which may be generated electrochemically.

In 1982, Huttner reported the preparation of $[Fe_3(CO)_7(\mu\text{-}S(CH_2)_nS]_2$ (n = 2(edt), 3(pdt)) as side products formed in low yields during the preparation of $[Fe_2(CO)_6(\mu\text{-}S(CH_2)_nS]$ (n = 2,3).[69] The analogous triruthenium clusters were prepared in 1996.[70]

Åkermark and coworkers reported the synthesis of the cluster $[Fe_3S_2(CO)_5(dppv)_2]$ (Figure 3.1a)[71] as a proton reduction catalyst from the reaction of $[Fe_2(CO)_6(\mu\text{-}SCH_2NRCH_2S)]$ (adt = SCH_2NRCH_2S) with dppv in the presence of Me_3NO (see

chapter 4). Recently Schollhammer and coworkers reported the triiron complex $[Fe_3(CO)_4(\kappa^2-P^{Ph}_2N^{Ph}_2))(\mu-CO)(\mu-pdt)_2]$ (Figure 3.1b) as well as the tetrairon complex $[Fe_4(CO)_6(pdt)_4]$ and studied the proton reduction catalysis of $[Fe_3(CO)_4(\kappa^2-dppe)(\mu-CO)(\mu-pdt)_2]^{72}$ (Figure 3.1c). These complexes were prepared from the reaction of the diiron complex $[Fe_2(CO)_6(\mu-pdt)_2]$ with the respective ligand. The electrochemical properties of $[Fe_3(CO)_4(\kappa^2-dppe)(\mu-CO)(\mu-pdt)_2]$ has been investigated. This complex undergoes quasi-reversible reduction and oxidation steps at -1.98 V and -0.21 V, respectively. A catalytic reduction of the complex is revealed around -2 V (*vs*, Fc^+/Fc, in CH_2Cl_2), which initiated by the one-electron reduction of the complex. Hogarth and coworkers have reported the tetrairon carbonyl complex $[Fe_4(CO)_{10}(\kappa^2-dppn)(\mu_4-O)]^{2-}$ (Figure 3.1d) and its ability to act as a catslyst for proton reduction.[73] The electrochemical behaviour reveals a reversible reduction at -1.02 V, followed by a second irreversible reduction at -1.59 V (*vs* Fc^+/Fc in CH_2Cl_2). In the presence of the relatively strong acid CF_3CO_2H a new catalytic wave appeared at -2.0 V with well-resolved current. Chiang and coworkers have prepared the higher nuclearity mixed-valent iron carbonyl complexes $[Fe_4(CO)_8(\mu,\mu,\kappa_2-bdt)_2(\mu-PPh_2)_2]$ and $[Fe_8(CO)_{18}(\mu,\mu,\kappa_2-bdt)_4(\mu-PPh_2)_4]$ and investigated the electrochemical properties of these complexes.[74] The complex $[Fe_4(CO)_8(\mu,\mu,\kappa_2-bdt)_2(\mu-PPh_2)_2]$ shows a quasi-reversible one-electron reduction at -1.05 V and an irreversible one-electron oxidation at +0.42 V; the complex $[Fe_8(CO)_{18}(\mu,\mu,\kappa_2-bdt)_4(\mu-PPh_2)_4]$ shows two single-electron reductions at -1.27 V and -1.73 V and one single-electron oxidation at +0.28 V (*vs* Fc^+/Fc, in CH_2Cl_2). Delgado and coworkers prepared $[Fe_3(CO)_7(\mu_3-SC_6H_2Cl_2S)_2]$ from the reaction of $[Fe_3(CO)_{12}]$ with $HSC_6H_2Cl_2SH$ (3, 6-dichloro-bdt) and examined proton reduction catalysis effected by this comound.[75] This complex shows a reduction potential at -0.69 V and oxidation potential at +1.11 V (*vs* SCE). In the presence of acid $HBF_4 \cdot OEt_2$ the reduction potential wave considerably increased and continued to grow in intensity with sequential addition of acid.
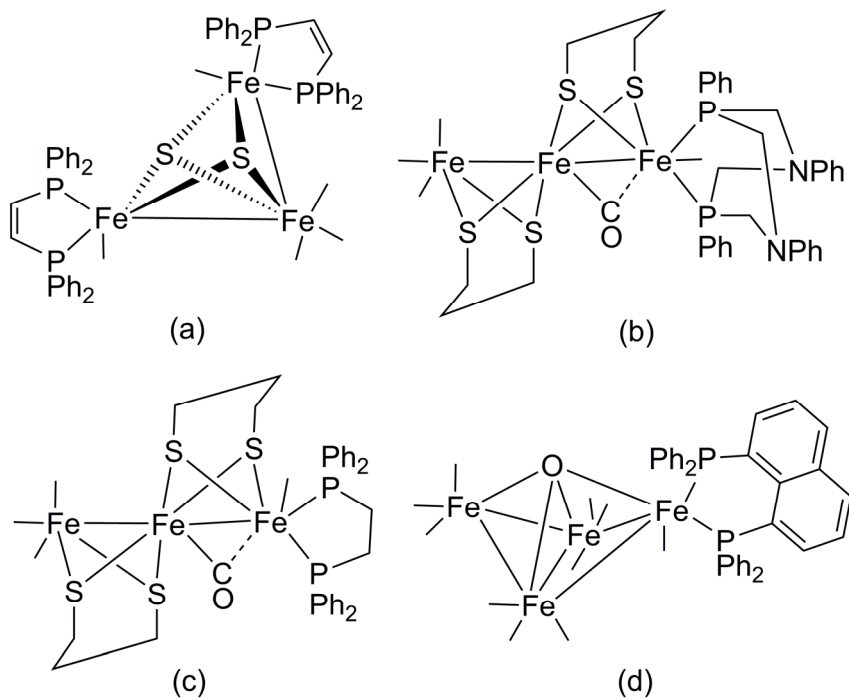
Figure 3.1 Higher nuclearity mixed-valent iron carbonyl complexes.

I have found a high yielding route to the synthesis of $[Fe_3(CO)_7(\mu\text{-}S(CH_2)_nS)]_2$ (n = 2,3)[76] (see below). This has permitted the preparation of these clusters in relatively large quantities, the synthesis of a number of phosphine derivatives of the parent clusters, and a relatively extensive study of the electrochemistry and the electrocatalytic efficiencies (for proton reduction) of these clusters. This chemistry is described in Paper I and will be discussed below.

3.2 Synthesis [Fe₃(CO)₇(μ-edt)₂]

The parent cluster $[Fe_3(CO)_7(\mu\text{-}edt)_2]$ (**3.1**) was synthesized by the reaction of Collman's reagent, $Na_2[Fe(CO)_4]$, with 1,2-ethanedithiol at room temperature in thf over 24 h, in higher yields than the previously reported methods.[69] Compound **3.1** and its propanedithiolate analogue $[Fe_3(CO)_7(\mu\text{-}pdt)_2]$ have been characterized by standard spectroscopic methods and single crystal X- ray diffraction studies (Figure 3.2), and characterising data are in accord with those reported earlier.[69]

(a)   (b)
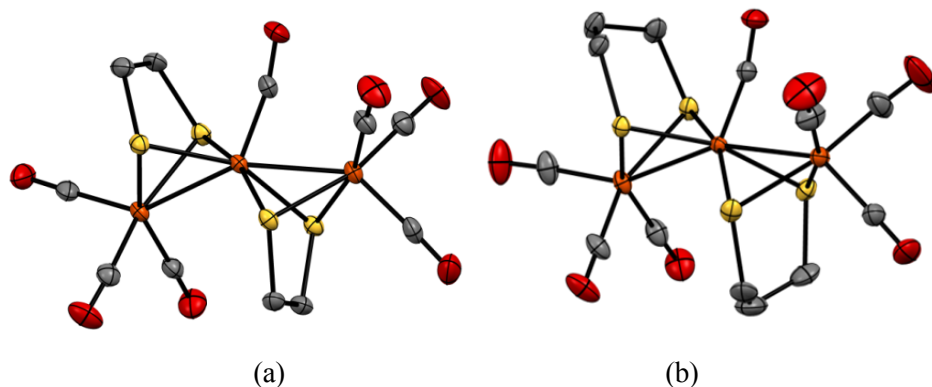
Figure 3.2 The molecular structures of (a) $[Fe_3(CO)_7(\mu\text{-edt})_2]$ (**3.1**) and (b) $[Fe_3(CO)_7(\mu\text{-pdt})_2]$.

3.3 Reactivity of $[Fe_3(CO)_7(\mu\text{-edt})_2]$ towards mono- and diphosphines

In order to increase the electron-density on the metal centers and thus render the clusters more susceptible to protonation, a number of phosphine and diphosphine derivatives of **3.1** were prepared. The reaction of **3.1** with one equivalent of PPh_3 gave the mono- and disubstituted triiron compounds $[Fe_3(CO)_6(\mu\text{-edt})_2(PPh_3)]$ (**3.2**) and $[Fe_3(CO)_5(\mu\text{-edt})_2(PPh_3)_2]$ (**3.3**), respectively, together with the known mono-substituted diiron compound $[Fe_2(CO)_5(\mu\text{-edt})(PPh_3)]$ (**3.4**), which results from cleavage of one metal-metal bond and formation of $Ph_3P{=}S$ (**3.5**) (Scheme 3.2). Complexes **3.2** and **3.3** have been characterized by a combination of spectroscopic data and single crystal X-ray diffraction studies.
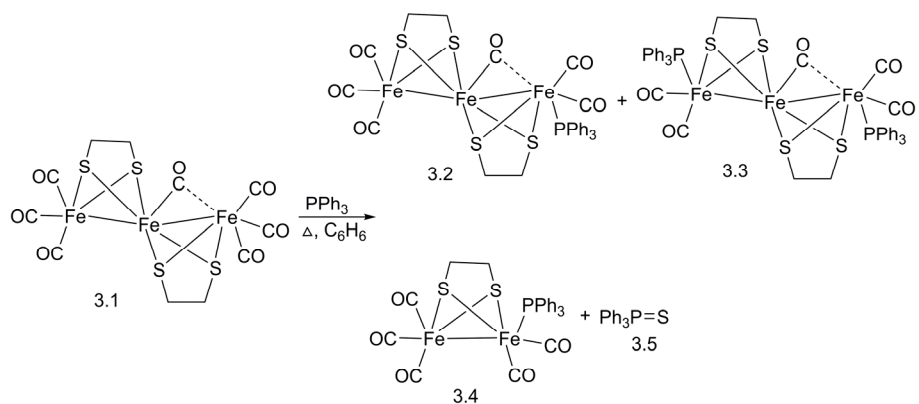
Scheme 3.2 New synthetic routes of complexes **3.2** and **3.3**

The $^{31}P\{^1H\}$ NMR spectrum of **3.2** shows two singlets in an approximate 3:1 ratio, which is attributed to the co-existence of two isomers. For **3.3**, three singlets are observed, which is attributed to two isomers; with one resonance attributed to overlapping singlets.
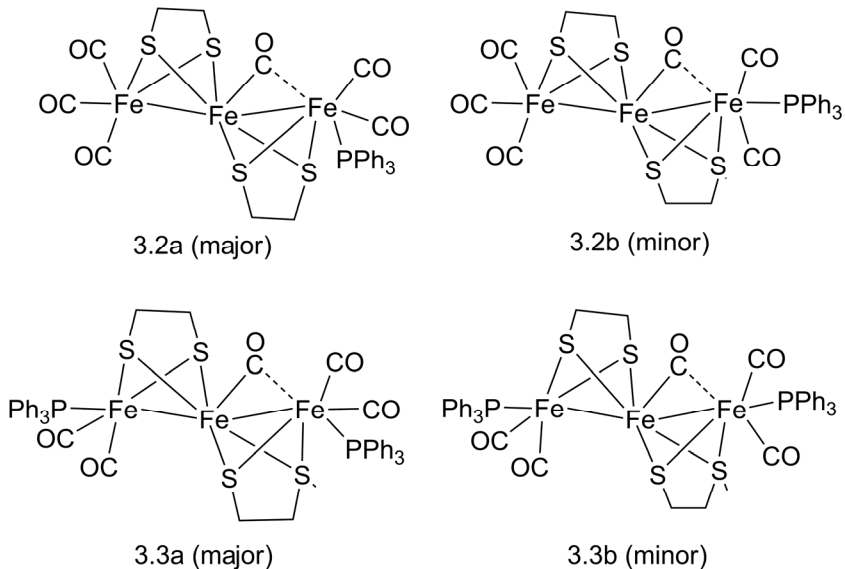
Scheme 3.3 Proposed major and minor isomers of **3.2** and **3.3**.

(a)   (b)
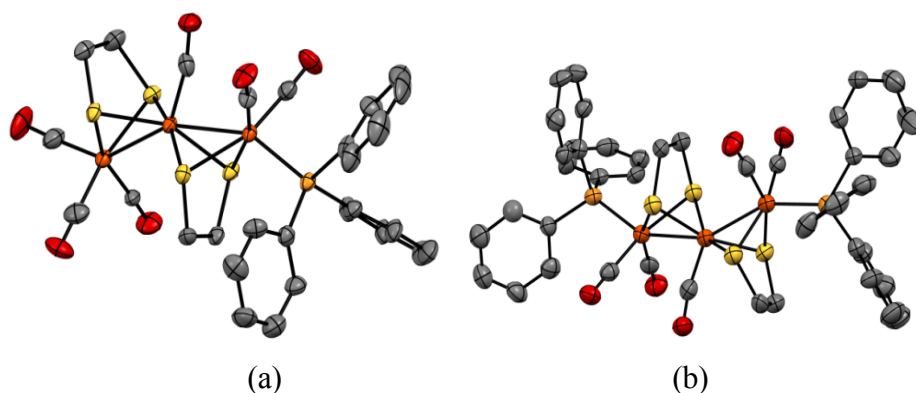
Figure 3.3 The molecular structures of (a) [Fe$_3$(CO)$_6$(μ-edt)$_2$(PPh$_3$)] (**3.2**) and (b) [Fe$_3$(CO)$_5$(μ-edt)$_2$(PPh$_3$)$_2$] (**3.3**)

Reaction of **3.1** with diphosphines afforded chelating complexes, the desired triiron complexes [Fe$_3$(CO)$_5$(k^2-diphosphine)(μ-edt)$_2$] (diphosphine = dppv, dppe, dppb, dppn) (**3.6-3.9**) together with the corresponding diiron species [Fe$_2$(CO)$_4$(k^2-diphosphine)(μ-edt)][77,78] as a result of one metal-metal bond cleavage (Scheme 3.4).[77,79,80]

3.6, X= CH=CH
3.7, X= CH$_2$CH$_2$
3.8, X = C$_6$H$_4$
3.9, X = C$_{10}$H$_6$
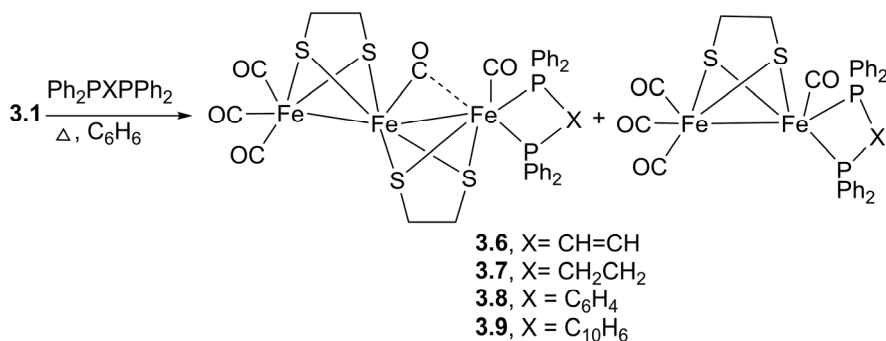
Scheme 3.4 Synthesis of complexes [Fe$_3$(CO)$_5$(k^2-diphosphine)(μ-edt)$_2$] (diphosphine = dppv, dppe, dppb, dppn) (**3.6-3.9**).

All of the triiron diphosphine complexes showed a weak absorption at ca. 1830 cm^{-1}, indicating that the semi-bridging carbonyl remained present. The ^{31}P{^{1}H} NMR spectra of **3.6-3.9** showed in all cases only a sharp singlet at even upon cooling to -60 ^{o}C this indicating that the ^{31}P nuclei are equivalent and the

complexes exist as single isomer. Crystallography and DFT studies on **3.6** supported that the coordination of the diphosphine occurs exclusively in the basal positions of one of the outer iron atoms (see Paper I).
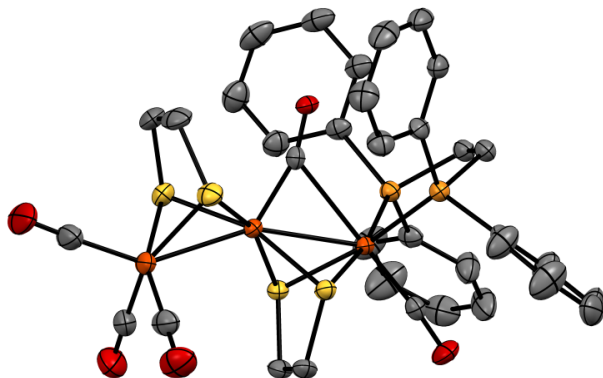
Figure 3.4 Solid-state molecular structure of $[Fe_3(CO)_6(\mu\text{-edt})_2(dppv)]$ (**3.6**)

3.4 Protonation of the triiron complexes

As discussed in Chapter 1, determination of whether a complex can be protonated in the presence of a Brönsted acid may help to understand whether the first step of a catalytic proton reduction mechanism is a protonation or a reduction process. Infrared spectroscopy showed that the $\nu(CO)$ bands go to lower wavenumbers from the unsubstituted **3.1** > mono-substituted complex **3.2** > di-substituted complex **3.3** due to the increased electron density on the Fe centers provided by the two PPh_3 ligands and consequent increased backbonding into CO anti-bonding orbitals.

Protonation experiments were monitored through the IR stretches of the CO ligands. On the addition of one equivalent of $HBF_4 \cdot Et_2O$ to the complex $[Fe_3(CO)_7(\mu\text{-edt})_2]$ (**3.1**) the bands of the IR spectrum did not change in intensity or position, indicating that protonation did not occur. Even on the addition of more acid there was no evidence for protonation. After 24 hours there was a color change and the bands of the IR spectrum shifted to higher wavenumbers. Performance of the same experiment on complex $[Fe_3(CO)_6(\mu\text{-edt})_2(PPh_3)]$ (**3.2**) also gave significant shift of the $\nu(CO)$ resonances after 21 h. For both clusters the IR signal for the semi-bridging CO was no longer present. There was no

clear evidence that the shift in the bands was due to protonation, or oxidation or decomposition. Further studies (see below) showed that the complexes were oxidized rather than protonated. For the di-substituted complex [Fe$_3$(CO)$_5$(μ-edt)$_2$(PPh$_3$)$_2$] (**3.3**) there was an immediate change in the IR spectrum on the addition of one equivalent HBF$_4$·Et$_2$O and the same phenomenon was observed also for the other complexes (**3.6-3.9**).

3.5 Oxidation of triiron clusters by ferrocenium

A possible explanation for the above-mentioned IR shifts upon the reaction with HBF$_4$·Et$_2$O is that the acid was reduced to form dihydrogen with the complex being oxidized rather than protonated. To investigate this possibility, the oxidation of **3.3** by the ferrocenium cation was studied. Upon the addition of 1 molar equivalent of ferrocenium ([Cp$_2$Fe][PF$_6$]) to the neutral complex, the spectrum showed a clear transition that is very similar to that found after the addition of HBF$_4$·Et$_2$O to the same complex. Further evidence for oxidation was obtained by NMR spectroscopy. On addition of HBF$_4$·Et$_2$O to the complex, the spectrum observed was characteristic of a paramagnetic species, suggesting it has been oxidized. There is no weak absorption spectrum for the bridging CO ligand in the IR spectrum of the oxidized complex, indicating that the oxidized complex does not exhibit a bridging CO ligand (Scheme 3.5).
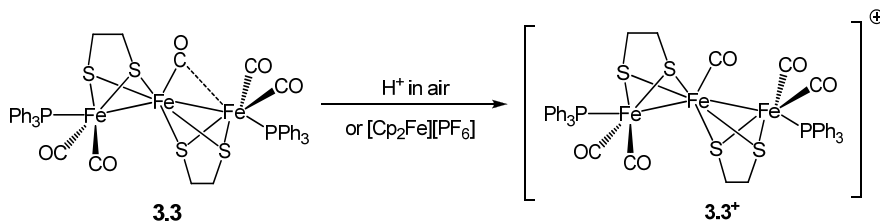
Scheme 3.5 Oxidation of **3.3** with [Cp$_2$Fe][PF$_6$] in dichloromethane

Repetition of the same experiment on the mono-substituted complex **3.2** gave an IR spectrum whose bands do *not* match those seen after the addition of HBF$_4$·Et$_2$O. It is therefore more likely that the acid is either protonating the complex or causing a slow decomposition of the complex rather than oxidizing it. The same behaviour that was observed for **3.3** was also found for the diphosphine complexes **3.6-3.9**. Addition of [Cp$_2$Fe][PF$_6$] led to generation of IR spectra that were not only indistinguishable between complexes **3.6-3.9** but

were also very similar those observed upon addition of HBF$_4$.Et$_2$O. This is consistent with oxidation and the formation of the cationic complexes [Fe$_3$(CO)$_5$(κ^2-diphosphine)(μ-edt)$_2$][BF$_4$] (Scheme 3.6). However, a notable difference to the behavior of **3.3** was the retention of the semi-bridging carbonyl as evidenced by IR spectroscopy.
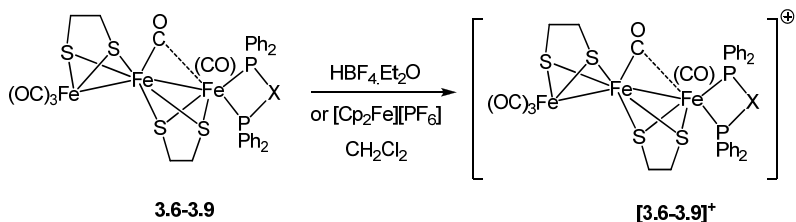
Scheme 3.6 Oxidation experiment of **3.6-3.9** with [Cp$_2$Fe][PF$_6$] in CH$_2$Cl$_2$.

3.6 Electrochemical studies

The cyclic voltammetry of all triiron complexes was carried out by David G. Unwin, University College London, UK. All triiron complexes were found to show similar behaviour in CH$_2$Cl$_2$ under an argon atmosphere - a quasi-reversible oxidation process and an irreversible reduction, which is followed by a small reduction peak.
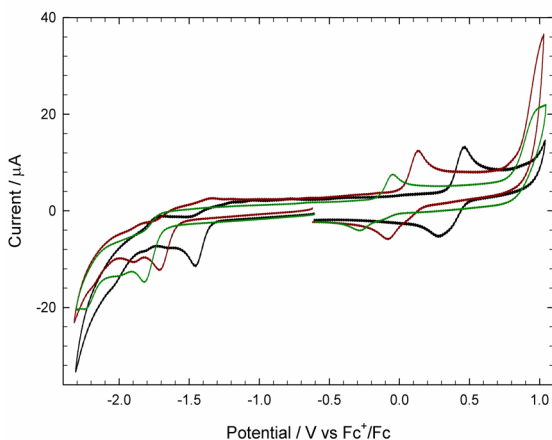
Figure 3.5 A comparison of the cyclic voltammograms of [Fe$_3$(CO)$_7$(μ-edt)$_2$] (**3.1**) (black), [Fe$_3$(CO)$_6$(μ-edt)$_2$(PPh$_3$)] (**3.2**) (red) [Fe$_3$(CO)$_5$(μ-edt)$_2$(PPh$_3$)$_2$] (**3.3**) (green).

A comparison of the cyclic voltammograms of complexes of each of the three riiron complexes **3.1-3.3** is shown in Figure 3.5. The first reduction of **3.1** shows at **-1.47** V. Upon substitution of one CO with a PPh$_3$ ligand, the first reduction in **3.2** is shifted 0.25 V more negative than in the unsubstituted **3.1** and upon a second substitution, the reduction potential in **3.3** is shifted a further 0.10 V more negative than that of **3.2**. In all cases, the oxidation and reduction potentials shifted to more negative potentials due to the PPh$_3$ ligands pushing more electron density onto the Fe centers.

The irreversible reduction of all complexes suggested that a chemical step (e.g. CO loss) takes place after the reduction process. Therefore, the electrochemical behaviour of **3.1** in a solution saturated with CO (which would suppress CO ligand loss) was investigated. The first oxidation and reduction take place at the same potentials but the second and third reductions occur with peak currents double that of the first reduction process (Figure 3.6).
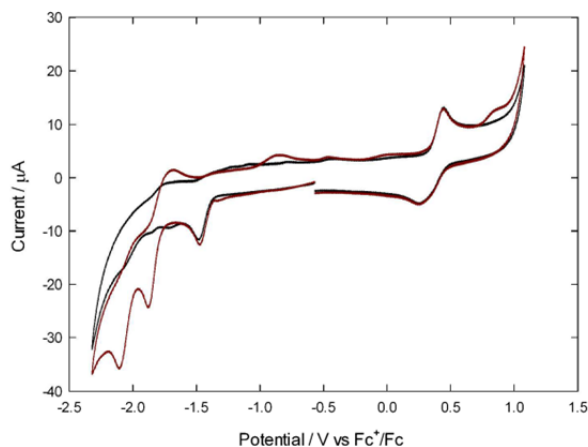
Figure 3.6 Cyclic voltammetry of **3.1** in CH$_2$Cl$_2$, [NBu$_4$][PF$_6$] saturated with CO (black line) and Ar (red line) (υ =0.1 Vs^{-1}, glassy carbon electrode; V vs Fc$^+$/Fc).
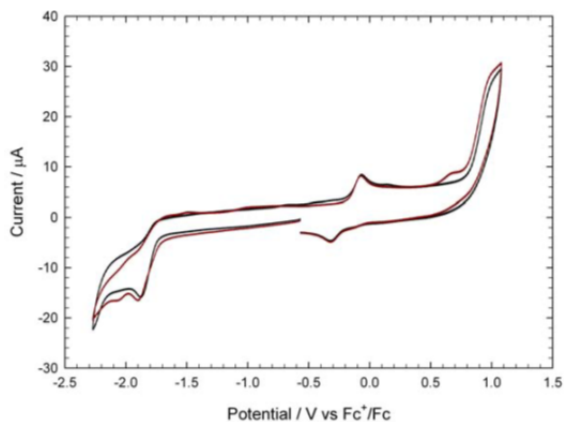
Figure 3.7 Cyclic voltammetry of **3.3** in CH_2Cl_2 [NBu$_4$][PF$_6$] saturated with CO (black line) and Ar (red line) (υ =0.1 Vs^{-1}, glassy carbon electrode; V vs Fc$^+$/Fc).

On the return scan, the re-oxidation peaks appear at different potentials. Scanning to anodic potentials, a second oxidation process appears at 0.82 V as a new peak under CO. In the presence of CO there is no change to the reversibility or position of the first reduction. This indicates that the irreversibility of the reduction is not due to CO ligand loss. Complex **3.3** has also been investigated under a CO atmosphere (Fig. 3.7) but the electrochemical behaviour was found to be almost similar compared to the Ar saturated system.

Cyclic voltammograms for all diphosphine derivatives [Fe$_3$(CO)$_5$(κ^2-diphosphine)(μ-edt)$_2$] (**3.6-3.9**) in CH_2Cl_2 are similar to those for **3.1-3.3** (See Supplementary Material, Paper 1). All diphosphine derivatives showed an irreversible reduction between -1.68 and -1.74 V and a quasi-reversible oxidation process takes place at E_p = 0.29 V for dppv, 0.20 V for dppe and 0.36 V for the dppb derivative; comparison of the oxidation peak height of complexes **3.6-3.9** with that for the oxidation of **3.3** suggests it is a one-electron process, consistent with its behavior on chemical oxidation with Fc$^+$.

3.7 A comparison between the triiron and the analogous diiron edt complexes.

To evaluate the potential benefit of adding the extra iron center in the triiron complexes, a comparison between the unsubstituted (**3.1**), mono-substituted (**3.2**) and di-substituted (**3.3**) triiron complex with the analogous unsubstituted diiron complex $[Fe_2(\mu\text{-edt})(CO)_6]$, mono-substituted $[Fe_2(CO)_5(\mu\text{-edt})(PPh_3)]$ and di-substituted $[Fe_2(CO)_4(\mu\text{-edt})(PPh_3)_2]$ was made. The results are shown in Figs. 3.8-3.10. It could be observed that the first reduction potential shifted 0.44 V less negative in **3.1** than the analogous unsubstituted diiron complex $[Fe_2(\mu\text{-edt})(CO)_6]$; for the mono-substituted triiron complex **3.2** the first reduction potential shifted 0.33 V less negative than the analogous mono-substituted diiron system and the di-substituted (**3.3**) triiron complex is again reduced at a significantly lower potential than the di-substituted diiron analogue, with a difference in reduction potential of 0.49 V. Furthermore, the first oxidation of the entire triiron complex also requires less energy than for the analogous diiron complex. This means that if any proton reduction catalyzed by these species involves the initial formation of an anion, the triiron complexes should be able to catalyze the reaction at lower overpotentials.
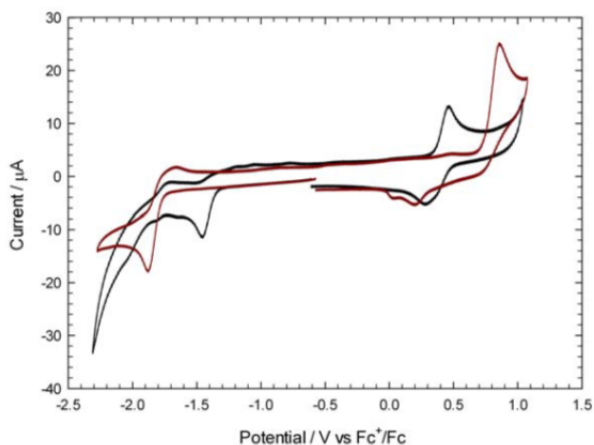
Figure 3.8 Cyclic voltammetry of **3.1** (black line) and $[Fe_2(CO)_6(\mu\text{-edt})]$ (red line) in CH_2Cl_2-$[NBu_4][PF_6]$ (υ =0.1 Vs^{-1}, glassy carbon electrode; V vs Fc$^+$/Fc).
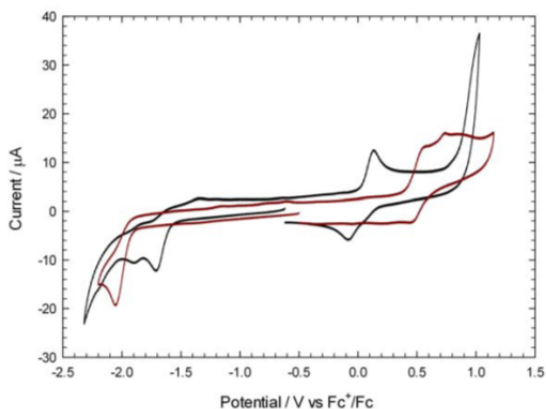
Figure 3.9 Cyclic voltammetry of **3.2** (black line) and [Fe$_2$(CO)$_5$(μ-edt)PPh$_3$] (red line) in CH$_2$Cl$_2$-[NBu$_4$][PF$_6$] (υ =0.1 Vs^{-1}, glassy carbon electrode; V vs Fc$^+$/Fc).
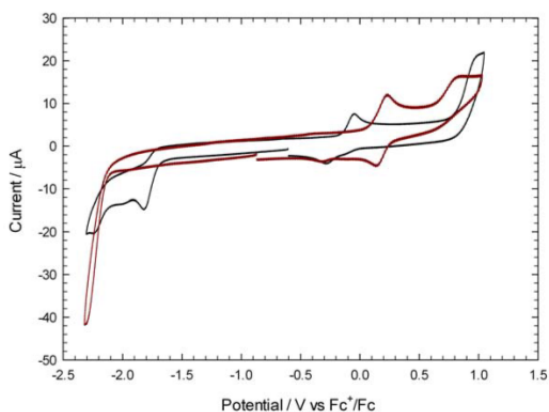
Figure 3.10 Cyclic voltammetry of **3.3 (**black line) and [Fe$_2$(CO)$_4$(μ-edt) (PPh$_3$)$_2$] (red line) in CH$_2$Cl$_2$-[NBu$_4$][PF$_6$] (υ =0.1 Vs^{-1}, glassy carbon electrode; V vs Fc$^+$/Fc).

3.8 Electrocatalytic studies

An investigation into whether the complexes are electrocatalysts towards proton reduction was also undertaken. The electrocatalytic activity of all triiron complexes was investigated in CH$_2$Cl$_2$ under argon, using HBF$_4$·Et$_2$O as the proton source. The electrocatalytic activity of the unsubstituted complex **3.1** is shown in Fig. 3.11. Upon addition of 1 molar equivalent of HBF$_4$·Et$_2$O, the peak

current of the first reduction process is twice that of the neutral complex and the remaining CV is very similar to that in the absence of acid. A new small reduction peak appeared at -1.80 V, and the heights of the both reduction waves continue to increase upon addition of further acid, indicating catalytic proton reduction.
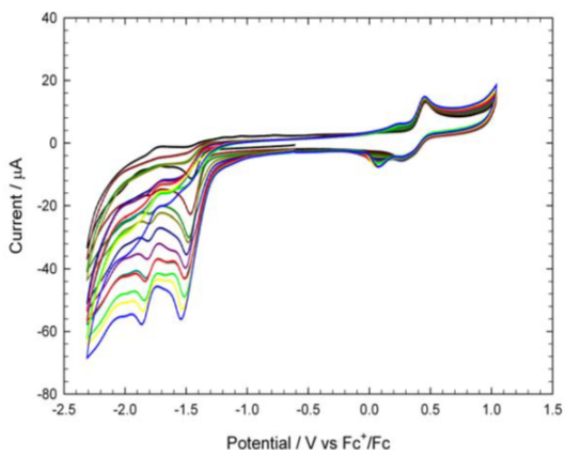
Figure 3.11 Cyclic voltammetry of **3.1** in CH_2Cl_2-$[NBu_4][PF_6]$ in the absence of acid and in the presence of up to 10 molar equivalents $HBF_4.Et_2O$ in steps of 1 molar equivalent ($v=0.1$ Vs^{-1}, glassy carbon electrode; V vs Fc^+/Fc).

The same behaviour was observed for **3.2** with the catalytic currents being approximately twice that of the unsubstituted complex **3.1** after the addition of 10 molar equivalents of $HBF_4.Et_2O$. With excess acid a new reduction peak appears at approximately -1.1 V and the first reduction seems to include a shoulder at 0.25 V less negative potential than the reduction of the neutral complex. This difference suggests that the singly reduced mono-substituted complex **3.2** is more readily protonated than the singly reduced unsubstituted **3.1** complex, which is consistent with the increased basicity of the Fe centers upon phosphine substitution. For the di-substituted complex **3.3** the first reduction peak becomes more broad, and grows slightly with addition of 1 molar equivalent of acid but the rest of the cyclic voltammogram is largely the same as in the absence of protons. For **3.1-3.3**, the oxidation peak remained unchanged from that of the neutral complex upon addition of acid, indicating chemical stability of the electrocatalysts.

The catalytic reduction potential of the triiron complex $[Fe_3(CO)_7(\mu\text{-edt})_2]$ (**3.1**) and the mono-substituted complex $[Fe_3(CO)_6(\mu\text{-edt})_2(PPh_3)]$ (**3.2**) are lower than the diiron analogues $[Fe_2(CO)_6(\mu\text{-edt})]$ and the mono-substituted complex $[Fe_2(CO)_5(\mu\text{-edt})(PPh_3)]$ (Figure 3.12). For both **3.1** and **3.2**, the improvement is ca. 0.40V lower overpotential. For the di-substituted triiron complex $[Fe_3(CO)_5(\mu\text{-edt})_2(PPh_3)_2]$ (**3.3**), the overpotential is lower than the di-substituted diiron analogous and the improvement is *ca* 0.25V.
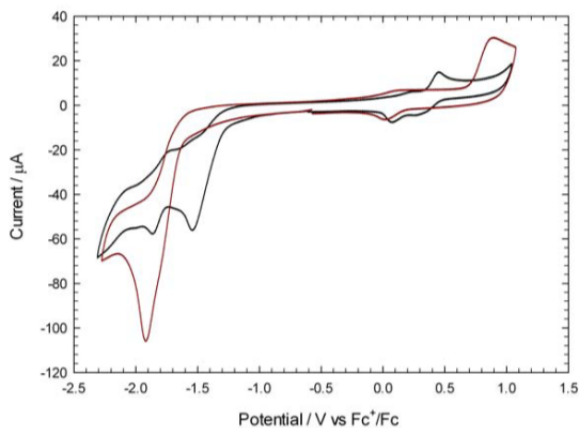
Figure 3.12 Cyclic voltammetry of **3.1**(black) and $[Fe_2(CO)_6(\mu\text{-edt})]$ (red) in CH_2Cl_2-$[NBu_4][PF_6]$ in the presence of 10 molar equivalents $HBF_4 \cdot Et_2O$ ($v=0.1$ Vs^{-1}, glassy carbon electrode; V vs Fc^+/Fc).

In dichloromethane, sequential addition of HBF_4 to **3.6-3.9** resulted in irreproducible cyclic voltammograms that suggested that the complexes were unstable under these conditions. It has been reported that electrocatalysis effected by binuclear complexes proceeds more cleanly in acetonitrile,[81] and electrocatalytic proton reduction by **3.6** was therefore studied in this solvent. Upon addition of one molar equivalent of acid, two new reduction peaks are observed at $E_p = -1.63$ V and $E_p = -2.26$ V, in addition to the reduction peaks at $E_p = -1.89$ V and $E_p = -2.70$ V associated with **3.6** (see Supporting Information, paper I). After addition of a second equivalent of acid the CV shows two prominent reductive features at $E_p = -1.76$ V and $E_p = -1.92$ V. Peak heights for both increase with acid concentration. After addition of two molar equivalents of acid a small reductive feature was also observed at $E_p = -1.50$ V, which splits into two distinct catalytic waves at higher acid concentrations (≥ 5 molar equiv.) and represent the principal catalytic events on the CV. However, the use of

43

different solvents means that it is difficult to draw definitive conclusions about the relative catalytic abilities of the two types of complexes.

3.9 Summary and Conclusions

For the complexes discussed in this Chapter, a significant improvement in the overpotential for proton reduction catalysis could be gained by using triiron complexes as catalysts instead of the analogous diiron complexes. The unsubstituted triiron complex is reduced at 0.36 V less negative potential than the equivalent diiron complex in the presence of $HBF_4 \cdot Et_2O$. It may be noted that DFT calculations indicate that the HOMO-LUMO separation is smaller in the triiron complex **3.1** than in the corresponding diiron complex (see Paper I), indicating that electrocatalysis involving initial reduction of the catalyst should be favored for the triiron complexes.

Mono or di-substitution by triphenylphosphine ligands or di-substitution by chelating diphosphines do not increase the basicity of the triiron bis(edt) complexes for protonation of the neutral molecules, even when strong Brönsted acids are used. Thus there is no overpotential advantage that may be gained from phosphine substitution. Consequently, the first step in the catalytic cycle is therefore always reduction of the complex. In fact, onset of (electro) catalysis is pushed to more negative potentials as the increased electron-density makes the complexes more difficult to reduce. However, one advantage of substitution seems to be the higher catalytic currents that can be achieved with the substituted complexes, indicating faster turnover.

Chapter 4 Chalcogenide-capped triiron clusters as proton reduction catalysts

4.1 Background

As mentioned in Chapters 1 and 3, the use of di- and triiron dithiolate clusters as models for the $[2Fe]_H$ subcluster of the active site of [FeFe] hydrogenase has led to a great interest in iron carbonyl thiolate clusters in general, and also iron carbonyl chalcogenide clusters (here, chalcogenide = S, Se, Te), as potential proton reduction catalysts. The presence of metal-metal bonds in chalcogenide-containing transition metal clusters depends on the size of the central main group element. Heavier main group elements generally bridge more open structures while the less heavier elements reinforce metal-metal bonding. Bridging chalcogenide ligands have been extensively used to promote the formation and stabilization of transition metal cluster complexes[82,83,84] and the mode of binding dictates the number of electrons contributed to the cluster by main group element. A large number of high nuclearity transition metal chalcogenide complexes containing bridging or chelating diphosphine ligands have been synthesized and structurally characterized.[85,86,87,88,89]
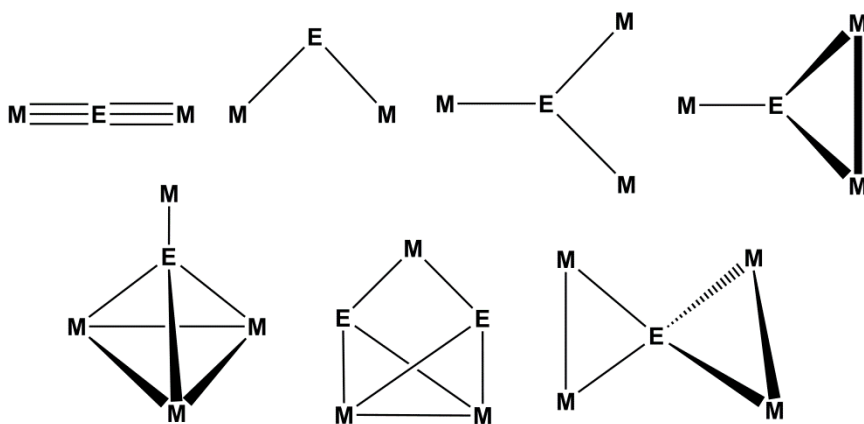
Figure 4.1 Examples of structural geometries of transition metal clusters containing group 16 elements; E = Group16 elements, M = d-block transition metals.

4.2 Electrocatalytic proton reduction by iron-chalcogenide complexes.

The μ_3-bridging coordination mode of chalcogenides is a common feature in transition metal chalcogenide cluster compounds. Such μ_3-capping chalcogenide entities have been shown to be effective in stabilization of metal clusters.[90,91,92,93,94,95,96] Although numerous μ_3-sulfido and μ_3-selenido metal clusters have been reported,[97,98,99] only the disulfide cluster $[Fe_3(CO)_9(\mu_3\text{-}S)_2]$ (**4.1S**)[100] has been investigated as a proton reduction catalyst.[101,102] Liu and coworkers studied proton reduction by **4.1S** and these investigators observed that the first reduction is reversible in MeCN, while in CH_2Cl_2 the monoanion $[Fe_3(CO)_9(\mu_3\text{-}S)_2]^-$ (**4.1S$^-$**) slowly loses CO to afford $[Fe_3(CO)_8(\mu_3\text{-}S)_2]^-$. In the presence of the strong acid $HBF_4.Et_2O$, both of these anions are active proton reduction catalysts in CH_2Cl_2 at -1.03 V and -1.30 V (vs Fc/Fc, respectively.[100a] Mebi and co-workers have shown that hydrogen production takes place at the second reduction potential (-1.75 V) in MeCN in the presence of a weak acid (acetic acid), thus suggesting that the dianion, $[Fe_3(CO)_9(\mu_3\text{-}S)_2]^{2-}$ (**4.1S^{2-}**) is an effective catalyst.[100b] This indicate that the monoanion is not basic enough to be protonated. Since $[Fe_3(CO)_9(\mu_3\text{-}S)_2]$ (**4.1S**) does not readily protonate even with strong acids, then initial reduction is a pre-requisite for proton reduction catalysis.

In biomimetics of the type $[Fe_2(CO)_6(\mu\text{-dithiolate})]$, the diiron core is likewise not susceptible to protonation unless very strong acids are used[103] and thus initial reduction is required. As discussed in earlier Chapters, a common strategy to favour protonation is the replacement of one or more of the carbonyls with electron-donating ligands such as phosphines.[104] An example of such a phosphine-substituted iron carbonyl chalcogenide cluster is $[Fe_3(CO)_5(\mu_3\text{-}S)_2(\kappa^2\text{-dppv})_2]$ [dppv = *cis*-1,2-bis(diphenylphosphino)ethylene], which was unexpectedly isolated by Åkermark and coworkers from reactions of $[Fe_2(CO)_6(\mu\text{-}SCH_2NRCH_2S)]$ with excess dppv, as described in Chapter 3.[71]This triiron cluster protonates readily with triflic acid and catalyses proton reduction at the first reduction peak of $[(\mu\text{-}H)Fe_3(CO)_5(\mu_3\text{-}S)_2(\kappa^2\text{-dppv})_2]^+$ at -0.98 V in CH_2Cl_2.

Although many tellurium-containing triiron carbonyl clusters have been synthesized,[105,106,107,108] their electrochemical and electrocatalytic behaviour has not been extensively studied. Song and coworkers have investigated a series of chalcogenide-containing trinuclear transition metal clusters

[(diphosphine)Ni(μ_3-E)$_2$Fe$_2$(CO)$_6$] (diphosphine = dppv, dppb, dppf, dppe, (Ph$_2$PCH$_2$)$_2$NR (R = Me, t-Bu; E = S, Se, Te)). Their electrochemical properties reveal that reduction of the three representative complexes [(dppv)Ni(μ_3-E)$_2$Fe$_2$(CO)$_6$] (E = S; Se; Te) becomes easier on going from the lighter to the heavier chalcogenide (*i.e.* from S to Se to Te). Furthermore, an electrocatalytic study demonstrated that in the presence of the proton source *p*-TsOH, complexes are catalysts for proton reduction to hydrogen.[109] Diiron carbonyl chalcogenolato complexes, [Fe$_2$(CO)$_6$(μ-EXE)] (E = S, Se, Te, X = arbitrary bridge), have been established as proton reduction catalysts by several groups.[110,111,112,113] The influence of the bridging chalcogen atoms in homologous diiron dithiolato, diselenolato, and ditellurolato complexes have been studied by Weigand and coworkers; these investigators found that the tellurium-containing complex being both the easiest to reduce and the easiest oxidize.[113]

The above mentioned proton reduction activities of triply capped triiron chalcogenide clusters and diiron chalcogenato clusters indicated that further exploration of such clusters as proton reduction catalysts is warranted. Therefore the chalcogenide-capped clusters [Fe$_3$(CO)$_9$(μ_3-E)$_2$] (**4.1**, E= S, Se,Te) and their phosphine derivatives were studied.

4.3 Synthesis and characterization of the chalcogenide-capped triiron clusters [Fe$_3$(CO)$_9$(μ_3-E)$_2$], [Fe$_3$(CO)$_7$(μ_3-CO)(μ_3-E)(μ-dppm)] and [Fe$_3$(CO)$_7$(μ_3-E)$_2$(μ-diphosphine)] (E = S, Se, Te) (Papers II and III).

The clusters [Fe$_3$(CO)$_7$(μ_3-CO)(μ_3-E)(μ-dppm)] (**4.2**) (E = S, Se, Te), [Fe$_3$(CO)$_9$(μ_3-Te)$_2$(PPh$_3$)](**4.3**), [Fe$_3$(CO)$_7$(μ_3-E)$_2$(μ-dppm)](**4.4**) (E = S, Se, Te) [Fe$_3$(CO)$_7$(μ_3-Te)$_2$(μ-dcpm)] (**4.5**) and [Fe$_3$(CO)$_7$(μ_3-Te)$_2$(μ-dppa)] (**4.6**) were prepared according to the Scheme 4.1 and were characterized by standard spectroscopic methods, including X-ray crystallography (see experimental details in Papers II and III). For **4.4S** and **4.4Se**, the ^{31}P{^{1}H} NMR spectrum shows a pair of doublets and a singlet, indicating that the clusters exist as a mixture of isomers in which the diphosphine bridges an iron-iron bonded or the non-bonded edge in solution (see Paper II). In the solid state, the diphosphine spans the non-bonded iron-iron edge of **4.4S** and **4.4Se** (Scheme 4.1). The ^{31}P{^{1}H} NMR spectra of **4.4-4.6Te** are identical; each showed a pair of doublets and suggesting that the diphosphine bridges across a metal-metal bond leading to chemical and magnetic inequivalence of the two phosphorus centers.
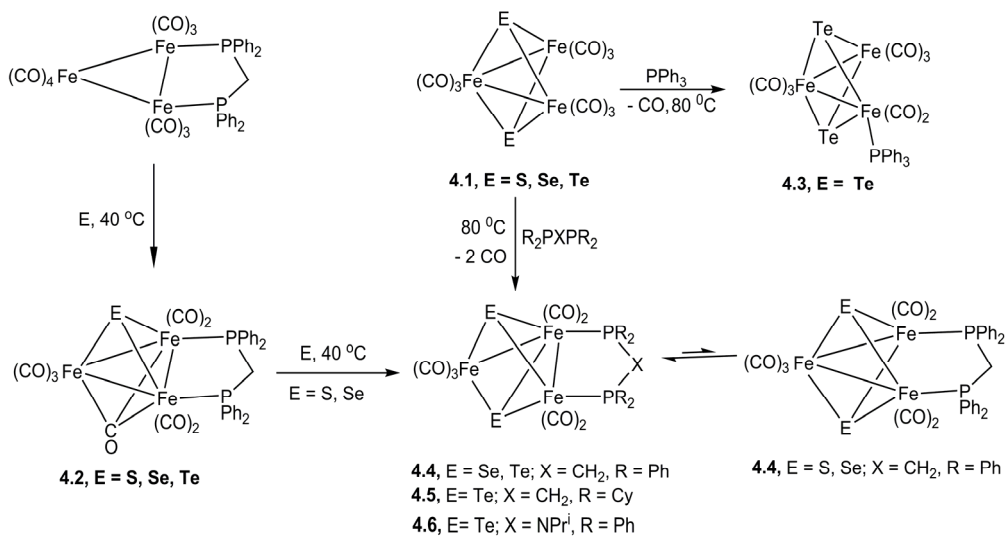
Scheme 4.1 Schematic representation of clusters **4.1-4.6**

[Fe$_3$(CO)$_7$(μ_3-CO)(μ_3-S)(μ-dppm)](**4.2S**)   [Fe$_3$(CO)$_7$(μ_3-S)$_2$(μ-dppm)](**4.4S**)
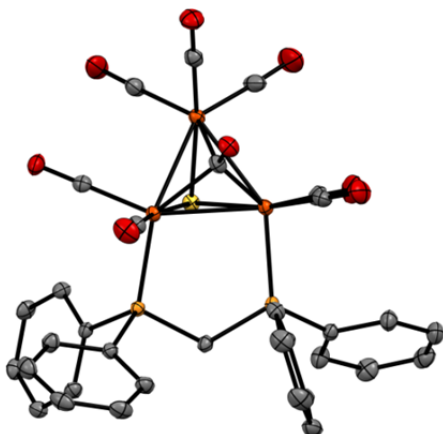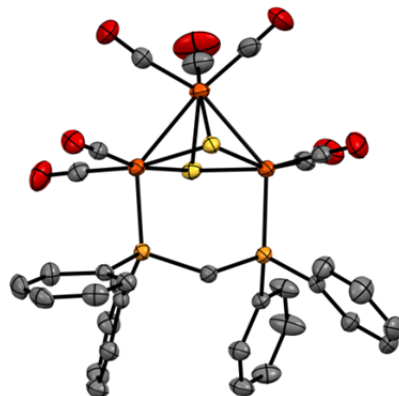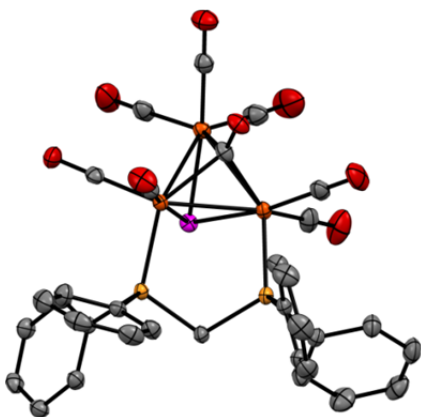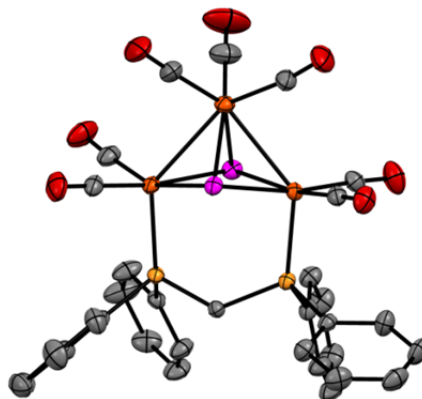
[Fe$_3$(CO)$_7$(μ_3-CO)(μ_3-Se)(μ-dppm)](**4.2S**)   [Fe$_3$(CO)$_7$(μ_3-Se)$_2$(μ-dppm)](**4.4Se**)

Figure 4.2 Molecular structures of chalcogenide-capped triiron clusters **4.2S**, **4.4S**, **4.2Se** and **4.4Se**. The crystal structures of **4.4S** and **4.4Se** have been published previously.[97d,101]

4.4 Synthesis and characterization of $[Fe_3(CO)_8(\mu_3\text{-Te})_2(\kappa^2\text{-diphosphine})]$ and $[Fe_4(CO)_{10}(\mu_3\text{-Te})_4(\kappa^2\text{-dppb})]$ (Paper IV).

Reaction of $[Fe_3(CO)_9(\mu_3\text{-Te})_2]$ **4.1Te** with the chelating tertiary diphosphine ligands dppe, dppp, dppv, dppb, dppf gave the "butterfly" complexes **4.7-4.12** as the main products (Scheme 4.2). In addition, small amounts of $[Fe_3(CO)_8(\mu_3\text{-Te})_2(\kappa^1\text{-diphosphine})]$, containing a diphosphine in a dangling coordination mode, were also formed (see the Experimental Section in Paper IV). Finally, the tetranuclear cluster $[Fe_4(CO)_{10}(\mu_3\text{-Te}_4)(\kappa^2\text{-dppb})]$ (**4.13**) was formed in good yield from the reaction of **4.1Te** with dppb. Clusters **4.7-4.13** have been characterized by standard spectroscopic methods, and the crystal structures of compounds **4.9-4.13** could be determined.

4.1, E = Te

4.7, dppe, X = CH_2CH_2
4.8, dppv, X = *cis*-CH=CH
4.9, dppb, X = $1,2\text{-}C_6H_4$
4.10, dppp ,X = $CH_2CH_2CH_2$
4.11, dppf, X = $1,1'\text{-}(C_5H_4)_2Fe$
4.12, dppbn, X = $C_{20}H_{12}$
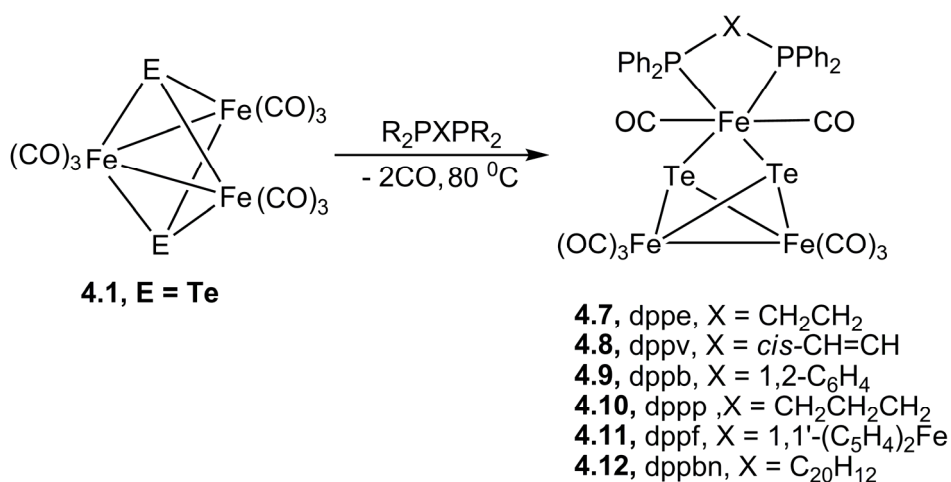
Scheme 4.2 Schematic representation of clusters **4.7-4.12**

[Fe$_3$(CO)$_8$(μ_3-Te)$_2$(κ^2-dppb)](**4.9**)   [Fe$_3$(CO)$_8$(μ_3-Te)$_2$(κ^2-dppp)](**4.10**)
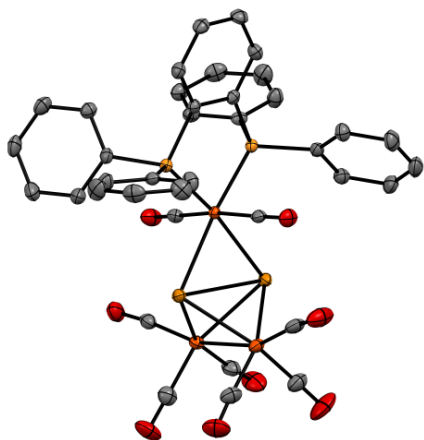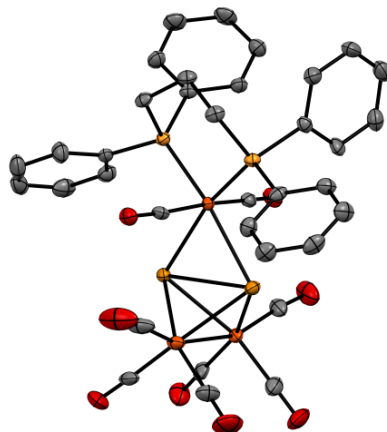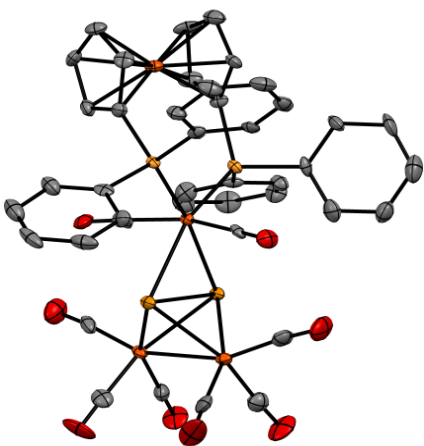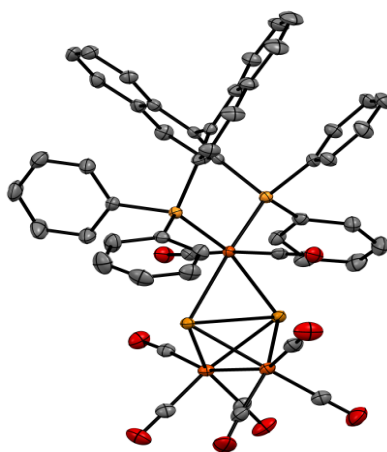
[Fe$_3$(CO)$_8$(μ_3-Te)$_2$(κ^2-dppf)](**4.11**)   [Fe$_3$(CO)$_8$(μ_3-Te)$_2$(κ^2-dppbn)](**4.12**)

Figure 4.3 Molecular structures of clusters **4.9**, **4.10**, **4.11** and **4.12** (Paper IV).
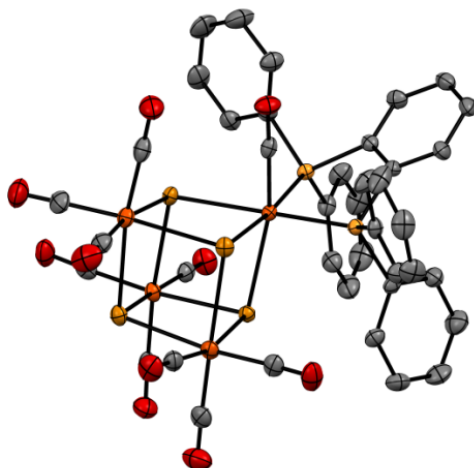
Figure 4.4 Molecular structure of **4.13** (Paper IV).

4.5. Protonation studies (Paper II, III and IV)

As described previously, protonation of the metal core of the cluster is a key feature of proton reduction catalysis. Initial protonation studies were carried out using the strong acid $HBF_4 \cdot Et_2O$. Reaction of this acid with clusters $[Fe_3(CO)_7(\mu_3\text{-Te})_2(\mu\text{-dppm})]$ (**4.4Te**), $[Fe_3(CO)_7(\mu_3\text{-Te})_2(\mu\text{-dcpm})]$ (**4.5**) and $[Fe_3(CO)_7(\mu_3\text{-Te})_2(\mu\text{-dppa})]$ (**4.6**) did not result in any significant changes to the IR spectrum, indicating that the triiron centre is not sufficiently basic to be protonated under these conditions (Paper III). On the other hand, addition of $HBF_4 \cdot Et_2O$ to CH_2Cl_2 solutions of $[Fe_3(CO)_7(\mu_3\text{-CO})(\mu_3\text{-S})(\mu\text{-dppm})]$ (**4.2S**) and $[Fe_3(CO)_7(\mu_3\text{-CO})(\mu_3\text{-Se})(\mu\text{-dppm})]$ (**4.2Se**) led to an immediate change in both cases, with all IR bands being shifted to higher wavenumbers by *ca.* 20-30 cm^{-1}. The magnitude of this change suggests that removal of electron-density has occurred not at the triiron centre, as metal-centered protonation is expected to result in a ~50-70 cm^{-1} positive shift.[36,37,38] Addition of a slight excess of piperidene resulted in regeneration of **4.2(S, Se)**, while addition of a slight excess of $BF_3 \cdot Et_2O$ to these cluster resulted in the same shift that was observed for addition of $HBF_4 \cdot Et_2O$. On the basis of the above experiments and DFT calculations (Figure 4.5 and Paper II), it was concluded that addition of both $HBF_4 \cdot Et_2O$ and $BF_3 \cdot Et_2O$ to **4.2(S, Se)** leads to formation of the BF_3 adduct $[Fe_3(CO)_7(\mu_3\text{-CO})(\mu_3\text{-EBF}_3)(\mu\text{-dppm})]$ (**4.2.BF₃**), where BF_3 coordinates to a capping chalcogenide (Paper II). Addition of 2 equivalents of *p*-TsOH (the acid used in catalytic studies, see below) to **4.2 (S, Se)** in CH_2Cl_2 did not lead to any

major changes in the IR spectrum, underscoring the fact that protonation of the neutral clusters is not favoured. Furthermore, monitoring of the reactions of **4.2(S, Se)** with HBF$_4$.Et$_2$O (in CDCl$_3$) by ^{1}H NMR spectroscopy revealed no evidence of formation of a hydride species.
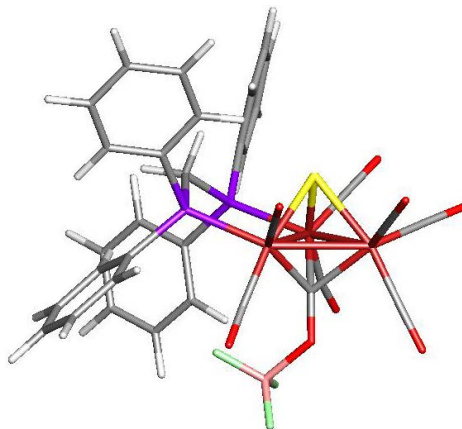
Figure 4.5 Structure of the calculated BF$_3$ adduct of [Fe$_3$(CO)$_7$(μ_3-CO)(μ_3-S)(μ-dppm)] (**4.2S**)

The reactions of [Fe$_3$(CO)$_7$(μ_3-S)$_2$(μ-dppm)] (**4.4S**) and [Fe$_3$(CO)$_7$(μ_3-Se)$_2$(μ-dppm)] (**4.4Se**) with HBF$_4$.Et$_2$O and *p*-TsOH were also investigated. Both of these clusters are protonated very slowly. The shifts to higher wavenumbers of *ca.* 50 cm^{-1} are consistent with protonation at the triiron core. The protonated species are tentatively assigned as [Fe$_3$(CO)$_7$(μ-H)(μ_3-E)$_2$(μ-dppm)][BF$_4$] (E = S, Se) (**4.4SH$^+$**, **4.4SeH$^+$**). However, attempts to observe these presumed hydride species by NMR spectroscopy were unsuccessful in both cases.

Addition of either HBF$_4$·Et$_2$O or CF$_3$CO$_2$H to CH$_2$Cl$_2$ solutions **4.7-4.12** in air led to the rapid disappearance of their characteristic four carbonyl absorptions bands, which were immediately replaced by four new bands at higher frequencies that were shifted by *ca* 25-30 cm^{-1}. Such an IR shift *may* be due to cluster protonation, but all attempts to collect good quality NMR spectra of the new products failed. The cyclic voltammograms of **4.7-4.12** (see below) showed that the clusters were easily oxidised, with oxidation potentials ranging from +0.14 V to 0.38 V (*vs* Fc/Fc$^+$). Addition of the oxidising agent [Cp$_2$Fe][PF$_6$] to a CH$_2$Cl$_2$ solution of **4.12** resulted in the rapid generation of the same IR spectrum as detected for addition of HBF$_4$·Et$_2$O or CF$_3$CO$_2$H (see Supplementary Material, Paper IV). Again, sharp NMR spectra could not be obtained upon

addition of a Brönsted acid. It is thus assumed that for **4.7-4.12**, *oxidation* rather than protonation takes place to yield cations of the type $[Fe_3(CO)_8(\mu_3\text{-Te})_2(\kappa^2\text{-diphosphine})]^+$.

4.6 Electrochemistry and catalytic studies of papers II-IV

As discussed above, two groups have independently studied proton reduction catalysis by $[Fe_3(CO)_9(\mu_3\text{-S})_2]$ (**4.1S**)[100] and this cluster is reported to undergo two one-electron reduction processes, the first one is fairly reversible and the second one is irreversible reduction process in CH_2Cl_2.[100a] In order to assess the effects of altering the chalcogenide moiety, the comparative electrochemical and catalytic proton-reduction activities of four different types of chalcogenide-capped clusters have been investigated. The four types of clusters are $[Fe_3(CO)_9(\mu_3\text{-E})_2]$ (**4.1** (**S, Se, Te**)), $[Fe_3(CO)_7(\mu_3\text{-CO})(\mu_3\text{-E})(\mu\text{-dppm})]$ (**4.2**), $[Fe_3(CO)_7(\mu_3\text{-E})_2(\mu\text{-}\kappa^2\text{-diphosphine})]$ (**4.4** (**S, Se, Te**); **4.5Te, 4.6Te**) and $[Fe_3(CO)_8(\mu_3\text{-Te})_2(\kappa^2\text{-diphosphine})]$ (**4.7-4.12**). Electrocatalytic proton reduction was investigated in CH_2Cl_2 in the presence of the strong acid *p*-toluenesulfonic acid (*p*-TsOH). All clusters were found to act as proton reduction catalysts and data are summarized in Tables 4.1 and 4.2. It was found that the nature of the chalcogenide does has an effect on the triiron core and consequent proton reduction capability. The mono-chalcogenide clusters **4**.2(**S, Se**) are reduced at relatively low potentials than the di-chalcogenide bicapped cluster **4**.4 (**S, Se**). The substitution of two carbonyls for the dppm ligand in **4**.4 (**S, Se, Te**) leads to an increase in the reduction potential of the cluster. The protonation of **4**.4 (**S, Se**) have shown to occur across an iron-iron bonded vector and not across the open edge or at one of the capping sulfide ligands.

In Paper III, electrochemical studies shows that each cluster $[Fe_3(CO)_9(\mu_3\text{-Te})_2]$ (**4.1Te**), $[Fe_3(CO)_7(\mu_3\text{-E})_2(\mu\text{-dppm})]$ (**4.4Te**) and $[Fe_3(CO)_7(\mu_3\text{-E})_2(\mu\text{-dcpm})]$ (**4.5Te**) reveals two reductive processes with good reversibility as well as in all cases showing that the 51-electron radical anions **4.1Te⁻**, **4.4Te⁻** and **4.5Te⁻** are quite stable. The reversibility of the second reduction process is highly dependent upon the nature of the supporting ligands such as the PPh$_3$ complex **4.5** is completely irreversible, while diphosphine such as dppm derivatives is quasi-reversible (paper III). During the catalysis experiments none of the iron telluride clusters react with this acid but they are able to act as proton-reduction catalysts at both their first and second reduction potentials. This indicates that the essential initial step in the catalytic proton reduction mechanism is reduction of the neutral cluster rather than protonation. As may be seen in Tables 4.2. The

reduction potential of the tellurium-containing cluster is lower and the reduced species are more stable than the sulfur and selenium analogues.

Complex	Peak potential reduction (V)		Peak potential Oxidation (V)		
	1st	2nd	1st	2nd	3rd
[Fe$_3$(CO)$_9$(μ_3-S)$_2$] (**4.1S**)	-1.03	-1.75	-	-	-
[Fe$_3$(CO)$_9$(μ_3-S)$_2$] (**4.1S**)^{MeCN}	-0.94	-1.75	+0.80	-	-
[Fe$_3$(CO)$_9$(μ_3-Se)$_2$](**4.1Se**)	-1.03	-1.68	+1.10	-	-
[Fe$_3$(CO)$_9$(μ_3-Se)$_2$](**4.1Se**) ^{MeCN}	-0.96	-1.70	+0.80	-	-
[Fe$_3$(CO)$_9$(μ_3-Te)$_2$](**4.1Te**)	-0.97	-1.51	-	-	-
[Fe$_3$(CO)$_7$(μ_3-CO)(μ_3-S)(μ_3-dppm)](**4.2S**)	-1.29	-	+0.81		-
[Fe$_3$(CO)$_7$(μ_3-CO)(μ_3-S)(μ_3-dppm)](**4.2S**) ^{MeCN}	-1.16	-	+0.20	-	-
[Fe$_3$(CO)$_7$(μ_3-CO)(μ_3-Se)(μ_3-dppm)](**4.2Se**)	-1.30	-	+0.55	+1.00	-
[Fe$_3$(CO)$_7$(μ_3-CO)(μ_3-Se)(μ_3-dppm)](**4.2Se**)^{MeCN}	-1.15	-	+0.28	-	-
[Fe$_3$(CO)$_9$(μ_3-Te)$_2$(PPh$_3$)](**4.3**)	-1.24	-2.01	-	-	-
[Fe$_3$(CO)$_7$(μ_3-S)$_2$(μ_2-dppm)](**4.4S**)	-1.55	-	+0.36	+0.57	-
[Fe$_3$(CO)$_7$(μ_3-Se)$_2$(μ_2-dppm)](**4.4Se**)	-1.45	-2.13	+0.38	+0.63	-
[Fe$_3$(CO)$_7$(μ_3-Te)$_2$(μ_2-dppm)](**4.4Te**)	-1.37	-1.77	+0.53	-	-
[Fe$_3$(CO)$_7$(μ_3-Te)$_2$(μ_2-dcpm)](**4.5**)	-1.51	-1.84	+0.34	+0.51	-
[Fe$_3$(CO)$_7$(μ_3-Te)$_2$(μ_2-dppa)](**4.6**)	-1.07	-1.58	-0.45	+94	-
[Fe$_3$(CO)$_8$(μ_3-Te)$_2$(μ-dppe)](**4.7**)	-1.80	-	+0.38	+0.50	+0.78
[Fe$_3$(CO)$_8$(μ_3-Te)$_2$(μ-dppv)](**4.8**)	-1.89	-	+0.33		-
[Fe$_3$(CO)$_8$(μ_3-Te)$_2$(μ-dppb)](**4.9**)	-1.85	-	+0.38	+0.55	+0.79
[Fe$_3$(CO)$_8$(μ_3-Te)$_2$(μ-dppp)](**4.10**)	-1.95	-	+0.38	-	-
[Fe$_3$(CO)$_8$(μ_3-Te)$_2$(μ-dppf)](**4.11**)	-1.72	-	-	-	-
[Fe$_3$(CO)$_8$(μ_3-Te)$_2$(μ-dppbn)](**4.12**)	-1.80	-	+0.14	+0.47	+0.87

Table 4.1 CVs data of complexes **4.1**–**4.12** in 1 mM solution in CH$_2$Cl$_2$, supporting electrolyte [NBu$_4$][PF$_6$], scan rate 0.25 Vs^{-1}, glassy carbon electrode, potential vs. Fc$^+$/Fc).

Complex	Reduction potential (V)			
	1st	2nd	3rd r	4th
$[Fe_3(CO)_9(\mu_3\text{-}S)_2]$ (**4.1S**)	-1.30	-	-	-
$[Fe_3(CO)_9(\mu_3\text{-}Se)_2]$(**4.1Se**)	-1.17	-1.78	-2.16	-
$[Fe_3(CO)_9(\mu_3\text{-}Te)_2]$(**4.1Te**)	-1.06	-1.53	-2.19	-
$[Fe_3(CO)_7(\mu_3\text{-}CO)(\mu_3\text{-}S)(\mu_3\text{-}dppm)]$(**4.2S**)	-1.36	-1.85	-2.10	-
$[Fe_3(CO)_7(\mu_3\text{-}CO)(\mu_3\text{-}Se)(\mu_3\text{-}dppm)]$(**4.2Se**)	-1.40	-1.82	-1.92	-
$[Fe_3(CO)_9(\mu_3\text{-}Te)_2(PPh_3)]$(**4.3**)	-1.31	-2.03	-2.23	-
$[Fe_3(CO)_7(\mu_3\text{-}S)_2(\mu_2\text{-}dppm)]$(**4.4S**)^{MeCN}	-1.51	-1.67,	-1.92	2.22
$[Fe_3(CO)_7(\mu_3\text{-}S)_2(\mu_2\text{-}dppm)]$(**4.4S**)	-1.70	-1.94	-2.12	-2.28
$[Fe_3(CO)_7(\mu_3\text{-}Se)_2(\mu_2\text{-}dppm)]$(**4.4Se**)^{MeCN}	-1.55,	-1.78,	-2.07	-2.10
$[Fe_3(CO)_7(\mu_3\text{-}Se)_2(\mu_2\text{-}dppm)]$(**4.4Se**)	-1.59	-2.16	-2.28	-
$[Fe_3(CO)_7(\mu_3\text{-}Te)_2(\mu_2\text{-}dppm)]$(**4.4Te**)	-1.45	-1.80	-	-
$[Fe_3(CO)_7(\mu_3\text{-}Te)_2(\mu_2\text{-}dcpm)]$(**4.5**)	-1.62	-1.99	-	-
$[Fe_3(CO)_7(\mu_3\text{-}Te)_2(\mu_2\text{-}dppa)]$(**4.6**)	-0.98	-1.24	-1.61	-
$[Fe_3(CO)_8(\mu_3\text{-}Te)_2(\mu\text{-}dppe)]$(**4.7**)	-1.53	-1.91	-2.18	-
$[Fe_3(CO)_8(\mu_3\text{-}Te)_2(\mu\text{-}dppv)]$(**4.8**)	-1.52	-1.93	-	-
$[Fe_3(CO)_8(\mu_3\text{-}Te)_2(\mu\text{-}dppb)]$(**4.9**)	-1.48	-1.90	-1.98	-
$[Fe_3(CO)_8(\mu_3\text{-}Te)_2(\mu\text{-}dppp)]$(**4.10**)	-1.48	-1.90	-	-
$[Fe_3(CO)_8(\mu_3\text{-}Te)_2(\mu\text{-}dppf)]$(**4.11**)	-1.53	-1.75	-2.15	-
$[Fe_3(CO)_8(\mu_3\text{-}Te)_2(\mu\text{-}dppbn)]$(**4.12**)	-1.45	-1.80	-2.10	-

Table 4.2 Observed potentials for onset of catalytic proton reduction by **4.1**–**4.12** in the absence and presence of 1–45 molar equivalents of TsOH (1 mM solution in CH_2Cl_2, supporting electrolyte $[NBu_4][PF_6]$, scan rate 0.25 Vs^{-1}, glassy carbon electrode, potential vs. Fc$^+$/Fc).

The electrochemical behaviour of clusters $[Fe_3(CO)_8(\mu_3\text{-}Te)_2(\mu\text{-}dppe)]$ (**4.7**), $[Fe_3(CO)_8(\mu_3\text{-}Te)_2(\mu\text{-}dppb)]$ (**4.9**) and $[Fe_3(CO)_8(\mu_3\text{-}Te)_2(\mu\text{-}dppbn)]$ (**4.12**) are very similar, three irreversible oxidation waves being observed. In contrast, clusters $[Fe_3(CO)_8(\mu_3\text{-}Te)_2(\mu\text{-}dppv)]$ (**4.8**), $[Fe_3(CO)_8(\mu_3\text{-}Te)_2(\mu\text{-}dppp)]$ (**4.10**) and $[Fe_3(CO)_8(\mu_3\text{-}Te)_2(\mu\text{-}dppf)]$ (**4.11**) showed somewhat different electrochemical behaviour. Clusters **4.7-4.12** each undergo irreversible reduction at between -1.72 and -1.95 V at all scan rates, and all catalyse proton reduction at their first reduction potentials. A third catalytic peak also appeared with increasing acid concentration, this reduction potential shifted towards more positive potentials (see Table 4.2) possibly due to either protonation or increased polarity of the medium with increasing acid concentration. Thus, the

potentials for onset of catalytic proton reduction occur at ca. 1 V more positive potential than for the uncatalyzed proton reduction.

4.7 Summary and Conclusions

Comparative studies of four different types of the chalcogenide-capped triiron clusters and their phosphine derivatives as proton reduction catalysts have been discussed in this Chapter. The parent clusters $[Fe_3(CO)_9(\mu_3\text{-}E)_2]$ (**4.1**) (E = S, Se, Te) and diphosphine complexes $[Fe_3(CO)_7(\mu_3\text{-}CO)(\mu_3\text{-}E)(\mu\text{-}dppm)]$ (**4.2**) (E = S, Se), $[Fe_3(CO)_7(\mu_3\text{-}E)_2(\mu\text{-}diphosphine)]$ (**4.4-4.6**) (E = S, Se, Te) (Paper II-III) and $[Fe_3(CO)_8(\mu_3\text{-}Te)_2(\kappa^2\text{-}diphosphine)]$ (**4.7-4.12**) (Paper IV). It is observed that the nature of the chalcogenide has a small but, in some instances, significant effect on the triiron core and consequent proton reduction ability. The main findings are summarized below:

(i) The comparative study on the electrochemical and electrocatalytic properties of $[Fe_3(CO)_9(\mu_3\text{-}E)_2]$ (**4.1**) (E = S, Se, Te) demonstrated that the tellurium-containing cluster is reduced at lower potentials and shows better stability and reversibility than the sulfur and selenium analogues. For example, **4.1Te** reduces at -1.06 V, **4.1Se** at -1.17 V and **4.1S** at -1.30 V in the presence of a proton source in CH_2Cl_2. The first catalytic reduction potentials occur in at ca. 0.25 V lower potential for **4.1Te** than for **4.1S** and **4.1S**e. The ability of these complexes to act as catalysts for the reduction of protons to hydrogen increases in the order, Te > Se > S. The same behaviour has been observed for diiron chalcogenide clusters.[109-113]

(ii) A similar behaviour to that described in (i) is observed for the diphosphine derivatives. Electrocatalytic proton reduction studies on $[Fe_3(CO)_7(\mu_3\text{-}E)_2(\mu\text{-}diphosphine)]$ (**4.4**) (E = S, Se, Te) show that **4.4Te** reduces at -1.45 V, **4.4Se** at -1.59 V and **4.4S** at -1.70 V.

(iii) The mono-chalcogenide capped clusters **4.2** (E = S, Se) are reduced at relatively lower potential than the di-chalcogenide bicapped clusters **4.4** (E = S, Se) (Paper II). The triply bridging CO is a site of Lewis basicity, reacting with the Lewis acid BF_3, while the triiron core is not basic enough to bind a proton even upon addition of strong Brönsted acids.

Chapter 5 Phosphido-bridged diiron and phosphinidene capped triiron clusters as proton reduction catalysts (Papers V-VI).

5.1 Background

As described in the previous Chapter, the chemistry of iron chalcogenato and chalcogenide complexes has been extensively explored in the context of biomimics of hydrogenase enzymes. Comparatively less attention has been paid to iron phosphido and phosphinidene complexes which bear both structural and electronic similarities to chalcogenide complexes.

The chemistry of electron-poor bicapped phosphido-containing diiron clusters have attracted extensive interest but their electrochemical and electrocatalytic behaviour are little studied as yet[114-120] although a few iron diphosphido complexes have been investigated as proton reduction catalysts.[121-128] Best and coworkers investigated $[Fe_2(\mu-PPh_2)_2(CO)_6]$ as an electrocatalyst for proton reduction. Two catalytic waves for proton reduction at -1.4V and -1.7 V (*vs* SCE) were found, the first wave grew from the primary two-electron reduction of the Fe_2P_2 dimer observed in the absence of acid.[125] Similarly, the linked phosphido-bridged analogue $[Fe_2(\mu,\mu-PPh(CH_2)_3(PPh)(CO)_6]$ exhibited a single reduction wave at -1.52 V corresponding to a two election reduction process. In the presence of *p*-TsOH the complex displayed electrocatalytic proton reduction waves at -1.55 V and -1.68 V (*vs* SCE). The electrochemical current at the first process was limited by the low rate for hydrogen production from $[Fe_2(\mu,\mu-PPh(CH_2)_3(PPh)(CO)_6H_2]$, but further reduction of this species resulted in rapid evolution of dihydrogen.[122] Shi and coworker reported the complex $[Fe_2(\mu-PPh_2)_2(CO)_6(\mu-k^2O,P-OPPh_2)]$ showed two irreversible reduction waves at -1.48 and -2.13V (*vs* Fc$^+$/Fc)[127] Colbran and coworkers have investigated proton reduction by diiron diphosphido species based on the primary phosphine FcPH$_2$ (Fc = ferrocenyl). The complexes $[Fe_2\{\mu_2-P(CH_2Fc)H\}_2(CO)_6]$ and $[Fe_2\{\mu_2-P(CH_2Fc)Me\}_2(CO)_6]$ (Figure 5.1)[128] catalyzed the reduction of protons at -2.18 and -2.11V (vs Fc$^+$/Fc), respectively, in the presence of *p*-TsOH in THF.

The reaction proceeds via the formation of a radical anion, that was detected *in situ*, by EPR spectroscopy. Subsequent slow elimination of H$_2$ yields the $[Fe_2\{\mu_2-P(CH_2Fc)H\}\{\mu_2-P(CH_2Fc)\}(CO)_6]^-$ anion in which one of the bridging

phosphido moieties has been deprotonated to a give μ-phosphinidene bridge (Scheme 5.1).
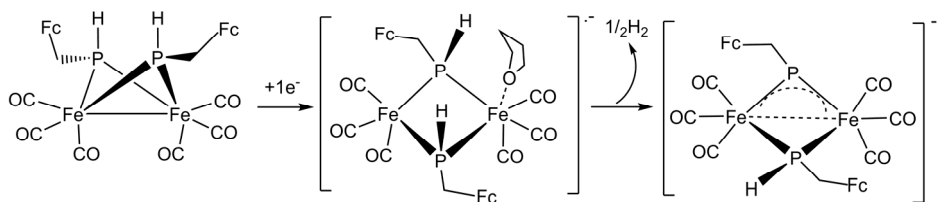
Scheme 5.1 The formation of the radical anion of $[Fe_2\{\mu_2\text{-}P(CH_2Fc)H\}_2(CO)_6]$ and its subsequent elimination of H_2.

In the presence of a proton source, protonation of the radical anion, and spontaneous reduction was proposed to lead to hydrogen elimination. Reprotonation of the product anion at phosphorus would then regenerate neutral cluster and close the catalytic cycle (Scheme-5.2).
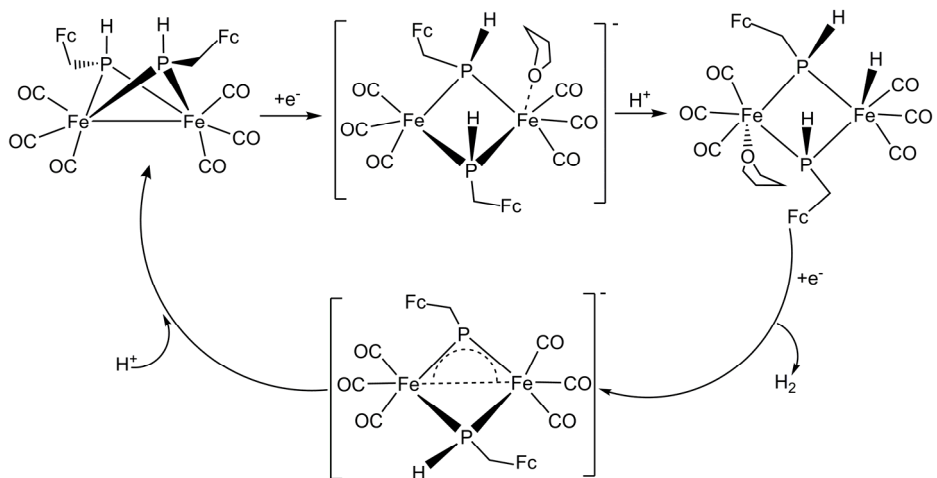
Scheme 5.2 Proposed catalytic pathway for dihydrogen evolution catalyzed by $[Fe_2\{\mu_2\text{-}P(CH_2Fc)H\}_2(CO)_6]$.[128]

5.2 Synthesis and characterization of diiron di-phosphido clusters

As discussed above, Colbran and co-workers had described the use of ferrocenyl-substituted phosphido-bridged diiron complexes as proton reduction catalysts.[128] Ferrocene potentially acts as an electron reservoir. Therefore, it was of interest to investigate other phosphido-bridged diiron dimers based on primary phosphines without electron donor substituents. Moreover, there are potentially three different structural isomers for the dimers of a specific primary phosphine (see Scheme 5.3) and it was interesting to see whether the isomers would give different chemistry and exhibit different electrocatalytic activities in proton reduction.
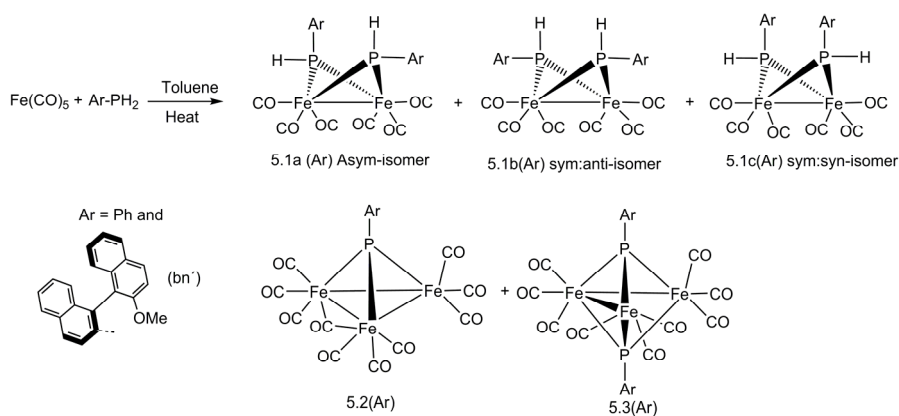
Scheme 5.3 Syntheses of the diiron isomers **5.1(a-c)** and the triiron clusters **5.2** and **5.3**.

Therefore, the clusters *asym*-[Fe$_2$(CO)$_6${(μ_2-P(Ar)H}$_2$] (**5.1a**, **Ar = Ph**, **bn′**), *sym:anti* [Fe$_2$(CO)$_6${(μ_2-P(Ar)H}$_2$] (**5.1b**, **Ar = Ph**, **bn′**), *sym:anti* [Fe$_2$(CO)$_6${(μ_2-P (Ar)H}$_2$] (**5.1c, Ar = Ph**), [Fe$_3$(CO)$_9$(μ_3-CO)(μ_3-PAr)] (**5.3, Ar = bn′**) and [Fe$_3$(CO)$_9$(μ_3-PAr)$_2$] (**5.3, Ar = Ph**, **bn′**) (**bn′** = 2′-methoxy-[1, 1′-binaphthalen]-2-ylphosphine) were synthesized by reaction of [Fe(CO)$_5$] with the respective primary phosphine (Scheme 5.3). In this work, the phenyl phosphido-bridged diiron dimers, **5.1(a, b)**, were isolated for the first time. The dimers, **5.1(a-c)**, were first identified in a mixture (not isolated) by Stelzer and coworkers.[118] It is also noteworthy that the isomers **5.1(a, b)** derived from the air-stable primary phosphine bn'PH$_2$ were also cleanly isolated.

The clusters **5.1(a-b)-5.3** were characterized by standard spectroscopic techniques (see paper V). Complexes **5.1a (Ar = Ph)**, **5.1b (Ar =Ph, bn´) 5.2 (Ar = bn´)** and **5.3 (Ar = Ph)** were also structurally characterized by single crystal X-ray diffraction studies (Figure 5.2).

asym-[Fe$_2$(CO)$_6${(μ_2-P(Ph)H}$_2$] (**5.1a(Ph)**)   *sym:anti*-[Fe$_2$(CO)$_6${(μ_2-P(Ph)H}$_2$] (**5.1b(Ph)**)

sym:anti-[Fe$_2$(CO)$_6${(μ_2-P(bn')H}$_2$] (**5.1b(bn')**)   [Fe$_3$(CO)$_9$(μ_3-CO)(μ_3-Pbn')] (**5.3(bn')**)
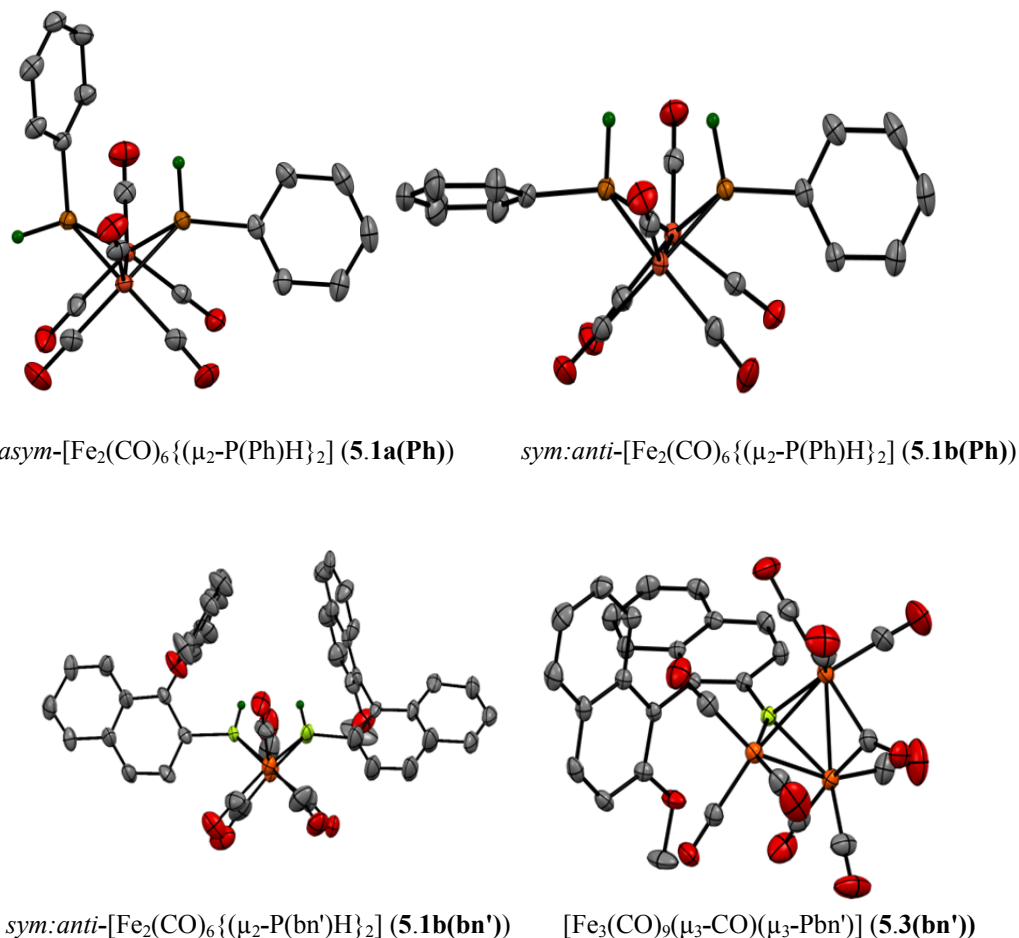
Figure 5.2 The molecular structures of the di-phosphido diiron carbonyl dimers *asym* **5.1a (Ar = Ph)** and *sym:anti*- **5.1b (Ar = Ph, bn')**, and of the triiron carbonyl cluster (**5.2bn´**).

The ^{1}H NMR spectra of the four Fe$_2$P$_2$ dimers **5.1** are not straightforward; in each case, a complicated second-order set of signals for an A$_2$(M)$_2$X$_2$ or AB(MN)XY (A, B, M, N = ^{1}H and X, Y = ^{31}P, see Figure 5.3 for an example)

61

spin system is observed for the phosphido protons, which was unravelled by simulation.
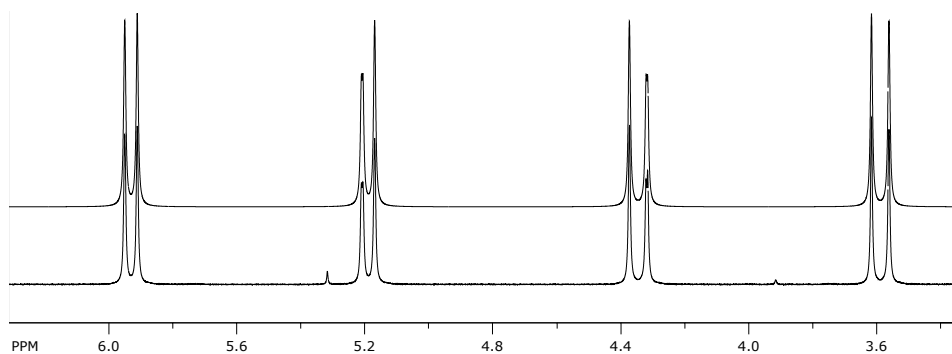
Figure 5.3 Experimental (bottom trace) and simulated (top trace) 500 MHz ^{1}H NMR spectra over the P–H region for **5.1a (Ar = Ph)**.

5.3 Synthesis and characterization of phosphinidene-dicapped triiron clusters (paper VI)

The chemistry of transition metal clusters having phosphinidene (PR) ligands has been of considerable interest in the organometallic research area.[129-131] The phosphinidene ligand is very versatile: for example, it can act as a two-electron or four-electron donor and can bind from one to four metal atoms in many different coordination modes, as depicted in Chart-5.1. The chemistry of phosphinidene-capped triiron clusters has been relatively thoroughly studied,[132-143] but their electrochemical and electrocatalytic behaviour remains relatively poorly investigated.

Perkinson *et al.*[139] have reported that triiron phosphinidene clusters [Fe$_3$(CO)$_9$(μ_3-P-*p*-C$_6$H$_4$X)(μ_3-P-*p*-C$_6$H$_4$X´) (X = X´ = NMe$_2$, OCH$_3$, Cl, CF$_3$, CN)] showed quasi-reversible electrochemical behavior with two one-electron reduction waves. The clusters with electron-withdrawing substituents in the *para* position of the phenylphosphinidene moiety were found to be reduced at more positive potentials than those with electron-donating substituents.
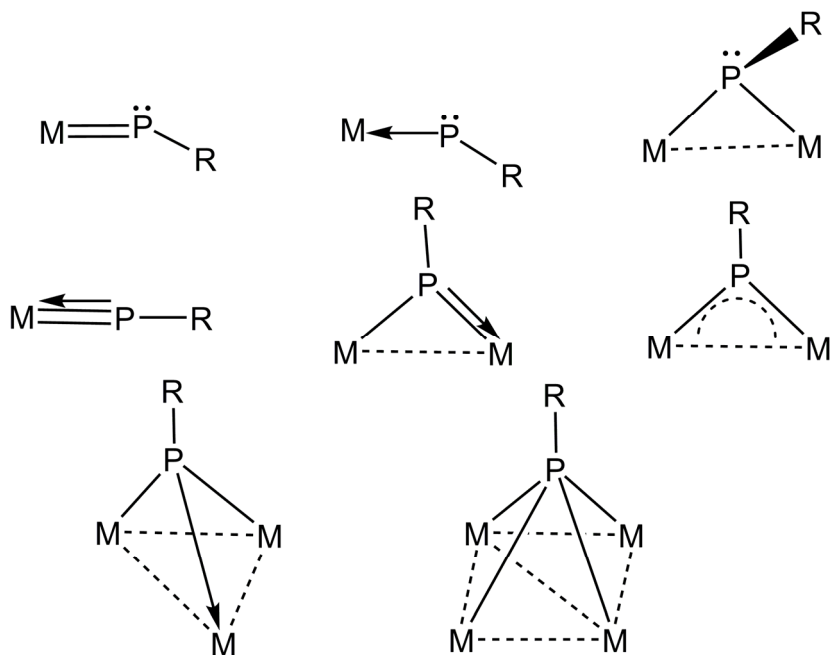
Chart 5.1 Different modes of metal binding by a phosphinidene (PR) ligand.

Ohst and Kochi[141] showed that the cluster $[Fe_3(CO)_9(\mu_3\text{-}PPh)_2]$ (**5.3**) (and its derivatives) undergoes successive, reversible one-electron reductions to produces the radical anion $[Fe_3(CO)_9(\mu_3\text{-}PPh)_2]^{\cdot-}$ and dianion $[Fe_3(CO)_9(\mu_3\text{-}PPh)_2]^{2-}$. These investigators also revealed that the radical was susceptible to opening of a phosphinidene bridge upon attack by even weak nucleophiles (*e.g.* THF solvent) and that the dianion readily protonated at phosphorus to afford $[Fe_3(CO)_9(\mu_3\text{-}PPh)(\mu_2\text{-}P(Ph)H]^-$. Given these results, further study of the catalytic properties of triiron phosphinidene clusters for the electro-reduction of protons, and the influence of suitable introduction of non-carbonyl ligands on the reactivity of the clusters, was deemed of considerable interest.

In order to investigate the capacity of a phosphinidene-capped triiron cluster to function as a proton reduction catalyst, the known bis-phosphinidene cluster $[Fe_3(CO)_9(\mu_3\text{-}PPh)_2]$ (**5.3**) was prepared and a number of diphosphine derivatives of this cluster were synthesized. The diphosphine derivatives were prepared because it was anticipated that these more electron-rich clusters would be more easily protonated than **5.3** (see discussion in earlier Chapters 1, section 1.7). All clusters were characterized by standard spectroscopic methods (see

paper VI). In addition, the minor products $[Fe_3(CO)_8(\mu_3\text{-PPh})_2(\kappa^1\text{-diphosphine})]$ (diphosphine = dppb, dppe, dppf) with a dangling diphosphine ligand were identified on the basis of IR and $^{31}P\{^1H\}$ NMR and spectroscopy. In addition, crystal structures could be determined for the cluster $[Fe_3(CO)_9(\mu_3\text{-PPh})_2]$ (**5.3**) (previously reported[143] but for a different polymorph), $[Fe_3(CO)_7(\mu_3\text{-PPh})_2(\kappa^2\text{-dppv})]$ (**5.4**), $[Fe_3(CO)_7(\mu_3\text{-PPh})(\mu_3\text{-}1\kappa^1\text{-}O,2,3\text{-}\kappa^2P\text{-}(OPPh_2)(1\kappa^2\text{-dppb})]$ (**5.5**) and $[Fe_3(CO)_7)(\mu_3\text{-PPh})_2(\mu\text{-dppf})]$ (**5.7**); (see Figure 5.4).

$[Fe_3(CO)_9(\mu_3\text{-PPh})_2]$ (**5.3**) $[Fe_3(CO)_7(\mu_3\text{-PPh})_2(\kappa^2\text{-dppv})]$ (**5.4**)

$[Fe_3(CO)_7(\mu_3\text{-PPh})(\mu_3\text{-}1\kappa^1\text{-}O,2,3$
$\kappa^2P\text{-}(OPPh_2)(1\kappa^2\text{-dppb})]$ (**5.5**) $[Fe_3(CO)_7)(\mu_3\text{-PPh})_2(\kappa^2\text{-dppf})]$ (**5.7**)
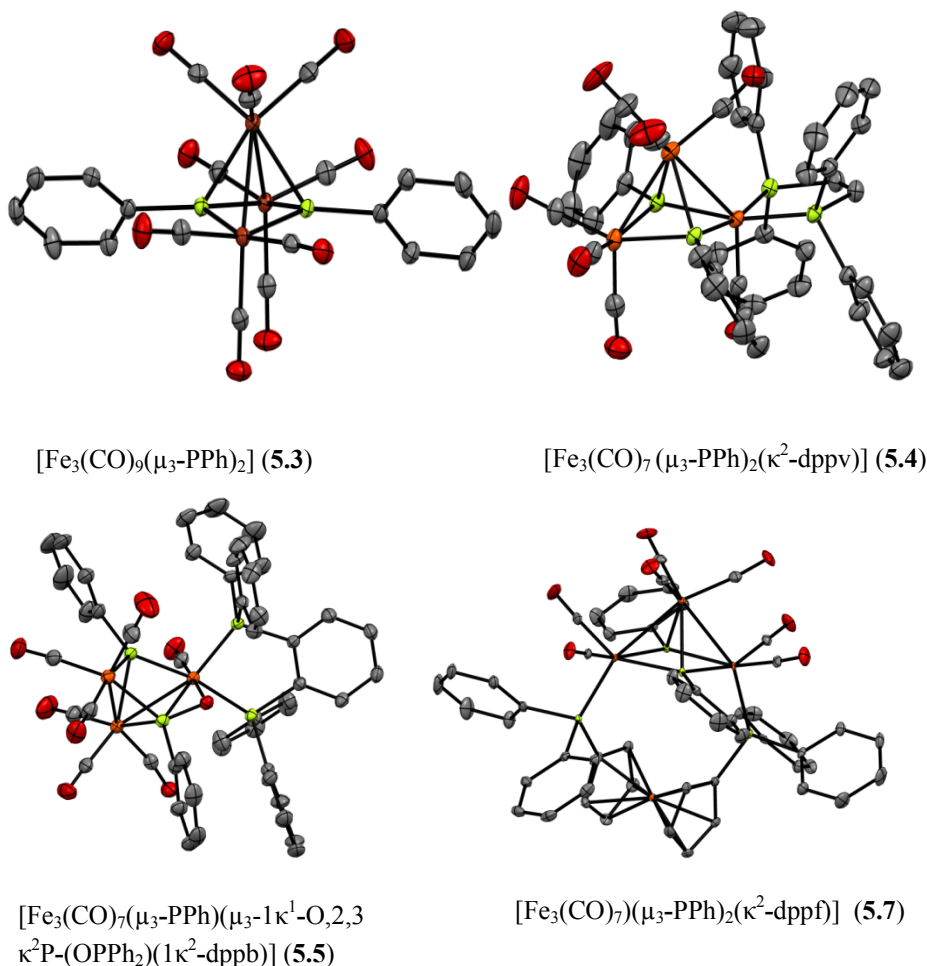
Figure 5.4 The molecular structure of bis(phosphinidene)-capped triiron carbonyl clusters **5.3Ph** and the electron rich diphosphine derivatives **5.4**, **5.5** and **5.7**.

5.4 Electrochemistry and electrocatalytic studies of diiron diphosphido carbonyl dimers (Paper V)

The electrochemical properties of the various isomers of the diiron diphosphido clusters **5.1(a-b)** (*cf.* Scheme 5.3) in tetrahydrofuran were investigated, and the findings may be summarized as follows (Paper V):

(i) Cyclic voltammograms of the asymmetric isomer **5.1a(Ph)** and the symmetric *anti*-isomers (*sym:anti*-) **5.1b(Ph)** and **5.1b(bn')** reveal essentially the same electrochemical behaviour: *i.e.,* a one-electron primary reduction at *ca.* -1.9 V, as well as some small peaks in the reverse positive sweep for oxidation of the reduction product(s). The primary reduction was irreversible for isomers **5.1a,b(Ph)** but exhibited some chemical reversibility for **5.1a,b(bn')**.

(ii) As the diphosphido dimers **5.1a(Ph), 5.1b(Ph), 5.1a(bn'), 5.1b(bn')** all exhibit a primary one-electron reduction process similarly to *sym:anti*-$[Fe_2(CO)_6\{\mu_2\text{-}P(CH_2Fc)H\}_2]$,[128] it appears that such one-electron reduction processes are common for $Fe_2(CO)_6$ dimers with primary phosphido bridges, irrespective of the orientation of the P–H bonds with respect to the Fe_2 core.
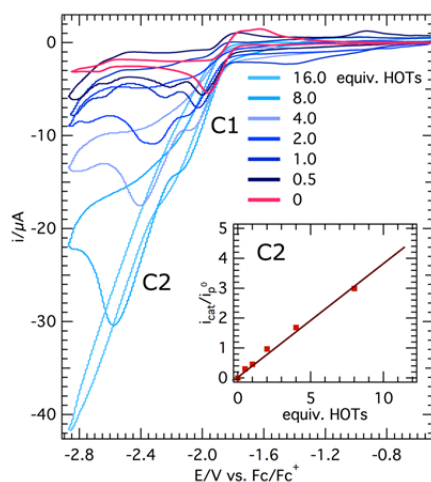
Figure 5.5. Electrocatalysis of proton reduction: CVs of *asym*-$[Fe_2(CO)_6\{\mu_2\text{-}P(bn')H\}_2]$ **5.1a(bn')** (1.0 mM) and added TsOH. Inset: Catalytic current ratio data for the catalytic wave *C2* versus equiv. of added acid.

(iii) In the presence of *p*-toluene sulfonic acid (*p*-TsOH) as a proton source, clusters **5.1** act as electrocatalysts for proton reduction. The currents for the first

reduction process and for a new second reduction peak increase with increasing
p-TsOH, consistent with catalysis of proton reduction (see Figure 5.5).

5.5 Electrochemistry and electrocatalytic studies of triiron bis(phosphinidene)-capped clusters (Paper VI)

The electrochemical behaviours of all bis(phosphinidene)-capped triiron
carbonyl clusters **5**.**3**–**5**.**7** were investigated, primarily to determine reduction
potentials at which electrocatalytic proton reduction activity in dichloromethane
was observed. Cluster **5**.**3** reveals two quasi-reversible, one-electron reduction
processes at -1.39 and -1.66 V, which is the same as previously reported for this
cluster.[139,141] The new diphosphine-substituted clusters **5**.**4** and **5**.**5** exhibited
quasi-reversible oxidation and reduction processes, at -1.57 V and +0.11 V for
5.**4** and at -1.57 V and +0.12 V for **5**.**5,** which differs from the two consecutive
reductions observed for parent cluster **5**.**3**. The reduction potentials of **5**.**4** and
5.**5** shift to more negative values due to the increasing electron density in the
cluster core upon diphosphine substitution. The cyclic voltammograms of
$[Fe_3(CO)_7](\mu_3\text{-}PPh)_2(\mu\text{-}dppe)]$ (**5**.**6**) exhibited a quasi-reversible first oxidation
couple at +0.08 V followed by second oxidation couple at +0.36 V, which
diminished in current with increasing scan rate. To negative potential, cluster
5.**6** revealed a quasi-reversible first reduction couple at –1.55 V followed by a
second reduction couple at –1.88 V. The current dependencies of the second
reduction and the second oxidation couples with scan rate indicated these
processes arose from species produced by chemical steps following the
reduction and the oxidation of **5**.**6**, respectively. Cyclic voltammograms of the
diphosphino-ferrocene-substituted triiron cluster **5**.**7** revealed three consecutive
quasi-reversible oxidation waves and one quasi-reversible reduction wave with
the reduction potential shifted to more negative than the values for the primary
reductions of **5**.**3**–**5**.**6**.

The electrocatalytic activity of complexes **5**.**3**–**5**.**7** towards proton reduction was
investigated by cyclic voltammetry in the presence of *p*-toluene sulfonic acid (*p*-
TsOH). Upon addition of increasing amounts of acid to cluster **5**.**3**, both the
reversibility of the first and second reduction couples was lost, accompanied by
increasing cathodic currents. In addition, two new peaks with high cathodic
current appeared at quite negative potentials. With increasing acid
concentration, the new (third and fourth) catalytic reduction waves substantially
increased in current and shifted to more negative direction.
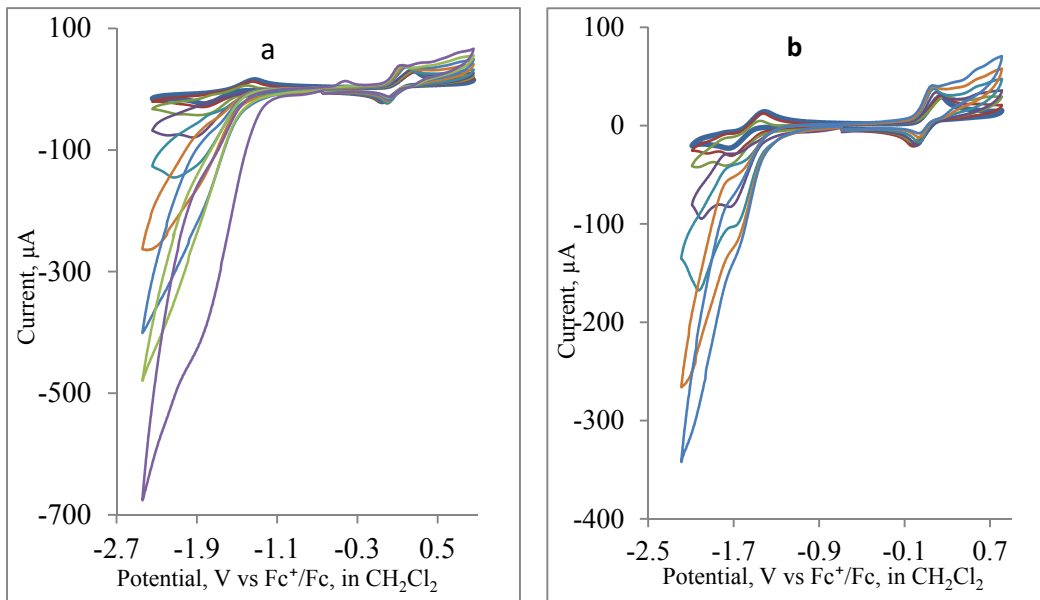
Figure 5.6 (CVs of complexes (a) **5.4** and (b) **5.5**, in the absence and presence of 1–19 molar equivalents of *p*-TsOH (1 mM solution in CH_2Cl_2 supporting electrolyte $[NBu_4][PF_6]$, scan rate 0.25 Vs^{-1}, glassy carbon electrode, potential vs. Fc^+/Fc).

Both clusters **5**.**4** and **5**.**5** show similar electrochemical responses to increasing amounts of acid and act as proton reduction catalysts (see figure 5.6). The chemical reversibility of the first reduction couple disappeared within the addition of one equivalent of acid. Both the first and second processes were found to show increasing cathodic current indicative of catalysis of proton reduction with increasing acid concentration. The oxidation couples of **5**.**4** and **5**.**5** are broadened, but are otherwise unperturbed, by increasing amounts of acid. For cluster **5**.**6** it was also observed that the cathodic currents of the first and second reductions increased with the concentration of acid, again suggestive for catalysis of proton reduction. The result indicates that both **5**.**6** $^{\bullet-}$ and **5**.**6**$^{2-}$ are catalytically competent species (see figure 5.7). A third reduction process was also observed and at higher acid concentrations dominates the current for proton reduction.
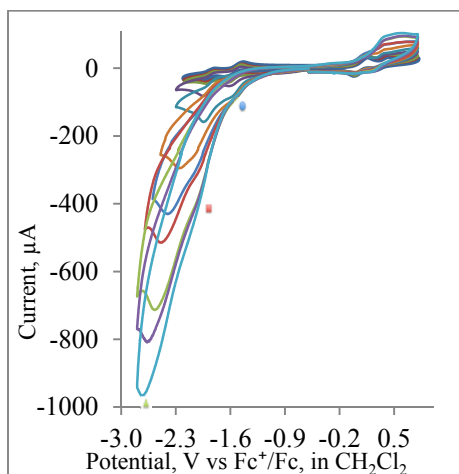
Figure 5.7 CVs of complex **5.6** (2mM) in the absence and presence of 1–45 molar equivalents of *p*-TsOH (100 mM) in CH_2Cl_2 – 0.1 mM $[NBu_4][PF_6]$; scan rate 0.25 Vs^{-1}, glassy carbon electrode, potential *vs*. the Fc^+/Fc couple.

5.6 Summary and Conclusions

The diphosphido diiron clusters *asym*-$[Fe_2(CO)_6\{(\mu_2\text{-}P(Ar)H\}_2]$ (**5.1a, Ar = Ph**), *sym:anti* $[Fe_2(CO)_6\{(\mu_2\text{-}P\ (Ar)H\}_2]$ (**5.1b, Ar = Ph, bn'**) and triiron cluster $[Fe_3(CO)_9(\mu\text{-}CO)(\mu\text{-}PAr]$ (**5.2, Ar = bn´**), all the clusters have been prepared, and fully characterized. Similarly, the bis(phosphinidene)-capped triiron carbonyl clusters $[Fe_3(CO)_9(\mu_3\text{-}PPh)_2]$ (**5.3**, **Ph**), including electron rich derivatives $[Fe_3(CO)_7(\mu_3\text{-}PPh)_2(\kappa^2\text{-}dppv)]$ (**5.4**), $[Fe_3(CO)_7(\mu_3\text{-}PPh)(\mu_3\text{-}1\kappa^1\text{-}O,2,3\text{-}\kappa^2P\text{-}(OPPh_2)(1\kappa^2\text{-}dppb)]$ (**5.5**) and $[Fe_3(CO)_7)(\mu_3\text{-}PPh)_2(\kappa^2\text{-}dppf)]$ (**5.7**) formed by substitution with chelating diphosphines clusters have been prepared, and fully characterized in this thesis. All clusters are capped by an anti-arrangement of two triply bridging μ_3-PPh$_2$ ligands, with the exception of cluster **5.5** where one phosphinidene has been converted to an unusual phosphinidoxo (κ^1-O,κ^2P-(OPPh)) ligand.

The electrochemical and electrocatalytic properties of all diiron carbonyl dimers was studied using cyclic voltammograms of the complexes in tetrahydrofuran. The dimers **5**.**1a(Ph)**, **5**.**1b(Ph)** and **5**.**1b(bn')** with primary phosphido bridges showed a broad and irreversible first reduction potential peak at –1.8 to –2.0 V for a one-electron process, which is the same reduction behaviour as was observed for $[(CO)_6Fe_2\{\mu\text{-}P(CH_2Fc)H\}_2]$.[128] *Asym*-**1a(bn')** revealed a quasi-reversible one-electron process, which was different from the other dimers. In

68

the presence of acid (*p*-TsOH), all of the dimers show similar behaviour with two consecutive catalytic waves for catalysis of proton reduction appearing in the cyclic voltammograms.

The triiron carbonyl cluster **5.3** exhibited two one electron quasi-reversible reduction waves. Upon addition of *p*-TsOH, cluster **5.3** shows a first catalytic wave at -1.57 V and two further proton reduction processes at -1.75 and -2.29 V, each with a good current response. The diphosphine-substituted derivatives **5.5**-**5.7** were reduced at more negative potentials than the parent cluster **5.3** due to the increase electron density on the triiron core. Clusters **5.4** and **5.5** show similar electrochemical properties to each other, but upon addition of acid, reduction of **5.5** occured at lower potential by *ca*. 0.1 V than for **5.4**. Cluster **5.6** exhibited different electrochemical behaviour with a good current response. Cluster **5.7** does not show any catalytic activity for proton reduction in the presence of *p*-TsOH. The phosphine substitution increases the electron density on the iron center but does not lead to lower overpotential for proton reduction.

The neutral phosphinidene-capped triiron clusters do not react with *p*-TsOH. As discussed above, Ohst and Kochi[141] reported that the dianion radical of the parent cluster **5.3** is protonated directly at the phosphinidene cap at -78°C. In the electrocatalytic experiments, the first and second proton reduction processes leading to formation of **5.3$^-$** and **5.3^{2-}** may be followed by protonation steps at both a phosphinidene cap and at a metal center (generating a hydride). Subsequent loss of dihydrogen may regenerate **5.3$^-$** and **5.3^{2-}** as active catalytic species.

A comparison of the electrochemical and electrocatalytic properties of of the phosphinidene-dicapped clusters $[Fe_3(CO)_9(\mu_3\text{-}E)_2]$ (E = PPh) with the analogous clusters $[Fe_3(CO)_9(\mu_3\text{-}E)_2]$ (**4.1**) (E = S, Se, Te) reveals that the chalcogenide-containing clusters are reduced at lower potentials than the corresponding phosphinidine-capped cluster and its electron-rich diphosphine substituted derivatives. The electrochemical stability and reversibility of the phosphinidene-(di)capped triiron cluster $[Fe_3(CO)_9(\mu_3\text{-}PPh)_2]$ (**5.3**) are better than for its sulfido and selenido analogues and similar with the tellurido analogues. Phosphinidene-containing clusters may thus offer the advantage of better electrochemical properties, but the quite negative potentials required for the onset of electrocatalytic proton reduction catalyzed by triiron phosphinidene cluster(s) make such catalysts less attractive than the tellurido-containing clusters, which offer the same good electrochemical properties but considerably more positive potentials for the onset of proton reduction catalysis.

Chapter 6 Concluding remarks and future perspectives

6.1 Concluding remarks

Using a bio-inspired approach, the research described in this thesis has investigated the ability of iron carbonyl clusters to function as electrocatalysts for proton reduction. A number of new di- and trinuclear iron carbonyl clusters have been prepared; they comprise di and triiron-dithiolato clusters, chalcogenide-capped triiron clusters, diphosphido-bridged diiron clusters and phosphinidine-capped triiron clusters. All of these different types of clusters have been found to catalyze the electrochemical reduction of protons to molecular hydrogen. The main findings of this dissertation are summarized below;

(i) In Paper I, the mixed-valence triiron complexes $[Fe_3(CO)_{7-x}(PPh_3)_x(\mu\text{-edt})_2]$ (x = 0, 1, 2; edt = SCH_2CH_2S) and the diphosphine derivatives $[Fe_3(CO)_5(\kappa^2\text{-diphosphine})(\mu\text{-edt})_2]$ have been synthesized and characterized. These formally Fe(I)-Fe(II)-Fe(I) complexes undergo one- or two-electron oxidation and reduction processes, depending on reaction conditions. The one-electron reduced states of the complexes are catalysts for the reduction of protons to hydrogen and the catalytic overpotential depends upon successive phosphine substitution processes. Phosphine substitution pushes the catalytic response to more negative potentials; however, the payoff is that higher catalytic currents can be achieved. In comparison to their diiron analogues, the triiron complexes catalyze proton reduction at up to 0.36 V less negative potentials, which is a significant energetic gain. Electronic structure calculations show that the HOMO-LUMO separation is smaller in the triiron complex than in the diiron complex

(ii) Papers II-IV describe the synthesis of four different types of chalcogenide-capped triiron clusters and selected phosphine and diphosphine derivatives of these clusters. The clusters are $[Fe_3(CO)_9(\mu_3\text{-E})_2]$ (E = S, Se, Te), the mono-chalcogenide capped clusters $[Fe_3(CO)_7(\mu_3\text{-CO})(\mu_3\text{-E})(\mu\text{-dppm})]$ (E = S, Se), the dichalcogenide dicapped clusters $[Fe_3(CO)_7(\mu_3\text{-E})_2(\mu\text{-diphosphine})]$ and the dicapped clusters $[Fe_3(CO)_8(\mu_3\text{-Te})_2(\kappa^2\text{-diphosphine})]$. The clusters have been examined as proton reduction catalysts. A comparative study of the tellurium-containing clusters relative to those containing the lighter chalcogenides sulfur and selenium found that the tellurium-containing clusters are relatively better

stable. The tellurium-containing cluster are reduced at lower potential and show better stability and reversibility than their sulfur and selenium analogues, leading to electrocatalytic proton reduction taking place at lower overpotentials for the tellurium-containing clusters.

(iii) In Paper V, the structural orientation and the influence of the substitution of the primary phosphido-bridged diiron clusters $[Fe_2(CO)_6(\mu\text{-}PR_2)_2]$ on the ability of the clusters to act as proton reduction catalysts has been studied. All complexes display two consecutive catalytic waves for catalysis of proton reduction. The maximum current ratio for the first catalytic wave is related to the maximum catalytic rate of proton reduction and varies with phosphido substitution but not between the isomers of the diiron dimers.

(iv) In Paper VI, synthesis and characterization of the bis(phosphinidene)-capped triiron carbonyl clusters, including diphosphine derivatives have been studied and examined as proton reduction catalysts. Triiron phosphinidene dicapped cluster reduced lower potential than the electron rich diphosphine derivatives. All diphosphine derivatives reveal reduction potential shifted more negative potential due to the increasing electron density on the triiron core.

As expected, phosphine substitution did not lead to any gain in overpotential in the cluster described in this thesis. Instead, phosphine substitution increased the electron density on the iron center and the reduction potential and onset of electrocatalytic proton reduction are pushed to more negative potentials. The advantage of the substitution seems to be the higher catalytic currents that can be achieved with the phosphine substituted clusters, indicating a faster turnover.

6.2 Future perspectives

The present work has opened some new directions towards the development of catalysts for electrochemical proton reduction by modulating the reactivity of synthetic iron clusters by utilizing proper ligands. It is necessary to develop new clusters with lower overpotential and higher turnover frequencies. The reduction potential may be considerably improved on moving from two- to three-iron center clusters. It is likely to be important to improve the reduction potential and modify the active site of the complexes with ligand substitution; strongly electron-donating (di)phosphine ligands will need to be introduced in order to make the clusters more prone to protonation. On the other hand, electron-withdrawing ligands would be expected to make further improvements to the reduction

potential and perhaps create a catalyst for proton reduction with an excellent overpotential; this aspect needs to be further explored. In addition, more studies such as computational modelling, bulk electrolysis experiments, electron paramagnetic resonance (EPR) measurements, and spectroelectrochemical studies (IR, UV-Vis, EPR) are required to characterize the species involved and determine the proton reduction mechanism(s) for the catalysts discussed in this thesis, as well as for new catalysts being developed.

There is significant scope for improvement in the catalytic efficiency of bio-inspired catalysts for hydrogen production. The ultimate goal should be to develop relatively simple, readily available catalysts based on cheap iron that can be widely used in proton reduction, including industrial scale reactions for hydrogen production.

Populärvetenskaplig sammanfattning

En utveckling av den s. k. väte-ekonomin, där vätgas (H_2) används som energibärare, skulle – rent teoretiskt – kunna lösa människans energiproblem då vatten skulle kunna användas som bränsle. För att nå detta mål krävs dock väsentlig teknologisk och vetenskaplig utveckling. Ur ett rent vetenskapligt perspektiv, måste bl a (energisnåla) kemiska metoder att skapa stora mängder vätgas utvecklas. Många forskare söker att efterhärma de fundamentala biologiska reaktioner som sker i fotosyntesen, bl a oxidation av vatten till syrgas, protoner (vätejoner, H^+) och elektroner. Det är lika viktigt att kunna omvandla protoner och elektroner till vätgas på ett effektivt sätt, och intensivt forskningsarbete bedrivs för närvarande inom detta område. Denna forskning har hittills fokuserat på att efterhärma de aktiva säten (bestående av järn-nickel eller järnkluster) i vissa enzymer – hydrogenaser – som kan katalysera jämvikten $2 H^+ + 2 e^- \leftrightarrow H_2$ (i båda riktningar). Denna forskning har lett till en djupare förståelse av de fundamentala kemiska principerna för hydrogenasreaktionerna, men har *inte* lett till goda katalysatorer. I denna avhandling beskrivs framställandet av ett antal järnkomplex som innehåller två, tre eller fyra järnatomer, och som besitter liknande kemiska egenskaper som hydrogenas-enzymer. Likt vissa sådana enzymer, kan komplexen katalysera elektrokemisk reduktion av protoner som skapar vätgas, d v s driva ovanstående jämvikt åt höger. Med hjälp av elektrokemiska metoder, spektroskopiska studier och datorberäkningar har mekanismen för protonreduktion studerats och för ett flertal katalysatorer har det mest sannolika första steget i reaktionen kunnat fastställas, nämligen om komplexet först binder en proton eller erhåller en elektron (reduceras).

Acknowledgement

I would like to express my indebtedness and deepest sense of gratitude to my honorable supervisor **Professor Ebbe Nordlander**, for all your patience, encouragement, thoughtful suggestions, proper guidance and supervision throughout the progress of my research work. Thank you Ebbe for allowing me to work in the interesting research field and to visit U.K. and Australia to complete my research. Ebbe, I am indebted to you more than you know.

Dr. Graeme Hogarth, Department of Chemistry, King's College London, I am thankful to you Graeme for your enthusiasm in developing such a nice project, encouraging me in the work, your kindness in allowing me to work in your lab (University College London), discussing the electrochemistry and writing whenever I needed your help. I also thankful to **Professor Stephen B. Colbran,** School of Chemistry, University of New South Wales, Sydney, Australia, Your valuable suggestion for our phosphido and phosphinidine brigde project, your kindness in allowing me to work in your lab, discussing the electrochemistry and writing.

I would like to thank Prof. Matti Haukka, Department of Chemistry, University of Jyveskylä, Finland and Prof. Derek A. Tocher, Department of Chemistry, University College London, U.K. for solving the X-ray structures; Prof. Michael G. Richmond, Department of Chemistry, University of North Texas, USA, for your computational work and nice discussing the chemistry during your visit in Lund; Prof. George C. Lisensky, Department of Chemistry, Beloit College,USA, for your helping in electrochemistry setup and discussion during your visit in Lund; Dr. Lee Higham, School of Chemistry, Newcastle University, U.K. for the primary phosphine and Dr. Luca Zuppiroli of the Department of Organic Chemistry "A. Mangini", University of Bologna, Italy for recording mass spectra.

I like to thank my co-supervisor Prof. Sofi Elmroth for your kind assistance and attention whenever I need.
There are a number of respected teachers in the Chemical Physics Department that I would like to thank for their inspiration, providing different types of services that strongly facilitated my research project and for your kind assistance and attention whenever I need; Prof. Villy sundström, Tönu, Arkady, Ivan Scheblykin, Donatas, Per Uvdal and Torbjörn Pascher.

I express my heartiest and sincere thanks to my former honorable supervisor Professor Shariff Enamul Kabir, Member, Bangladesh Public Service Commission, former Vice-chancellor, Jahangirnagar University, who teach me how to do the research; for his encouragement, thoughtful suggestions, proper guidance. I also thankful to Professor Fakir

Rafiqul Alam, Department of Chemistry, National University, Gazipur, Dhaka for his guidance, inspiration and cooperation not only for my research work but also all the discussions covering small and large things in my life.

I convey special acknowledgment to Thomas and Maria for their indispensable help dealing with travel funds, administration and bureaucratic matters during my stay and also Katarina Fredriksson for her help to ordering chemical.

During my Ph D I had very nice time with so many good people around the world. I would like to thank all the present and past members of Nordlander group. In particular, Amrendra, Martin, Reena, Arup, shilpi, Kamlesh, Lotta, Erik, Mainak, Biswanath, Ahmed, Satish, Arun da, Maitham, Kamal , Fatma, Reda and Nasi for providing excellent working atmosphere in our shared lab and office. I would also like to thanks all the department mates (Jens, Pavel, Aboma, Nils, Mohamed, Kaibo, Dimali, Azahar,Ujjal, Karki, Amal, Eva, Alice, Rafael, Wei Zhang, Sesha, Alireza and Junsheng) for offering me such a nice working environment, helps during my research at this department and Friday morning Fika. I am going to miss you all.

I am dedicating the thesis to the soul of my father Abul Hasen (Hasi) who put the fundament my learning character, showing me the joy of intellectual pursuit ever since I was a child. Special thanks goes to My reverend Mother Dudmeher Begum, is the one who sincerely raised me with her caring and prayers. Thanks a lot to my mother-in-law Mahfuza Akter and Ummey Kulsum Rosy for their continuous inspiration, help, support and prayer. Thank you to my brothers Ataur Rahman, brother in-law, Zakir Chowdhury, my sisters Johara Begum and sisters in-law Israt Jahan Shila for their sacrifice, cooperation, continuous inspiration support, understanding and encouragement in whatever choices I have made in life and always believing in me.

There are no words in my vocabulary to express my appreciation to my beloved wife Marufa Akter Rupa, whose dedication, love and persistent confidence in me, has taken the load off my shoulder. I could literally not have done it without all your support. I wish you all the best in your future. My loving son Ahnaf Abid Rahman Ta-seen who is inspiration of my life when you said "best of luck with your writing daddy" every day during my writing and when I went to lab during weekend you said "daddy today is weekend!!!" I felt inspiration from you Ta-seen. Thank you very much and I love you daddy; My sweetheart Moin, Mohid, Shihab, Jarif, Saurov and shohag; I wish you all prosperous future ahead, a lifetime of love, knowledge, achievement and happiness.

Special thanks go to my all Bangladeshi friends and relatives for their sacrifice, cooperation and continuous inspiration during my research work. Thank you all member of Lund Summer Cricket (Jhijhipoka) and Bangladeshi Cultural Association in Skåne (BCAS) to organize a lots of enjoyable events. I wish to offer my warm thanks to all the friends I have made during my PhD. There are too many people to mention but you know who you are you've made my PhD very enjoyable.

Above all, I am grateful to almighty Allah for His great blessings to complete this research work in time.

Reference

1. Zuttel, A. Borgschulte, L. Sachlapbach, *Hydrogen as a Future energy Carrier*, (2008) 1st ed. *Wiley-VCH Verlag GmbH & Co.* ISBN: 978-3-527-30817-0.
2. J. R. Petit, *Nature,* 1999, **399**, 429.
3. R.T. Watson, *Climate Change 2001: Synthesis Report*, Cambridge University Press,
4. Tard, C. Pickett, *Chem. Rev.*, 2009, **109**, 2245.
5. J. A. Cracknell, K. A. Vincent, F. A. Armstrong, *Chem. Rev.*, 2008, **108**, 2439.
6. M. Stephenson, L. H. Stickland, *J. Biochem.*, 1931, **25**, 205.
7. R. K. Thauer, A. R. Klein, G. C. Hartmann, *Chem. Rev.,* 1996, **96**, 3031.
8. P. Vignais, B. O. Billoud, *Chem. Rev.,* 2007, **107**, 4206.
9. M. Frey, *Chem Bio Chem.*, 2002, **3**, 153.
10. M. W. W. Adams, *Biochim. Biophys. Acta,* 1990, **1020**, 115.
11. E. C. Hatchikian, N. Forget, V. M. Fernandez, R. Williams, R. Cammack, *Eur. J. Biochem.,* 1992, **209**, 357.
12. Y. Nicolet, A. L. de Lacey, X. Vernede, V. M. Fernandez, E. C. Hatchikian, J. C. Fontecilla-Camps, *J. Am. Chem. Soc.,* 2001, **123**, 1596.
13. (a) D. J. Evans, C. J. Pickett, *Chem. Soc. Rev.*, 2003, **32**, 268; (b) L. -C. Song, *Acc. Chem. Res.*, 2005, **38**, 21; (c) W. Lubitz, W. Tumas, *Chem. Rev.,* 2007, **107**, 3900; (d) M. Gräetzel, *Acc. Chem. Res.,* 1981, **14**, 376; (e) A. J. Bard, M. A. Fox, *Acc. Chem. Res.,* 1995, **28**, 141; (f) J. Alper, *Science*, 2003, **299**, 1686; (g) R. Cammack, M. Frey, R. Robson, *Hydrogen as a Fuel: Learning from Nature, Taylor & Francis, London,* 2001.
14. J. W. Peters, W. N. Lanzilotta, B. J. Lemon, L. C. Seefeldt, *Science,* 1998, **282**, 1853.
15. Y. Nicolet, C. Piras, P. Legrand, C. E. Hatchikian, J. C. Fontecilla-Camps, *Structure,* 1999, **7**, 13.
16. M. Adams, *Biochim. Biophys. Acta,* 1990, **1020**, 115.
17. B. L. Vallee, R. J. Williams, *Proc. Natl. Acad. Sci., USA* 1968, **59**, 498.
18. M. Bruschi, C. Greco, P. Fantucci, L. De Gioa, *Inorg. Chem.,* 2008, **47**, 6056.
19. B. J. Lemon, J. W. Peters, *Biochemistry,* 1999, **38**, 12969.
20. Y. Nicolet, B. J. Lemon, J. C. Fontecilla.-Camps, J. W. Peters, *Trends Biochem. Sci.,* 2000, **25**, 138.

21. Greco, M. Bruschi, L. De Gioia, U. Ryde, *Inorg.Chem.*, 2007, **46**, 5911.

22. H. Reihlen, A. Gruhl, G. Hessling, Liebigs, *Ann. Chem.*, 1929, **472**, 268.

23. Lawrence, H. X. Li, T. B. Rauchfuss, M. Benard, M. M. Rohmer, *Angew. Chem., Int. Ed.,* 2001, **40**, 1768.

24. Winter, L. Zsolnai, G. Huttner, B. Naturforsch, *Anorg. Chem. Org. Chem.*, 1982, **37**, 1430.

25. R. B. King, *J. Am. Chem. Soc.,* 1963, **85**, 1584.

26. (a) Q. Francois, P. Guillaume, G. Frederic, *Energy Environ. Sci.,* 2012, **5**, 7757; (b) S. Lennart, P. S. Singh, L. Eriksson, R. Lomoth, S. Ott, *C. R. Chimie*, 2008, **11**, 875; (c) A. Javier, M. Cabeza, A. M. -Garcia, R, Victor. A. Diego, G. -G. Santiago, *Organometallics,* 1998, **17**, 1471; (d) G. A. N. Felton, A. K. Vannucci, J. Chen, L. T. Lockett, N. Okumura, B. J. Petro, U. I. Zakai, D. H. Evans, R. S. Glass, D. L. Lichtenberger, *J. Am. Chem. Soc.*, 2007, **129**, 12521; (e) F. Gloaguen, D. Morvan, J. -F. Capon, P. Schollhammer, J. Talarmin, *J. Electroanalytical Chem.*, 2007, 603; (f) J. -F. Capon, F. Gloaguen, P. Schollhammer, J. Talarmin, *J. Electroanalytical Chem.,* 2006, 595; (g) J. -F. Capon, F. Gloaguen, P. Schollhammer, J. Talarmin, *J. Electroanalytical Chem.,* 2004, 566; (h) P. Li, M. Wang, J. Pan, Li. Chen, N. Wang, L. Sun, J. *Inorg. Biochem.*, 2008, **102**, 952; (i) J. Zhao, Z. Wei, Xi. Xeng, Xi. Liu, *Dalton Trans*., 2012, **41**, 11125.

27. (a) E. S. Donovan, G. S. Nichol, G. A. N. Felton, *J. Organomet. Chem.,* 2013, **726**, 9; (b) G. A. N. Felton, B. J. Petro, R. S. Glass, D. L. Lichtenberger, D. H. Evans, *J. Am. Chem. Soc.,* 2009, **131**, 11291; (c) E. Xu, Z. Xiao, H. Liu, Li, Long, L. Li, Xi. Liu, *RSC Adv.,* 2012, **2**, 10171; (d) S. J. Borg, J. W. Tye, M. B. Hall, S. P. Best, *Inorg. Chem.*, 2007, **46**, 2.

28. (a) F. Gloaguen, J. D. Lawrence, M. Schmidt, S. R. Wilson, T. B. Rauchfuss, *J. Am. Chem. Soc.,* 2001, **123**, 12518; (b) Z. Xiao, Z. Wei, Li Long, Y. Wang, D. J. Evans, Xi. Liu, *Dalton Trans.,* 2011, **40**, 4291; (c) L. E. Roy, E. R. Batista, P. J. Hay, *Inorg. Chem.*, 2008, **47**, 20; (d) T. Liu, B. Li, M. L. Singleton, M. B. Hall, M. Y. Darensbourg, *J. Am. Chem. Soc.,* 2009, **131**, 23; (e) J. Danielle, J. A. Crouthers, R. D. Denny, D. G. Munoz, M. Y. Darensbourg, *Organometallics,* 2014, **33**, 4747; (f). S. Dey, A. Rana, D. Crouthers, B. Mondal, P. K. Das, M. Y. Darensbourg, A. Dey, *J. Am. Chem. Soc.,* 2014, **136**, 8847; (g). S. J. Borg, S. K. Ibrahim, C. J. Pickett, S. P. Best, *C. R. Chimie,* 2008, **11**, 852 (h). J. -F. Capon, S. Ezzaher, F. Gloaguen, F. Y. Pe´tillon, P. Schollhammer, J.

Talarmin, T. J. Davin, J. E. McGrady, K. W. Muir, *New J. Chem.,* 2007, **31**, 2052; (i) M. -Q. Hu, C. -B. Ma, Y. -T. Si, C. -N. Chen, Q. -T. Liu. *J. Inorg. Biochem.,* 2007, **101**, 1370; (j) P. Li, M. Wang, C. He, G. Li, X. Liu, C. Chen, B. Åkermark, L. Sun. *Eur. J. Inorg. Chem.,* 2005, 2506; (k) S. J. Borg, T. Behrsing, S. P. Best, M. Razavet, X. Liu, C. J. Pickett *J. Am. Chem. Soc.,* 2004, **126**, 16988; (l) R. M. -Rodriguez, D. Chong, J. H. Reibenspies, M. P. Soriaga, M. Y. Darensbourg. *J. Am. Chem. Soc.,* 2004, **126**, 38; (m) D. Chong, I. P. Georgakaki, R. M. -Rodriguez, J. S. -Chinchilla, M. P. Soriaga, M. Y. Darensbourg. *Dalton Trans.,* 2003, 4158.

29. J. Lyon, I. P. Georgakaki, J. H. Reibenspies, M. Y. Darensbourg, *Angew. Chem., Int. Ed.,* 1999, **38**, 3178.

30. M. Schmidt, S. M. Contakes, T. B. Rauchfuss, *J. Am. Chem. Soc.,* 1999, **121**, 9736.

31. L. Cloirec, S. P. Best, S. Borg, S. C. Davies, D. J. Evans, D. L. Hughes, C. J. Pickett, *Chem. Commun.,* 1999, 2285.

32. L. Schwartz, PhD Thesis.

33. A. Felton, C. A. Mebi, B. J. Petro, A. K. Vannucci, D. H. Evans, R. S. Glass, D. L. Lichtenberger, *J. Organomet. Chem.*, **2009,** **694**(17), 2681.

34. Tard, X. M. Liu, S. K. Ibrahim, M. Bruschi, L. De Gioia, S. C. Davies, X. Yang, L. S. Wang, G. Sawers and C. J. Pickett, *Nature*, 2005, **433**, 610.

35. (a) S. Tschierlei, S. Ott, R. Lomoth, *Energy Environ. Sci.*, 2011, **4**, 2340; (b) M. I. Grace, C. M. Whaley, N. Lehnert. *Inorg. Chem.,* 2010, **49**, 3201.

36. (a) F. Gloaguen, J. D. Lawrence, T. B. Rauchfuss, *J. Am. Chem. Soc.,* 2001, **123**, 9476; (b) L. Schwartz, G. Eilers, L. Eriksson, A. Gogoll, R. Lomoth, S. Ott, *Chem. Commun.,* 2006, 520; (c) F. I. Adam, G. Hogarth, I. Richards, *J. Organomet. Chem.*, 2007, **692**, 3957; (d) F. I. Adam, G. Hogarth, S. E. Kabir, I. Richards, *C. R. Chim.*, 2008, **11**, 890; (e) I. P. Georgakaki, M. L. Miller, M.Y. Darensbourg, *Inorg. Chem.*, 2003, **42**, 2489.

37. (a) J. F. Capon, F. Gloaguen, P. Schollhammer, J. Talarmin, *Coor. Chem. Rev.,* 2005, **249**, 1664; (b) J. F. Capon, F. Gloaguen, F. Y. Pe´tillon, P. Schollhammer, J. Talarmin, *Coor. Chem. Rev.,* 2009, **253**, 1476.

38. (a) S. Ezzaher, J. F. Capon, F. Gloaguen, F. Y. Pe´tillon, P. Schollhammer, J. Talarmin, *Inong. Chem.*, 2007, **46**, 3426; (b) J. F. Capon, F. Gloaguen, F. Y. Pe´tillon, P. Schollhammer, J. Talarmin. *Eur. J. Inor. Chem.*, 2008, 4671.

39. F. A. Cotton, G. Wilkinson, *Adv. Inorg. Chem.*, *Wiley*: New York, 1988, Chapter 23.

40. R. B. King, *Inorg. Chim. Acta,* 1986, **116**, 119.

41. D. M. P. Mingos, T. Slee, *J. Organomet. Chem.*, 1990, **394**, 679.

42. P. Lemoine. *Coord. Chem. Rev.*, 1982, **47**, 55.

43. (a) B. H. S. Thimmappa, *Coord. Chem. Rev.*, 1995, **143**, 1; (b) R. D. Johnston, *Adv. Inorg. Radiochem.*, 1970, **13**, 471; (c) P. Chini, G. Lononi, V. G Albano, *Adv. Organomet. Chem.*, 1976, **14**, 285.

44. (a) P. Chini, B. T. Heaton, *Top. Curr. Chem.*, 1977, **71**, 1; (b) E. Band, E. L. Muetterties, *Chem. Rev.,* 1978, **78**, 639; (c) G. L. Geoffroy, *Acc. Chem. Res.*, 1980, **13**, 469.

45. (a) W. L. Gladfetter, G. L. Geoffroy, *Adv. Organomet. Chem.*, 1980, **18**, 207; (b) D. A. Roberts, G. L. Geoffroy, Comp. *Organomet. Chem.*, G. Wilkinson, F. G. A. Stone, E Abel, Eds. Pergamon: Oxford, 1982; Vol. **6**, p 763; (c) K. Wade, *In Transition Metal Clusters*, B. F. G. Johnson, *Ed., Wiley*: 1980; Chapter 3; (d) C. Bianchini, A. Meli, *J. Chem. Soc., Dalton Trans.,* 1996, **6**, 801.

46. B. F. G. Johnson, *In Transition Metal Clusters*, *Wiley*: New York, 1980; Chapter 3.

47. I. Haiduc, J. J. Zuckerman, Basic *Organomet. Chem.*; Walter de Gruyter, Berlin and New York, 1985; p 233.

48. (a) J. J. Brunet, M. Taillefer, *J. Organomet. Chem.*, 1988, **348**, C5; (b) H. Alper, K. E. Hashem. *J. Am. Chem. Soc.*, 1981, **103**, 6514.

49. C. Pac, K. Miyake, T. Matsuo, S. Yanagida, H. Sakurai, *J. Chem. Soc., Chem. Commun.*, 1986, 1115.

50. J. Palágyi, L. Marko, *J. Orgament. Chem.*, 1982, **236**, 343.

51. J. Dewar, H. O. Jones, *Proc. Roy. Soc.,* (London) Ser. 1905, **B 76**, 564.

52. B. E. Hanson, E. C. Lisic, J. T. Petty, G. A. *Inorg. Chem.*, 1986, **25**, 4062.

53. H. Ogino, S. Inomate, H. Tobita, *Chem. Rev.*, 1998, **358**, 2093.

54. C. H. Wei, C. G. R. Wilkes, P. M. Treichel, L. F. Dahl, *Inorg. Chem.*, 1966, **5**, 900.

55. W. Hieber, W. Z. Beck, *Allg. Anorg. Chem.*, 1958, **296**, 91.

56. P. M.-Lausarot, G. A. Vaglio, M. Valle, *Inorg. Chim. Acta,* 1977, **25**, L104.

57. H. U. Blase, A. Indolese, A. Schnyder, *Science*, 2000, **78**, 1336.

58. (a) I. P. Georgakaki, L. M. Thomson, E. J. Lyon, M. B. Hall, M. Y. Darensbourg, *Coord. Chem. Rev.*, 2003, **238-239**, 255; (b) D. J. Evans, C. J. Pickett, *Chem. Soc. Rev.,* 2003, **32**, 268.

59. (a) T. B. Rauchfuss, *Inorg. Chem.,* 2004, **43**, 14; (b) L. Sun, B. Åkermark, S. Ott, *Coord. Chem. Rev.,* 2005, **249**, 1653.

60. (a) X. Liu, S. K. Ibrahim, C. Tard, C.J. Pickett, *Coord. Chem. Rev.,* 2005, **249**, 1641; (b) M. Y. Darensbourg, E. J. Lyon, J. J. Smee, *Coor. Chem. Rev.,* 2000, **533**, 206.

61. M. Bruschi, C. Greco, M. Kaukonen, P. Fantucci, U. Ryde, L. De Gioia, *Angew. Chem., Int. Ed.,* 2009, **48**, 3503.

62. C. Greco, P. Fantucci, L. De Gioia, R. Suarez-Bertoa, M. Bruschi, J. Talarmin, P. Schollhammer, *Dalton Trans.,* 2010, **39**, 7320.

63. C. Greco, G. Zampella, L. Bertini, M. Bruschi, P. Fantucci, L. De Gioia, *Inorg. Chem.,* 2007, **46**, 108.

64. P. Surawatanawong, J. W. Tye, M. Y. Darensbourg, M. B. Hall, *Dalton Trans.,* 2010, **39**, 3093.

65. P. I. Volkers, C. A. Boyke, J. Chen, T. B. Rauchfuss, C. M. Whaley, S. R. Wilson, H. Yao, *Inorg. Chem.,* 2008, **47**, 7002.

66. J. Windhager, M. Rudolph, S. Bräutigam, H. Görls, W. Weigand, *Eur. J. Inorg. Chem.,* 2007, 2748.

67. C. Tard, X. Liu, D. L. Hughes, C. J. Pickett, *Chem. Commun*., 2005, 133.

68. M. H. Cheah, C. Tard, S. J. Borg, X. Liu, S. K. Ibrahim, C. J. Pickett, S. P. Best, *J. Am. Chem. Soc.*, 2007, 1**29**, 11085.

69. A. Winter, L. Zsolnai, G. Huttner, *Zeit. Natur.,* 1982, **37B**, 1430.

70. R. D. Adams, J.H. Yamamoto, *J. Cluster Sci.,* 1996, **7**, 643.

71. W. Gao, J. Sun, M. Li, T. Akermark, K. Romare, L. Sun, B. Akermark, *Eur. J. Inorg. Chem.*, 2011, 1100.

72. (a) S. Lounissi, J. **-**F. Capon, F. Gloaguen, F. Matoussi, F. Y. Pe´tillon, P. Schollhammer, J. Talarmin, *Chem. Commun.,* 2011, **47**, 878 ; (b)L. Beaume, M. Clemancey, G. Blondin, C. Greco, F. Y. Pe´tillon, P. Schollhammer, J. Talarmin, *Organometallics*, 2014, **33**, 6290; (c) K. Charreteur, J. F. Capon, F. Gloaguen, F. Y. Pe´tillon, P. Schollhammer, J. Talarmin, *Eur. J. Inorg. Chem.,* 2011, 1038.

73. S. Ghosh, K. B. Holt, S. E. Kabir, M. G. Richmond, G. Hogarth, *Dalton Trans*., 2015, **44**, 5160.

74. K. T. Chu, Y. C. Liu, Y. L. Huang, G. H. Lee, M. C. Tseng, M. H. Chiang, *Chem. Eur. J.* 2015, **21**, 6852.

75. S. Bruna, I. Cuadrado, E. Delgado, C. J. G. Gracia, D. Hernandez, E. Hernandez, R. Llusar, A. Martin, N. Menendez, V. Polo, F. Zamora, *Dalton, Trans.,* 2014, **43**, 13187.

76. S. Ghosh, G. Hogarth, K. B. Holt, S. E. Kabir, A. Rahaman and D. G. Unwin, *Chem. Commun.,* 2011, **47**, 11222.

77. A. K. Justice, G. Zampella, L. De Gioia, T. B. Rauchfuss, J. I. V. Vlugt, S. R. Wilson, *Inorg. Chem.,* 2007, **46**, 1655.

78. A. Rahaman, S. Ghosh, N. Hollingsworth, S. E. Kabir, M. G. Richmond, E. Nordlander, G. Hogarth, unpublished results.

79. (a) F. I. Adam, G. Hogarth, I. Richards, *J. Organomet. Chem*., 2007, **692**, 3957; (b) F. I. Adam, G. Hogarth, I. Richards, B. E. Sanchez, *Dalton Trans*., 2007, 2485; (c) F. I. Adam, G. Hogarth, S. E. Kabir, I. R. Richards, *C. R. Chimie*, 2008, **11**, 890; (d) G. Hogarth, I. Richards, *Inorg. Chem. Commun*., 2007, **10**, 66.

80. (a) S. Ezzaher, J. -F. Capon, F. Gloaguen, F. Y. Pe´tillon, P. Schollhammer, J. Talarmin, *Inorg. Chem*. 2007, **46**, 9863; (b) S. Ezzaher, J. -F. Capon, F. Gloaguen, F.Y. Pe´tillon, P. Schollhammer, J. Talarmin, R. Pichon, N. Kervarec, *Inorg. Chem*., 2007, **46**, 3426; (c) S. Lounissi, J. -F. Capon, F. Gloaguen, F. Matoussi, F. Y. Pe´tillon, P. Schollhammer, J. Talarmin, *Chem. Commun*., 2011, **47**, 878.

81. S. Ghosh, G. Hogarth, N. Hollingsworth, K. B. Holt, I. Richards, M. G. Richmond, B. E. Sanchez, D. Unwin, *Dalton Trans.,* 2013, **42**, 6775.

82. P. Mathur, Md. M. Hossain, P. B. Hitchcock, J. F. Nixon, *Organometallics,* 1995, **14**, 3101.

83. R. D. Adams, D. F. Shriver, H. D. Kaesz, R. D. Adams, *the Chemistry of Metal Cluster complexes.*

84. D. A. Roberts and G. L. Geoffroy, S. G. Wilkinson, F. G. A. Stone, E. W. Abel, *Comprehensive Organometallic Chemistry.*

85. G. Hogarth, N. J. Taylor, A. J. Carty, A. Meyer, *J. Chem. Soc., Chem. Commun*., 1988, 834.

86. R. D. Adams, J. E. Babin, P. Mathur, K. Natarajan, J.–G. Wang, *Inorg. Chem*. 1989, **28**, 1440.

87. (a) D. Cauzzi, C. Graiff, C. Massera, G. Predieri, A. Tiripicchio, D. Acquotti, *J. Chem. Soc*., *Dalton Trans*., 1999, 3515; (b) D. Cauzzi, C. Graiff, G. Predieri, A. Tiripicchio, C. Vignali, *J. Chem. Soc*., *Dalton Trans*., 1999, 237; (c) D. Cauzzi, C. Graiff, M. Lanfranchi, G. Predieri, A. Tiripicchio, *J. Organomet. Chem.,*1997, **536**, 497; (d) D. Cauzzi, C. Graiff, M. Lanfranchi, G. Predieri, A. Tiripicchio, *J. Chem. Soc*., *Dalton Trans*., 1995, 2321.

88. (a) P. Baistrocchi, M. Cared, D. Cauzzi, C. Graiff, M. Lanfranchi, P. Martini, G. Prcdicri, A. Tiripicchio, *Inorg. Chim. Acta,* 1996*, **252**, 307;

(b) P. Baistrocchi, D. Cauzzi, M. Lanfranchi, G. Predieri, A. Tiripicchio, M. T. Camellini, *Inorg. Chim. Acta*, 1995, **235**, 173.

89. (a) P. Mathur, S. Chatterjee, Y. V. Torubaev, *J. Clust. Sci.*, 2007, **18**, 505; (b) M. Shieh, C. –Y. Miu, Y. –Y. Chu, C. –N. Lin, *Coord. Chem. Rev.*, 2012, **256**, 637.

90. M. D. H Sikder, S. Ghosh, S. E. Kabir, G. Hogarth, D. A. Tocher, *Inorg. Chim. Acta*, 2011, **376**, 170.

91. M. I. Hyder, N. Begum, M. D. H. Sikder, G. M. G. Hossain, G. Hogarth, S. E. Kabir, C. J. Richard, *J. Organomet. Chem.*, 2009, **694**, 304.

92. T. Akter, N. Begum, D. T. Howarth, D. W. Bennett, S. E. Kabir, Md. A. Miah, N. C. Sarker, T. A. Siddiquee, E. Rosenberg, *J. Organomet. Chem.*, 2004, **689**, 2571.

93. T. Akter, A. J. Deeming, G. M. G. Hossain, S. E. Kabir, D. N. Mondal, E. Nordlander, A. Sharmin, D. A. tocher, *J. Organomet. Chem.*, 2005, **690**, 4628.

94. M. –H. Hsu, C. **-**Y Miu, Y. –C. Lin, M. Shieh, *J. Organomet. Chem.* 2006, **691**, 966.

95. M. G. Humphrey, B. L. **-**Gillett, M. Samoc, B. W. Skelton ,V. A. Tolhurst, A. H. White, A. J. Wilson, B. F. Yates, *J. Organomet. Chem.*, 2005, **690**, 1487.

96. R. D. Pergola, L. G. Chellihem, *J. Chem. Soc., Dalton Trans.*, 1986, 2463.

97. (a) L. Markö, T. Madach, H. Vahrenkamp, *J. Organomet. Chem.*, 1980, **190**, C67; (b) R. D. Adams, J. E. Babin, M.Tasi, *Organometallics*, 1988, **7**, 219; (c) R. D. Adams, I. T. Horvath, H. S. Kim, *Organometallics*, 1984, **3**, 548; (d) D. Cauzzim, C. Graiff, M. Lanfranchi, G. Predieri, A. Tiripicchio, *J. Organomet. Chem.*, **1997**, 536–537*,* 497; (e) C. Graiff, G. Predieri, A. Tiripicchio, *Eur. J. Inorg. Chem.,* 2003, 1659**.**

98. (a) S. N. Konchenco, A. V. Virovets, S. V Thachev, *Zh. Strukt. Khim.* 1998, **39**, 894; (b) A. V. Virovets, S. N. Konchenko, D. Fenske, *J. Struc. Chem.*, 2002, **43**, 694.

99. D. Belletti, D. Cauzzi, C. Graiff, A. Minarelli, R. Pattacini, G. Predieri, A. Tiripicchio, *J. Chem. Soc., Dalton Trans.*, 2002, 3160**.**

100. (a) Z. Li, X. Zeng, Z. Niu, X. Liu, *Electrochimica Acta*, 2009, **54**, 3638; (b) C. A. Mebi, K. E. Brigance, R. B. Bowman, *J. Braz. Chem. Soc.*, 2012, **23**, 186.

101. M. Kaiser, G. Knör, *Eur. J. Inorg. Chem.,* 2015, 4199.

102. (a) M. D. Rail, L. A. Berben, *J. Am. Chem. Soc.,* 2011, **133**, 18577**;** (b) A. D. Nguyen, M. Rail, M. Shanmugam, J. C. Fettinger, L. A. Berben, *Inorg. Chem.,* 2013, **52**, 12847.

103. S. L. Matthews, D. M. Heinekey, *Inorg. Chem.*, 2010, **49**, 9746.

104. (a) J. –F. Capon, F. Gloaguen, F. Y. Pe´tillon, P. Schollhammer, J. Talarmin, *Eur. J. Inorg. Chem.,* 2008, 4671; (b) E. J. Lyon, I. P. Georgakaki, J. H. Reibenspies, M. Y. Darensbourg, *J. Am. Chem. Soc.*, 2001, **123**, 3268; (c) X. Zhao, I. P. Georgakaki, M. L. Miller, R. Mejia-Rodriguez, C.**-**Y. Chiang, M. Y. Darensbourg, *Inorg. Chem.*, 2002, **41**, 3917; (d) F. Gloaguen, J. D. Lawrence, T. B. Rauchfuss, M. Bénard, M. **-** M. Rohmer, *Inorg. Chem.*, 2002, **41**, 6573; (e) J. F. Capon, S. El. Hassnaoui, F. Gloaguen, P. Schollhammer, J. Talarmin, *Organometallics,* 2005, **24**, 2020; (f) P. Li, M. Wang, C. He, G. Li, X. Liu, C. Chen, B. Åkermark, L. Sun, *Eur. J. Inorg. Chem.,* 2005, **44**, 2506; (g) P.**-**Y. Orain, J. **-**F. Capon, F. Gloaguen, F. Y. Pe´tillon, P. Schollhammer, J. Talarmin, G. Zampella, L. De Gioia, T. Rosinel, *Inorg. Chem.*, 2010, **49**, 5003**;** (h) B. E. Barton, G. Zampella, A. K. Justice, L. De Gioia, T. B. Rauchfuss, S. R. Wilson, *Dalton Trans.*, 2010, **39**, 3011.

105. (a) S. Chatterjee, S. K. Patel, S. M. Mobin, *J. Organomet. Chem.*, 2011, **696**, 1782; (b) S. Chatterjee, S. K. Patel, V. Tirkey, S. M. Mobin. *J. Organomet. Chem.*, 2012, **699**, 12.

106. (a) D. A. Lesch, T. B. Rauchfuss, *Inorg. Chem.,* 1981, **20**, 3583; (b) D. A. Lesch, T. B. Rauchfuss, *Organometallics*, 1982, **1**, 499; (c) V. W. Day, D. A. Lesch, T. B. Rauchfuss, *J. Am. Chem. Soc.,*1982, **104***,* 1290; (d) D. A. Lesch, T. B. Rauchfuss, *Inorg. Chem.,* 1983, **22**, 1854; (e) L. E. Bogan, D. A. Lesch, T. B. Rauchfuss, *Organomet. Chem.,* 1983, **250**, 429.

107. (a) P. Mathur, *Adv. Organomet. Chem.*, 1997, **41**, 243; (b) P. Mathur, I. J. Mavunkal, J. *Organomet. Chem.*, 1988, **350**, 251; (c) P. Mathur, I. J. Mavunkal, V. Rugmini, J. Organomet. Chem., 1989, **367**, 243; (d) P. Mathur, V. D. Reddy, *J. Organomet. Chem.*, 1990, **385**, 363; (e) A. L. Rheingold, R. L. Ostrander, P. Mathur. *Acta Cryst.*, 1993, **C49**, 1741; (f) P. Mathur, A. K. Bhunia, A. Kumar, S. Chatterjee, S. M. Mobin, *Organometallics*, 2002, **21**, 2215.

108. (a) S. Klose, U. Flörke, H. Egold, P. Mathur. *Organometallics*, 2003, **22**, 3360; (b) P. Mathur, A. K. Dash, Md. M. Hossain, S. B. Umbarkar, *Organometallics,* 1996, **15**, 1356; (c) P. Mathur, I. J. Mavunkal, V. Rugmini. *Inorg. Chem.,* 1989**, 28**, 3616.

109. L. –C. Song, X. –J. Sun, G. –J. Jia, M. –M. Wang, H. –B. Song. *J. Organomet. Chem.*, 2014, **761**, 10.

110. C. M. Thomas, O. Rüdiger, T. Liu, C. E. Carson, M. B. Hall, M. Y. Darensbourg, *Organometallics,* 2007, **26**, 3976.

111. (a) M. K. Harb, T. Niksch, J. Windhager, H. Görls, R. Holze, L. T. Lochett, N. Okumura, D. H. Evans, R. S. Glass, D. L. Lichtenberger, M. El. Khateeb, W. Weigand, *Organometallics*, 2009, **28**, 1039; (b) M. K. Harb, H. Görls, T. Sakamoto, G. A. N. Felton, D. H. Evans, R. S. Glass, D. L. Lichtenberger, M. El. Khateeb, W. Weigand *Eur. J. Inorg. Chem.*, 2010, 3976; (c) M. K. Harb, U. **-**P. Apfel, T. Sakamoto, M. El. Khateeb, W. Weigand, *Eur. J. Inorg. Chem.*, **2011**, 986.

112. (a) L. **-**C. Song, Q. **-**L. Li, Z. **-**H. Feng, X. **-**J. Sun, Z. **-**J. Xie, H. **-**B. Song, *Dalton Trans.*, 2013, **42**,1612; (b) L. **-**C. Song, B. Gai, H. **-**T. Wang, Q. **-**M. Hu, J. *Inorg. Biochem.*, 2009, **103**, 805.

113. M. K. Harb, U. **-**P. Apfel, J. Kubel, H. Gorls, G. A. N. Felton, T. Sakamoto, D. H. Evans, R. S. Glass, D. L. Lichtenberger, M. El. Khateeb, W. Weigand, *Organometallics,* 2009, **28,** 6666.

114. (a) D. Seyferth, T. G. Wood, J. P. Jr. Fackler, A. M. Mazany, *Organometallics,* 1984, **3**, 1121; (b) D. Seyferth, T. G. Wood, R. S. Henderson, *J. Organomet. Chem.,* 1987, **336**, 163.

115. (a) D. Seyferth, T. G. Wood, *Organometallics,* 1987, **6**, 2563; (b) D. Seyferth, T. G. Wood, *Organometallics,* 1988, 7, 714; (c) R. B. King, F. **-**J. Wu, N. D. Sadani, E. M. Holt, *Inorg. Chem.,* 1985, **24,** 4450; (d) R. B. King, F. **-**J. Wu, E. M. Holt, *Inorg. Chem.,* 1986, **25**, 1733; (e) R. B. King, F. **-**J. Wu, E. M. Holt, *J. Am. Chem. Soc.,* 1987, **109**, 7764; (f) J. S. McKennis, E. P. Kyba, *Organometallics,* 1983, **2**, 1249; (g) E. P. Kyba, R. E. Davis, C. N. Clubb, S. **-**T. Liu, H. O. Aldaz Palacio, J. S. McKennis, *Organometallics,* 1986, 5, 869. (h) E. P. Kyba, M. C. Kerby, S. P. Rines, *Organometallics,* 1986, **5**, 1189; (i) T. C. Flood, F. J. DiSanti, K. D. Campbell, *Inorg. Chem.,* 1978, **17**, 1643; (j) A. L. Rheingold, *Acta Crystallogr.,* 1985, **C41**, 1043; (k) P. M. Treichel, W. M. Douglas, W. K. Dean, *Inorg. Chem.,* 1972, **7,** 1615.

116. (a) D. Seyferth, R. S. Henderson, L.-C. Song, *Organometallics,* 1982, **1**, 125; (b) D. Seyferth, G. B. Womack, R. S. Henderson, M. Cowie, B. W. Hames, *Organometallics,* 1986, **5**, 1568.

117. (a) J. D. Lawrence, H. Li, T. B. Rauchfuss, *Chem. Commun.,* 2001, 1482; (b) H. Li, T. B. Rauchfuss, *J. Am. Chem. Soc.,* 2001, 124, 726; (c) J. D. Lawrence, H. Li, T. B. Rauchfuss, M. Benard, M. **-**M. Rohmer,

Angew. Chem., Int. Ed., 2001, **40**, 1768; (d) S. Ott, M. Kritikos, B. Åkermark, L. Sun, *Angew. Chem., Int. Ed.,* 2003, **42**, 3285; (e) S. Ott, M. Borgstrom, M. Kritikos, R. Lomoth, J. Bergquist, B. Åkermark, L. Hammarström, L. Sun, *Inorg. Chem.,* 2004, **43**, 4683.

118. (a) P. M. Treichel, W. K. Dean, W. M. Douglas, *Inorg. Chem.,* 1972, **11**, 1609; (b) R. Bartsch, S. Hietkamp, S. Morton, O. Stelzer, *J. Organomet. Chem.,* 1981, **222**, 263; (c) J. P. Collman, R. K. Rothrock, R. G. Finke, E. J. Moore, F. R. Munch, *Inorg. Chem.,* 1982, **21**, 146; (d) R. G. Hayter, *Inorg. Chem.,* 1964, **3**, 711; (e) P. E. Garrow, *Chem. Rev.,* 1981, **81**, 229.

119. (a) W. Clegg, *Inorg. Chem.,* 1976, **15**, 1609; (b) M. R. Adams, J. Gallucci, A. Wojcicki, G. Long, *J. Inorg. Chem.,* 1992, **31**, 2; (c) R. E. Ginsburg, R. K. Rothrock, R. G. Finke, J. P. Collman, L. F. Dahl, *J. Am. Chem. Soc.,* 1979, **101**, 6550.

120. (a) R. E. Dessy, R. L. Kornmann, C. Smith, R. Haytor, *J. Am. Chem. Soc.,* 1968, **90**, 2001; (b) Y. F. Yu, J. Gallucci, A. Wojcicki, *J. Am. Chem. Soc.,* 1983, **105**, 4826; (c) R. E. Ginsburg, R. K. Rothrock, R. G. Finke, J. P. Collman, L. F. Dahl, *J. Am. Chem. Soc.,* 1979, **101**, 6550; (d) M. -H. Baik, T. Ziegler, C. K. Schauer, *J. Am. Chem. Soc.,* 2000, **122**, 9143; (e) J. G. M. V. Linden, J. Heck, B. Walther, H. C. Boettcher, *Inorg. Chim. Acta,* 1994, **217**, 29; (f) S. G. Shyu, A. Wojcicki, *Organometallics,* 1985, **4**, 1457; (g) A. Wojcicki, *Inorg. Chim. Acta,* 1985, **100**, 125.

121. R. Zaffaroni, T. B. Rauchfuss, A. Fuller, L. D. Gioia, G. Zampella, *Organometallics,* 2013, **32**, 232.

122. M. H. Cheah, S. J. Borg, S. P. Best, *Inorg. Chem.,* 2007, **46**, 5, 1741.

123. J. G. M. V. Linden, J. Heck, *Inorg, Chim. Acta,* 1994, **217**, 29.

124. R. E. Ginsburg, R. K. Rothrock, R. G. Finke, J. P. Collman, L. F. Dahl, *J. Am.Chem. Soc.,* 1979, **101**, 6550.

125. M. H. Cheah, S. J. Borg, M. I. Bondin, S. P. Best, *Inorg. Chem*., 2004, **43**, 5635.

126. P. Das, J. -F. Capon, F. Gloaguen, F. Y. Pe´tillon, P. Schollhammer, J. Talarmin, *Inorg. Chem.,* 2004, **43**, 8203.

127. Y. -C. Shi, W. Yang, Y. Shi, D. –C. Cheng, *J, Coord. Chem*., 2014, **67**, 2330.

128. C. G. Surinach, M. Bhadbhade, S. B. Colbran, *Organometallics,* 2012, **31**, 3480.

129. (a) H. Aktas, J. C. Slootweg, K. Lammerstma, *Angew. Chem., Int. Ed*. 2010, **49**, 2; (b) R. Waterman, *Dalton Trans*., 2009, 18; (c) F. Mathey,

Dalton Trans., 2007, 1861; (d) K. Lammertsma, *Top. Curr. Chem.,* 2003, **229**, 95; (e) R. Streubel, *Top. Curr. Chem.,* 2003, **223**, 91.

130. (a) F. Mathey, *Angew. Chem., Int. Ed. Engl.*, 2003, **42**, 1578; (b) K. Lammertsma, M. Vlaar, *J. M. Eur. J. Org. Chem.,* 2002, 1127; (c) F. Mathey, N. H. Tran-Huy, A. H. Marinetti, *Chim. Acta*, 2001, **84**, 2938; (d) D. W. Stephan, *Angew. Chem., Int. Ed. Engl.*, 2000, **39**, 314; (e) S. Shah, J. D. Protasiewicz, *Coord. Chem. Rev.*, 2000, **210**, 181.

131. (a) R. R. Schrock, *Acc. Chem. Res.*, 1997, **30**, 9; (b) A. H. Cowley, *Acc. Chem. Res.,* 1997, **30**, 445; (c) A. H. Cowley, A. R. Barron*, Acc. Chem. Res.*, 1988, **21**, 81; (d) G. Huttner, K. Knoll, *Angew. Chem., Int. Ed. Engl.*, 1987, **26**, 743; (3) G. Huttner, K. Evertz, *Acc. Chem. Res.,* 1986, **19**, 406.

132. V. D. Patel, A. A. Cherkas, D. Nucciarone, N. J. Taylor, A. Carty, *Organometallics,* 1985, **4***, 1792.**

133. M. Shieh, C. **-**H. Ho, W. **-**S. Sheu, B. **-**G. Chen, Y.**-**Y. Chu, C. –Y. Miu, H. **-**L. Liu, C. **-**C. Shen, *J. Am. Chem. Soc.,* 2008, **130**, 14114.

134. C. Caryn, B. Breen, M. T. Bautista, C. K. Schauer, P. S. White, *J. Am. Chem. Soc.,* 2000, **122***, 3952.**

135. G. D. Williams, G. L. Geoffrey, R. R. Whittle, *J. Am. Chem. Soc.,* 1985*, **107**, 3,

136. M. T. Bautista, P. S. White, C. K. Schauer, *J. Am. Chem. Soc.,* 1991, **113**, 23.

137. H. H. Ohst, J. K. Kochi, *J. Chem. Soc., Chem. Commun.*, 1986**,** 21.

138. M. Shieh, C. **-**Y. Miu, K. **-**C. Huang, C. **-**F. Lee, B. G. Chen, *Inorg. Chem.*, 2011, **50,** 7735.

139. J. L. Perkinson, M. H. Baik, G. E. Trullinger, C. K. Schauer, P. S. White, *Inorg. Chimica. Acta,* 1999, **294**, 140.

140. N. A. Pushkarevsky, D. A. Bashirov, T. G. Terent'eva, A. V. Virovets, E. V. Peresypkina, H. Krautscheid, S. N. Konchenk, *Russ. J. Coor. Chem.,* 2006, **32**, 6.

141. H. H. Ohst, J. K. Kochi, *Inorg. Chem.,* 1986, **25***, 2066.

142. R. M. De. Silva, M, J. Mays, J. A. Solan, *J. Organomet. Chem.*, 2002, **664**, 27.

143. S. L. Cook, J. Evans, L. R. Gray, M. Webster, *J**. Organomet. Chem.*, 2002*, **236**, 367.

Ahibur Rahaman was born on 31st December 1981 in Narsingdi, Bangladesh. After finishing his early education in Narsingdi, he received his Master of Philosophy (M. Phil) degree in Chemistry from Jahangirnagar University, Dhaka, Bangladesh, in 2011. During his M.Phil studies, he performed research under the joint supervision of Prof. Shariff Enamul Kabir and Prof. Fakir Rafiqul Alam resulting in the thesis 'Di-iron Carbonyl Complexes Bearing Dithiolato, Thienyl and Furyl Ligands: Synthesis, Structures and Reactivity'. During that period he was awarded a Jahangirnagar University Fellowship and a National Science and Information and Communication Technology Fellowship.

In the same year, 2011, he was nominated for an Erasmus Mundus Europe Asia (EMEA) Fellowship from the European Union and joined as a PhD student in Prof. Ebbe Nordlander's research group at Chemical Physics, Department of Chemistry, Lund University, Sweden. His PhD research involved synthesis and reactivity studies of functional models for hydrogenase active sites, which resulted in this thesis. During his PhD work, he also collaborated and worked with Dr. Graeme Hogarth, King's College London and University College London, UK, and with Prof. Stephen B. Colbran, University of New South Wales, Sydney, Australia. Mr. Rahaman is interested in the fields of organometallic synthesis/inorganic synthetic chemistry, proton reduction catalysis and the development of solar fuels.

LUND
UNIVERSITY